NEW INSIGHTS INTO THE ROLE OF EQUINE INFECTIOUS ANEMIA VIRUS S2 PROTEIN IN DISEASE EXPRESSION

A Dissertation

by

LINA MARIA COVALEDA SALAS

Submitted to the Office of Graduate Studies of
Texas A&M University
in partial fulfillment of the requirements for the degree of

DOCTOR OF PHILOSOPHY

May 2010

Major Subject: Veterinary Microbiology

NEW INSIGHTS INTO THE ROLE OF EQUINE INFECTIOUS ANEMIA VIRUS S2 PROTEIN IN DISEASE EXPRESSION

A Dissertation

by

LINA MARIA COVALEDA SALAS

Submitted to the Office of Graduate Studies of
Texas A&M University
in partial fulfillment of the requirements for the degree of

DOCTOR OF PHILOSOPHY

Approved by:

Chair of Committee,	Susan Payne
Committee Members,	Judith M. Ball
	C. Jane Welsh
	Van G. Wilson
Head of Department,	John R. August

May 2010

Major Subject: Veterinary Microbiology

ABSTRACT

New Insights Into the Role of Equine Infectious Anemia Virus S2 Protein in Disease Expression. (May 2010)

Lina Maria Covaleda Salas, B.S., Universidad de los Andes, Colombia

Chair of Advisory Committee: Dr. Susan Payne

Equine infectious anemia virus (EIAV) is an important animal model to study the contribution of macrophages in viral persistence during lentiviral infections. EIAV is unique amongst the lentiviruses in that it causes a rapid, rather than the very slow disease progression, characteristic of other lentiviral infections. The accessory gene, S2, unique to EIAV, is an important determinant in viral pathogenesis. A functional S2 gene is required to achieve high-titer viremia and the development of disease in infected horses. Despite its essential role, the mechanisms by which S2 influences EIAV pathogenesis remain elusive. The goal of this research was to gain insight into the role of S2 in pathogenesis. To accomplish this goal we: (i) Examined the effects of EIAV and its S2 protein in the regulation of the cytokine and chemokine responses in macrophages, (ii) Assessed the influence of EIAV infection and the effect of S2 on global gene expression in macrophages and (iii) Identified host cellular proteins that interact with S2 as a starting point for the identification of host factors implicated in S2 function.

The results from this study provide evidence for a role of S2 in enhancing a pro-inflammatory cytokine and chemokine response in infected macrophages. Specifically, S2 enhances the expression of IL-1α, IL-1β, IL-8, MCP-2, MIP-1β, IP-10 and a newly discovered cytokine, IL-34. Involvement of S2 in cytokine and chemokine dysregulation may contribute to disease development by optimizing the host cell environment to promote viral dissemination and replication. Microarray analyses revealed an interesting set of differentially expressed genes upon EIAV infection. Genes affected by EIAV were involved in the immune response, transcription, translation, cell cycle and cell survival.

Finally, we used the yeast two-hybrid system to identify S2 host cellular interacting proteins. We identified osteosarcoma amplified 9 (OS-9) and proteasome 26S ATPase subunit 3 (PSMC3) proteins as interacting partners of S2. Additional evidence is needed to demonstrate the physiological relevance of these interactions *in vivo*.

In summary, the results from this study contribute towards our understanding of the role S2 in disease expression and allow the formulation of new hypotheses as to the potential mechanisms of action of S2 during EIAV infection.

DEDICATION

To Alejandro

ACKNOWLEDGEMENTS

I would like to thank my committee chair, Dr. Susan Payne, for her encouragement, patience and helpfulness. I feel very lucky to have had the opportunity to join her lab.

Also I would like to thank my committee members, Dr. Judith Ball, Dr. Jane Welsh and Dr. Van Wilson, for their priceless guidance and support throughout the course of this research.

Thanks also go to my friends and lab-mates for making my time at Texas A&M University a great experience.

Finally, I want to thank my husband Alejandro, my mother, father and siblings for their encouragement, love and support.

TABLE OF CONTENTS

LIST OF FIGURES

LIST OF TABLES

CHAPTER I

AN INTRODUCTION TO EQUINE INFECTIOUS ANEMIA VIRUS, THE DISEASE AND THE S2 PROTEIN

History

Equine Infectious Anemia (EIA), also known as "swamp fever", is a worldwide infectious disease that affects members of equine family. Although the disease was first described in France in 1843, it was not until 1976 that the etiological agent, equine infectious anemia virus (EIAV) was classified as a retrovirus (Charman et al., 1976). In 1978 it was classified within the subfamily Lentiviridae (Gonda et al., 1978). EIAV has an important place in the history of retroviruses because it is the (i) first animal disease proven to be caused by a filterable agent (virus) in 1904, (ii) the first retrovirus confirmed to be transmitted by insects (deerflies and horseflies), (iii) the first retrovirus for which antigenic drift was described and (iv) the first retrovirus for which a diagnostic test was approved (Coggins et al., 1972; Kono et al., 1973; Stein, 1942; Vallée H., 1904). The diagnostic test, approved in the 1970s, is an agar-gel immunodiffusion assay commonly known as the Coggins test developed to identify EIAV-infected carrier animals. Although other serologic and PCR based assays have been developed, the Coggins test is the international "gold standard" procedure for routine testing of EIA (Cook et al., 2002; Issel and Cook, 1993; Nagarajan and Simard, 2001).

This dissertation follows the style and format of Virology.

EIAV Transmission and Control

The main route of EIAV transmission is through mechanical transfer of blood by blood-feeding insects such as horse and deer flies (Kemen et al., 1978). EIAV also can be spread by contaminated needles, through semen of an infected stallion or by *in-utero* passage from mare to foal (Kemen MJ Jr, 1972; Metcalf, 2001). Although there is no effective treatment or approved vaccine for EIA, the disease has been successfully managed in most countries by the establishment of mandatory measures to control the spread of disease (Issel et al., 1990). The regulations include: surveillance testing (Coggin's test), mandatory reporting of positive EIAV carriers, life-long quarantine or destruction of infected animals and mandatory testing for imported horses.

EIAV Structure, Genome Organization and Gene Expression

EIAV virions exhibit the morphology and virion organization characteristic of other lentiviruses. As depicted in Fig. 1.1A, EIAV particles have a roughly spherical shape of about 100-200 nm in diameter partly covered by distinctive surface projections, which consist of two viral glycoproteins gp90 and gp45 (Nakajima et al., 1974). The matrix (M) protein lies underneath the viral envelope forming the inner shell, the capsid (CA) protein forms a conical core that surrounds the nuclecapsid (NC) which coats and protects the RNA genome. The genome consists of two identical copies of positive single-stranded RNA, each of which is associated with a molecule of cellular tRNALys3 required as a primer for the initiation of reverse transcription (Arts et al., 1996).

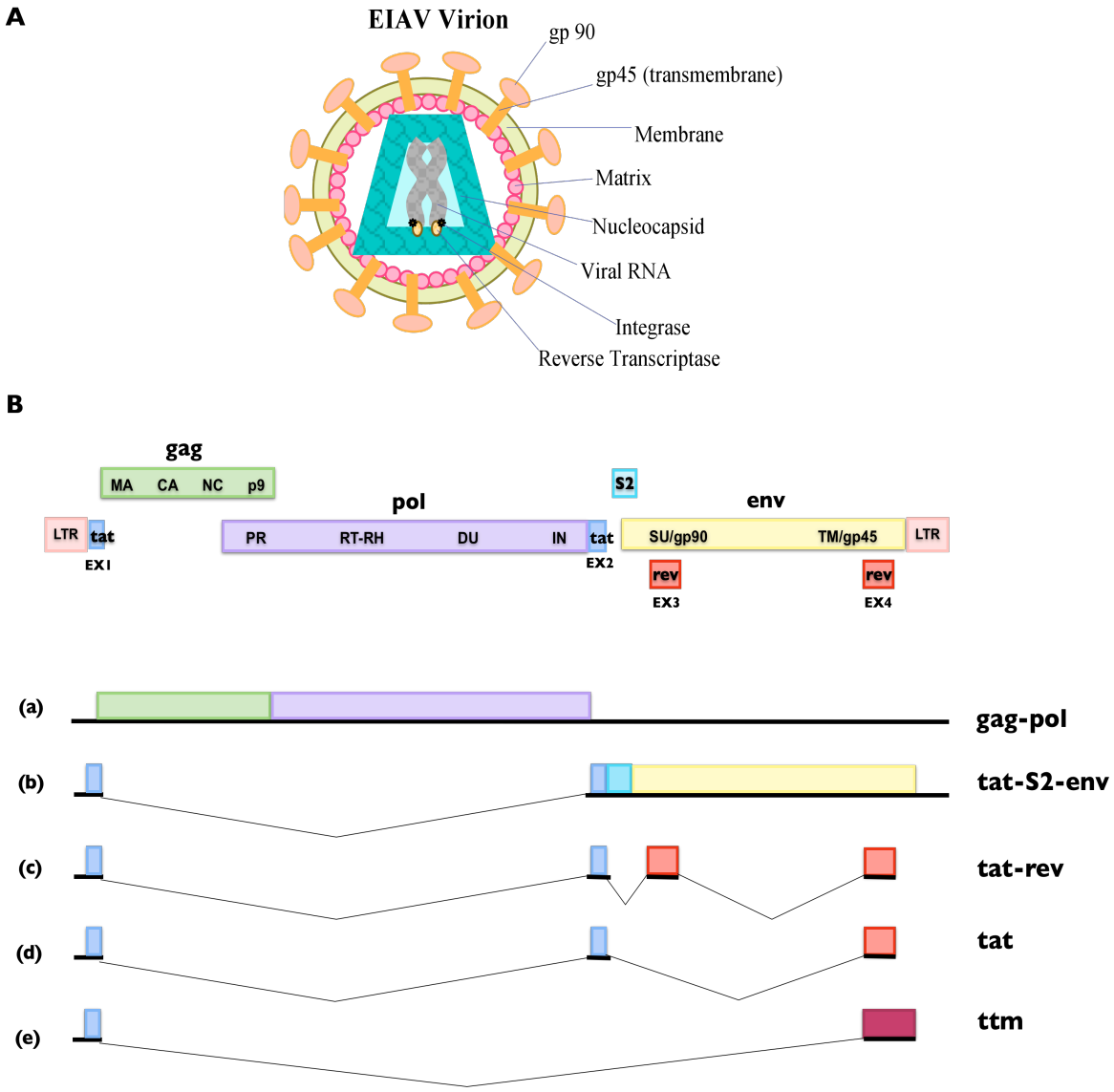

Figure 1.1. EIAV virion, genome organization and transcription map. (A) EIAV virion structure. **(B)** Schematic representation of the EIAV genome and transcripts. The 8.2 kb viral genome encodes the genes *gag*, *pol*, *env*, *tat*, *rev* and *S2*. The major EIAV mRNA transcripts are: (a) an unspliced transcript with a dual role as template for translation of the Gag and Gag-Pol polyproteins or as full-length RNA that is packaged into the virions (b) single spliced transcript that encodes the Tat, S2 and Env proteins, (c,d) multiply spliced mRNAs encoding both the Tat and Rev proteins, and (e) single spliced mRNA that encodes the Ttm protein.

Among the lentiviruses, the EIAV genome is the smallest and genetically the simplest. The EIAV genome is 8.2 kb and contains only 6 genes that are classified into

three categories: structural, regulatory and accessory genes (Fig. 1.1B). The structural genes *gag*, *pol* and *env*, common to all retroviruses, are required for particle formation and replication. The regulatory genes S1 (*tat*) and S3 (*rev*) are essential for viral gene expression and replication both *in vivo* and *in vitro* (de Parseval and Elder, 1999; Miller et al., 2000). The accessory gene S2, whereas dispensable for viral replication *in vitro*, is necessary for robust viral replication and disease expression *in vivo* (Fagerness et al., 2006; Li et al., 1998; Payne, 2006). Long terminal repeat (LTR) sequences present at both the 5' and 3' ends of the proviral genome are involved in controlling viral transcription thus are key players in cell tropism and virulence (Derse et al., 1987; Payne et al., 1999; Payne et al., 2004).

Analyses using several EIAV-specific probes have identified at least 5 specific transcripts that share the same 5' sequences (Maury, 1998). As seen in Fig. 1.1B, the major EIAV mRNA transcripts are: (a) the 8.2 kb unspliced transcript which can either serve as template for translation of Gag and Gag/Pol polyproteins or as genome-length RNA that is packaged into progeny virions, (b) the 3.5 kb, single spliced transcript that encode Tat, S2 and Env, (c,d) the ~ 2 kb, multiply spliced mRNAs that express Tat and Rev, and (e) the single spliced transcript that encodes the Ttm protein (Beisel et al., 1993; Noiman et al., 1990; Schiltz et al., 1992).

Lentiviruses have a distinctive pattern of gene expression that can be separated into early and late phases. Early gene expression is characterized by the appearance of multiply spliced transcripts encoding Tat and Rev proteins. Late gene expression

corresponds to unspliced or partially spliced mRNAs that code for Gag and Gag-Pol structural proteins and the accessory proteins S2 and Ttm (Clements and Zink, 1996).

EIAV transcription is regulated in a cell type and differentiation dependent manner by a complex interplay among cellular transcription factors, the virally encoded transactivator of transcription Tat and the EIAV LTRs (Maury, 1998). The U3 region in the LTR acts as a constitutive viral promoter and contains cis-acting DNA elements that are known to be binding sites for transcription factors such as MDBP, PEA2, Oct, CRE and PU.1 (Carvalho et al., 1993). Studies have shown that PU.1 binding sites in the LTR are critical for EIAV LTR expression in primary macrophages, while in fibroblastic cell lines the PEA2, Oct and CRE binding motifs are important (Hines et al., 2004; Lichtenstein et al., 1999; Maury et al., 2000)

EIAV Proteins and Their Function

Although the EIAV genome contains only 6 genes, it is capable of generating 14 distinct proteins (Table 1.1) by alternative splicing, production of bicistronic mRNA, ribosomal frameshifting, ribosomal leaky scanning mechanisms and proteolytic processing (Carroll and Derse, 1993; Montelaro, 2003; Payne, 2006).

Table 1.1. EIAV structural and regulatory proteins

Gene	Protein	Function
gag	CA (p26)	Capsid protein
	MA (p15)	Matrix protein
	NC (p11)	Nucleocapsid protein
	p9	Critical for virion release
pol	PR (p12)	Protease
	RT (p66/p51)	Reverse transcriptase/RNase H
	DU (p15)	dUTPase
	IN	Integrase
env	SU (gp90)	Surface unit protein
	TM (gp45)	Transmembrane protein
S1	Tat	Transcriptional transactivator
S2	S2	Virulence factor
S3	Rev	mRNA Splicing/nuclear export
	Ttm	Unknown

The *gag* gene encodes the precursor polyprotein $Pr55^{gag}$, which is proteolytically cleaved upon virion maturation by the viral-encoded protease (PR). The cleavage products from the N-terminus are matrix (MA) p15, capsid (CA) p26, nucleocapsid (NC) p11 and p9 (Hussain et al., 1988). The Gag precursor plays an essential role not only in the course of virus assembly but also during the budding process (Leroux et al., 2004).

Even though the *gag* and *pol* genes are in different reading frames, in approximately 5% of Gag translation events, a Gag-Pol polyprotein is made by a -1 ribosomal frameshifting (Chen and Montelaro, 2003). The *pol* gene is expressed as a Gag-Pol precursor protein (Pr180) that is also cleavage by the viral protease into the

mature Gag proteins and into the reverse transcriptase-RNaseH (RT-RNaseH) p66/p51, protease (PR) p12, integrase (IN) and a dUTPase. The EIAV dUTPase is required for productive viral replication in non-dividing cells such as macrophages (Le Grice et al., 1991; Lichtenstein et al., 1995; Threadgill et al., 1993; Wohrl et al., 1994).

The *env* gene, the most variable region of the EIAV genome encodes a glycosylated precursor polyprotein gp135 (Payne et al., 1987). Gp135 has both receptor-binding and fusion activities and is processed by proteolytic cleavage to yield the mature surface glycoprotein gp90 (SU). SU is responsible for recognition of the cell surface receptor (ELR1) and gp45 (TM), a transmembrane protein is essential for membrane fusion (Rice et al., 1990; Sun et al., 2008).

SU is a highly glycosylated and highly variable surface protein (Montelaro et al., 1984). Since SU is a major target of the humoral immune response, these properties allow the virus to evade the immune response by escaping neutralizing antibody recognition (Howe et al., 2002). In fact, neutralizing antibodies are produced to regions that lie predominantly within the variable region in SU (Hussain et al., 1987). In addition to a role in immune evasion, studies have shown that SU is also a virulence determinant (Ball et al., 2005; Payne et al., 2004).

In contrast to other lentiviruses, EIAV is unique in that the TM protein undergoes an additional carboxyl-terminal processing, which yields an N-terminal glycosylated 32kDa (p32) and a non-glycosylated 20kDa (p20) proteins (Rice et al., 1990). Similar to SU, TM is also subject to genetic variation but is not as variable as the SU region (Leroux et al., 1997; Maury et al., 2005).

Tat is an 8 kDa regulatory protein, expressed early in the replication cycle and essential for optimal transactivation of viral gene expression and viral replication (Noiman et al., 1991). In the absence of Tat, most of the viral transcripts are prematurely released from the DNA template, leading to the accumulation of short transcripts and a substantial decrease in the production of fully elongated mRNAs (Maury et al., 1994; Selby et al., 1989). Similar to other known lentiviral Tat proteins, EIAV Tat has a modular structure containing separate RNA-binding and transcriptional activation domains (Derse and Newbold, 1993). Tat binds directly to an RNA stem-loop regulatory element designated TAR (trans-activation-responsive region) present at the 5' end of all nascent viral mRNA transcripts and stimulates transcription elongation by recruitment of the positive transcription elongation factor b (P-TEFb) complex to the TAR element (Anand et al., 2008). P-TEFb recruitment is mediated by the specific interaction of Tat with the Cyclin T1 (CycT1) component of the P-TEFb complex, increasing the affinity of Tat for TAR (Bieniasz et al., 1999). Binding of CycT1 or P-TEFb to TAR does not occur in the absence of Tat (Jing Zhang, 2000). After binding to TAR, Tat induces the kinase activity of the second P-TEFb component, CDK9, a cyclin-dependent kinase to hyperphosphorylate the C-terminal domain (CTD) of RNA polymerase II (Pol II) (Taube et al., 2000). Hyperphosphorylation of Pol II increases its processivity, thus leading to enhanced efficiency of transcriptional elongation of the nascent viral mRNA (Karn, 1999). Tat mediated transactivation increases viral transcription by greater that 100-fold (Garber et al., 1998). Analysis of EIAV Tat associated cellular proteins revealed the presence of at least three unidentified proteins involved in Tat transactivation in addition

of the known CycT1, CDK9 and SF1 (Tat associated cofactor), suggesting there are additional factors that modulate EIAV Tat activity (Sune et al., 2000).

Rev is the second regulatory protein essential for lentiviral gene expression and hence, for viral replication. Similar to Tat, Rev is encoded by a fully spliced transcript and is produced early during the viral replication cycle. EIAV Rev not only functions at the posttranscriptional level by mediating the nuclear export of unspliced and incompletely spliced viral mRNA, but also plays a key role in alternative splicing and viral mRNA stability (Belshan et al., 2000; Martarano et al., 1994). Rev function is critical for the switch in viral gene expression from the early regulatory phase to the late structural phase (Huffman et al., 1999). Since export of cellular mRNAs is tightly controlled by regulating nuclear exit of only fully spliced mRNAs, this poses a problem for lentiviruses that require export of both unspliced and partially spliced viral mRNA from the nucleus to the cytoplasm to serve as template for translation of the structural proteins, S2 and Ttm or to serve as the viral genome (Cullen, 2000). Lentiviruses overcome this limitation by the expression of Rev, the presence of a Rev-responsive element (RRE) within the viral pre-mRNA and the hijacking of cellular mRNA export adaptors (Sandri-Goldin, 2004). The EIAV Rev protein harbors a nuclear localization signal (NLS), a leucine-rich nuclear export signal (NES) and an RNA-binding domain composed of two short discontinuous motifs (Ihm et al., 2009; Lee et al., 2006). Both the NLS and NES domains are essential for Rev function allowing it not only to shuttle in and out of the nucleus but also for the specific interaction with RRE (Stauber et al., 1998). Briefly, the sequential steps involved in Rev- mediated nuclear export are: (a)

binding to the RRE, a specific sequence present in all unspliced and partially spliced viral pre-mRNAs, (b) Rev multimerization, (c) formation of a nuclear export ribonucleoprotein complex composed of Rev-RRE, cellular nuclear export factor (CRM1) and RanGTP, which targets viral mRNA for nuclear export, (d) cargo release in the cytoplasm and (e) Rev recycling whereby Rev is imported back into the nucleus to interact with newly transcribed viral pre-mRNAs (Askjaer et al., 1998; Otero et al., 1998).

S2 is unique to EIAV and does not display significant sequence homology with any other retroviral or cellular protein. S2 gene is located in the *pol-env* intergenic region and encodes a small 65 amino acid, 7 kDa protein. S2 is synthesized at a late phase of the viral life cycle by a leaky ribosome scanning mechanism from either a singly spliced tricistronic mRNA encoding Tat, S2 and Env or from bicistronic mRNA encoding S2 and Env (Carroll and Derse, 1993; Schiltz et al., 1992). Immunolocalization studies suggest that S2 is mainly localized to the cytoplasm with a punctuate pattern towards the perinuclear region. In the same study S2 was found to directly interact with the EIAV Gag precursor *in vitro*, suggesting a role in viral particle assembly, however S2 does not appear to be incorporated into the EIAV particles (Yoon et al., 2000). Antibodies against S2 can be detected in sera from EIAV infected horses indicating that it can elicit a humoral immune response (Schiltz et al., 1992).

Examination of S2 viral sequences from natural or experimentally infected horses during persistent infection reveals a high level of conservation, indicating that S2 plays an important functional role during natural infection (Craigo et al., 2009; Leroux et

al., 2004; Li et al., 2000). As seen in Fig. 1.2, amino acid sequence alignments of available S2 proteins indicate several putatively conserved, well-characterized protein motifs and therefore are presumed to play an important role in S2 function *in vivo*: an N-terminal myristoylation motif (GVTWSA), the nucleoporin motif (GLFG), the nuclear localization signal (RRKQETKK) motif, the proline rich (PxxP) SH3 binding motif, a casein kinase II (CKII) phosphorylation motif and at least two protein kinase phosphorylation sites (Leroux et al., 2004; Li et al., 2000). However, is important to note that the PxxP motif has recently been found to be absent (substitution of the first proline (P) to leucine (L) from a recently characterized virulent field isolate ($EIAV_{PA}$) (Craigo et al., 2009). Analysis of S2 sequences from additional virulent field strains is warranted.

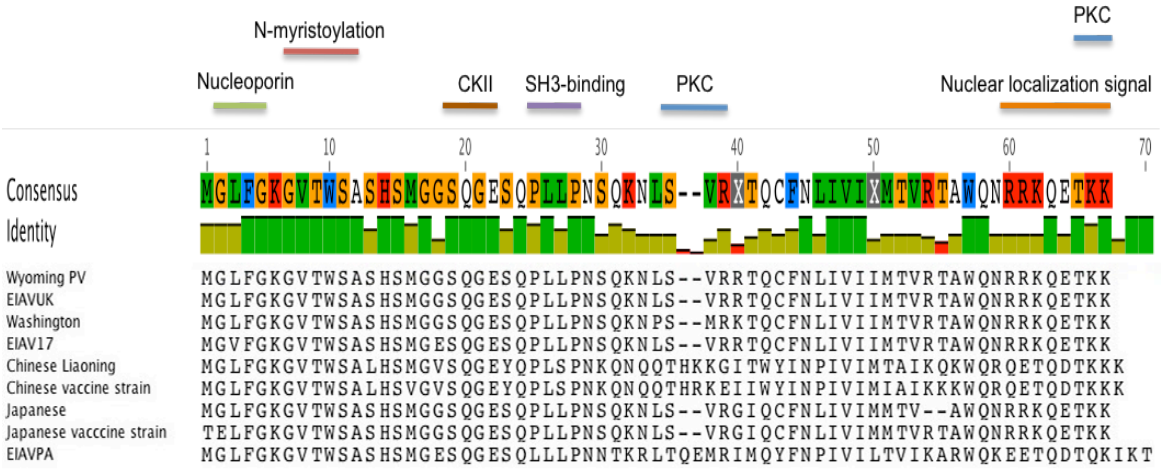

Figure 1.2. Alignment of published EIAV S2 amino acid sequences. The labels to the left indicate the virus isolate designation. The Consensus line shows the amino acid present in the majority of isolates at each position. Below the consensus identity sequence the dark green color indicates that the residue is the same across all sequences, light green indicates less than complete identity and red, very low or no identity. Dashes are use to indicate amino acid deletions in the alignment. Several putative motifs are indicated. Nucleoporin motif, N-terminal myristoylation site, caseine kinase II phosphorylation site, (PXXP) SH3-binding motif, protein kinase C phosphorylation site and the nuclear localization signal.

EIAV Cell Tropism

The identification of macrophages as the predominant cellular targets of EIAV in the natural host came from analysis of tissues from acutely infected horses by direct immunofluoresence and *in-situ* hybridization (McGuire et al., 1971; Sellon et al., 1992). During acute or asymptomatic infection viral DNA and RNA are predominantly detected in mature tissue macrophages of the liver, lymph nodes, kidney, bone marrow and the spleen. The spleen is estimated to contribute to over 90% of the tissue viral burden during acute disease (Harrold et al., 2000; Oaks et al., 1998). In addition, viral RNA has been detected in endothelial cells suggesting that these cells can harbor the virus, but their role or contribution to pathogenesis is unknown (Oaks et al., 1999). Peripheral blood monocytes are susceptible to viral infection but differentiation of monocytes into macrophages is a prerequisite step for active replication (Maury, 1994; Sellon et al., 1992; Sellon et al., 1996). Even though EIAV-infected monocytes do not support productive infection, they may serve not only as a vehicle for viral dissemination to macrophage rich target organs but they also can act as reservoirs for the virus.

In vitro, both wild-type and cell-adapted EIAV strains can replicate in equine monocyte-derived macrophages and tissue macrophage derived from the spleen or bone marrow (Raabe et al., 1998b). In addition, some wild-type isolates of EIAV have been adapted to growth in equine dermis (ED), fetal equine kidney (FEK), feline embryonic fibroblast (FEA), canine D17 osteosarcoma and canine macrophage-like (DH82) cell lines (Bouillant et al., 1986; Carpenter and Chesebro, 1989; Hines and Maury, 2001; Klevjer-Anderson et al., 1979). However, attenuation of wild-type strains has been

reported to occur after repeated passage in cell culture although some strains have been shown to revert to a fully virulent phenotype after serial passages in horses (Carpenter and Chesebro, 1989; Orrego et al., 1982). Recently, an equine macrophage-like cell line that supports propagation of a virulent EIAV strain was characterized (Fidalgo-Carvalho et al., 2009).

Clinical Course of EIAV Infection

Natural or experimental infection of horses with EIAV causes a rapid rather than a very slow disease progression characteristic of most lentiviral infections (Cheevers and McGuire, 1985). As seen in Fig. 1.3, the clinical course of EIAV infection is divided into three distinct stages: acute, chronic and inapparent. The symptoms associated with acute disease usually occur within one to four weeks after infection and are of short duration. Symptoms of acute EIA include fever, depression, rapid weight loss, anemia, thrombocytopenia, and high levels of viremia (Russell et al., 1999).

Some infections progress to chronic EIA, in which infected animals develop recurrent cycles of fever, associated with high viral load and clinical signs similar to the acute phase (McGuire et al., 1990; Sellon, 1993). Recurrences appear during an interval of 6 to 8 months and are interspersed with normal clinical periods (weeks or months). Approximately 8 to 12 months postinfection more than 90% of infected horses progress to a life-long inapparent carrier stage characterized by very low viral loads and lack of clinical signs (Li et al., 2003; Sellon et al., 1994). The inapparent carrier stage seems to be associated with the establishment of a strict immunological control over virus

replication. Inapparent carriers are a constant source of transmission to uninfected horses (Hammond et al., 2000; Issel et al., 1982).

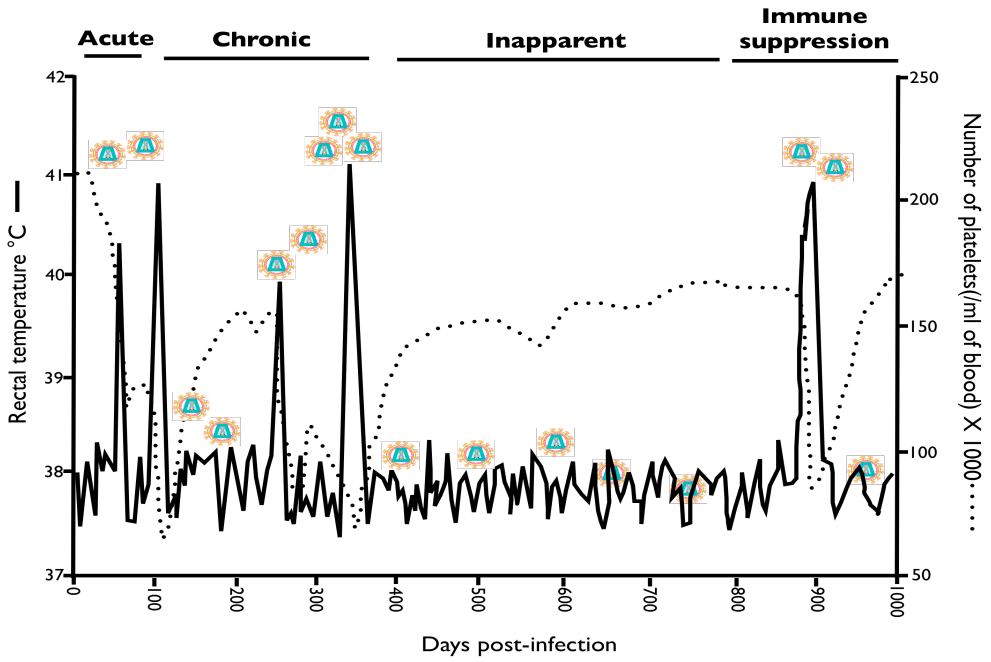

Figure 1.3. Clinical course of EIAV infection (adapted from Leroux et al. 2004).

Cellular, Humoral and Cytokine Responses during EIAV Infection

The success of EIAV persistence is linked to its overall ability to evade the host antiviral defenses by the generation of antigenic variants (quasispecies), which arise mainly through mutation of the *env* gene (Howe et al., 2002; Leroux et al., 1997; Lichtenstein et al., 1996; Montelaro et al., 1984). Each recurrent viremic episode during EIAV infection (chronic phase) is associated with the appearance of antigenic variants (Zheng et al., 1997). The initial humoral response is characterized by a high titer of low avidity antibodies (i.e., poor neutralizing activity). Emergence of quasispecies in

infected animals leads to a delayed production of neutralizing antibodies (6 to 8 months). EIAV-specific cytotoxic T-lymphocytes (CTL) appear within 3 to 4 weeks post-infection and are associated with the resolution of initial viremia (McGuire et al., 2002; Oaks et al., 1998). The inapparent phase is characterized by the presence of high avidity antibodies (i.e., effective neutralizing activity) and high levels of CTL activity to EIAV Gag and Env proteins. Therefore, suppression of viral replication and disease during the inapparent stage of EIAV infection is associated with strong CTL and neutralizing antibody responses (McGuire et al., 2004).

A main feature during lentiviral infection is the dysregulation of the cytokines and chemokines with resulting detrimental effects on the host immune response. During the course of HIV, SIV, and FIV infections, cytokines are known to modulate viral replication, persistence and disease progression in the host. In contrast, the dynamics of the cytokine/chemokine responses during the course of EIAV infection have not been fully determined. It has been shown that early during infection (0.5-1 h post-infection) there is a pro- and anti-inflammatory response to EIAV infection *in vitro*. eMDMs infected with $EIAV_{17}$ display significantly increased expression of interleukin 1 alpha (IL-1α), interleukin 1 beta (IL-1β), interleukin 6 (IL-6), interleukin 10 (IL-10) and tumor necrosis factor alpha (TNF-α) early during infection (0.5-1 h post-infection) suggesting a role of these pro-inflammatory cytokines during the initial response to EIAV infection (Lim et al., 2005). Some studies have reported that during EIAV infection, serum levels of TNF-alpha, transforming growth factor beta (TGF-β) and interferon alpha (IFN-α) are significantly increased and might be associated with the development of

thrombocytopenia in EIAV-infected foals (Tornquist et al., 1997). In addition, increased levels of pro-inflammatory cytokines such as IL-6 and TNF-α are found in the serum of infected ponies and are associated with high levels of viremia (Tornquist et al., 1997).

Changes in cytokine and chemokine levels during the course of EIAV infection could have a major impact in the immune system and may influence pathogenesis by enhancing or suppressing EIAV replication as well as favoring the formation of virus reservoirs.

EIAV S2 Is a Virulence Factor

Although its mode of action is not understood, studies have shown that S2 is essential for maintenance of high viral load and disease expression in the Shetland pony model (Fagerness et al., 2006; Li et al., 2000). The functional role of S2 in EIAV replication was formally assessed *in vitro* by infecting either EIAV permissive cell lines or primary equine monocyte-derived-macrophages (eMDM) with wild-type or S2 mutant proviruses. In these assays, S2 was found to be largely dispensable for viral replication *in vitro*, although its presence may confer a slight growth advantage (Fagerness et al., 2006; Li et al., 1998).

In contrast to the results *in vitro*, the biological importance of S2 in EIAV infection came from two different *in vivo* studies using the Shetland pony model. In the first study (Li et al., 2000), ponies were infected with either $EIAV_{UK,}$ a cell adapted virulent molecular clone or $EIAV_{UK}$ lacking S2. Ponies infected with $EIAV_{UK,}$ experienced a reduction in platelet count compared with ponies infected with the S2-deleted virus, although this was not considered to be clinically relevant. Moreover,

plasma RNA levels were significantly greater in ponies infected with the parental virus compared with the S2-deleted virus, suggesting a role of S2 in viral replication *in vivo*. However, in this study, ponies infected with the $EIAV_{UK}$ virus failed to develop the characteristic clinical signs of EIAV infection such as febrile episodes and thrombocytopenia, making it hard to judge the importance of S2 in disease expression.

In the second study by Fagerness et al. (2006) ponies infected with $EIAV_{17}$, a highly virulent molecular clone, displayed the typical signs of EIA disease, including key features such as: febrile episodes, thrombocytopenia, and high levels of viremia. In contrast, ponies infected with an S2-deleted virus ($EIAV_{17\Delta S2}$) display a decreased viral load and failed to develop any clinical signs of the disease (Fig. 1.4). Taken together, these studies reveal a role for S2 not only for enhancement of viral replication in the infected animal, but also for the development of disease.

Finally, amino acid sequence comparison between the EIAV Japanese virulent strain V70 and the attenuated strain V26 reveals that the initiation codon of S2 is absent in the attenuated virus, likely abolishing the expression of S2. *In vitro*, V26, replicates at high levels but when is used in *in vivo* experiments exhibits a marked reduction in replication, suggesting that S2 is a key determinant of viral replication and pathogenicity *in vivo* (Zheng et al., 2000).

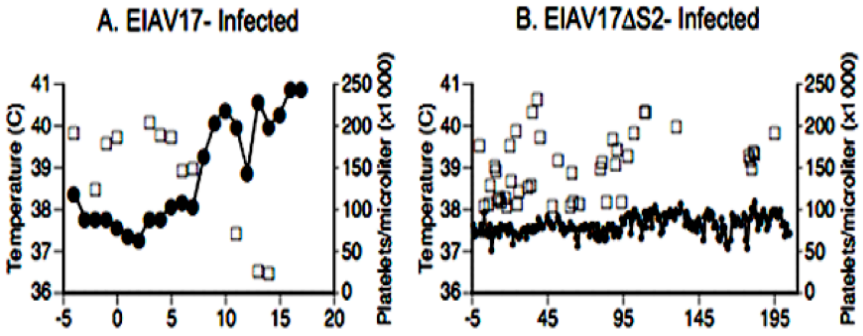

Figure 1.4. Clinical profiles of ponies infected with (A) $EIAV_{17}$ or (B) $EIAV_{17\Delta S2}$. Rectal temperature (●); Platelets (□). Figure courtesy of Dr Susan Payne, Texas A&M University.

EIAV Vaccines

After more than three decades since its classification as a retrovirus, there is still not an U.S. Food and Drug Administration-approved vaccine or treatment for EIAV. Several attempts have been made to develop a safe and effective EIAV vaccine, but have not been successful. However, these studies have been important in understanding the interaction between the immune response and vaccine candidates, which is key to developing an effective EIAV vaccine.

Different vaccine design strategies have been tested. The first vaccine against EIAV, known as the donkey leukocyte-attenuated vaccine (DLV), was developed and has been used in China since the late 1970s. This vaccine was generated by serial passages of the LN40 field isolate first in donkeys and then *in vitro* in primary donkey macrophages (Shen, 1985; Shen et al., 2006). Although the researchers have reported that the vaccine protects horses and donkeys against EIAV infection and is stable and safe for animal use (Wei et al., 2009; Zhang et al., 2007), this vaccine is not acceptable

in most of the countries worldwide. There is the potential risk of this vaccine reverting to virulence, and as would be expected, vaccinated horses will have a positive Coggin's test, making it impossible to distinguish between vaccinated and EIAV infected animals.

An EIAV whole-virus inactivated vaccine and a viral envelope glycoprotein-based subunit vaccine developed by Issel et al. (1992) protected vaccinated ponies after challenge with the homologous EIAV strain but failed to protect them after challenge with a virulent heterologous EIAV strain ($EIAV_{PV}$). In addition, the subunit vaccine had the capability to enhance the disease after challenge with the $EIAV_{PV}$ strain (Issel et al., 1992). Similar results were obtained in animal trials using a baculovirus-expressed recombinant vaccine (rgp90), developed by Wang et al. (1994), where the vaccine failed to protect immunized ponies from infection after challenge with the virulent $EIAV_{PV}$ strain. Moreover, a wide range of clinical signs, from marked exacerbation to no symptoms of the disease, were observed in the vaccinated ponies (Raabe et al., 1998a; Wang et al., 1994). Although it was hypothesized that the antibody response could be responsible for vaccine-induced enhancement of the disease, the authors did not find an association between antibody levels and the exacerbation of the disease.

Recently, an EIAV SU codon-optimized vaccine was also evaluated for its ability to elicit immune responses in immunized ponies (Cook et al., 2005). Immunized ponies were able to elicit a specific humoral and cellular response after immunization with the codon-optimized SU vaccine but similar to the other vaccines, the generated immune response failed to confer effective protection against challenge with $EIAV_{PV}$.

One of the most successful vaccine trials reported was the use of a live attenuated

EIAV proviral vaccine were the S2 gene is mutated ($EIAV_{UK}\Delta S2$) (Li et al., 2003). As mentioned before, absence of S2 has been shown to severely reduce viral replication and disease expression *in vivo* (Fagerness et al., 2006; Li et al., 2000). When used to infect ponies, this vaccine provided protection from infection after challenge with the virulent strain $EIAV_{PV}$. Protection was correlated with the development of both mature Env-specific cellular and humoral responses. Additional trials need to be conducted using different EIAV field isolates to determine if the immune response elicited by this vaccine is able to confer protection against other known EIAV strains.

Significance and Goals of the Study

EIAV serves a valuable animal model not only as a macrophage-tropic lentivirus, but also as a model for host immune control to lentiviral infection. Although S2 has been recognized to play an important role in disease expression since the early 2000's, its mechanism(s) of action are not clearly elucidated. The primary goals of this work were (i) To examine the effects of EIAV and its S2 protein in the regulation of the cytokine and chemokine responses in primary macrophages at different time points post-infection, (ii) To assess the influence of EIAV infection and the effect of S2 on gene expression in primary macrophages and (iii) To identify host cellular proteins that interact with S2 and could act as mediators of S2 function.

CHAPTER II

EIAV S2 ENHANCES PRO-INFLAMMATORY CYTOKINE AND CHEMOKINE RESPONSE IN INFECTED MACROPHAGES✶

Overview

Equine infectious anemia virus (EIAV) infection is distinctive in that it causes a rapid onset of clinical disease relative to other retroviruses. In order to understand the interaction dynamics between EIAV and the host immune response, we explored the effects of EIAV and its S2 protein in the regulation of the cytokine and chemokine response in macrophages. EIAV infection markedly altered the expression pattern of a variety of pro-inflammatory cytokines and chemokines monitored in the study. Comparative studies in the cytokine response between $EIAV_{17}$ and $EIAV_{17\Delta S2}$ infection revealed that S2 enhances the expression of IL-1α, IL-1β, IL-8, MCP-2, MIP-1β and IP-10. Moreover, S2 specifically induced the expression of the newly discovered cytokine, IL-34. Taken together, these results may help explain the effect of cytokine and chemokine dysregulation in EIAV pathogenesis and suggest a role of S2 in optimizing the host cell environment to promote viral dissemination and replication.

✶Reprinted with permission from "EIAV S2 enhances pro-inflammatory cytokine and chemokine response in infected macrophages" by Covaleda, L., Fuller, F.J., and Payne, S.L., 2010. Virology 397 (1), 217-223. Copyright 2010 by Elsevier.

Introduction

Equine Infectious Anemia (EIA), commonly known as swamp fever, is a worldwide disease of equids. The causative agent of EIA is equine infectious anemia virus, or EIAV (genus lentivirus, family *Retroviridae*), closely related to human immunodeficiency virus (HIV). EIAV is transmitted primarily through biting flies, such as the blood-feeding horseflies and deerflies (Foil and Issel, 1991). Natural or experimental infection of horses with EIAV causes a rapid, rather than the very slow disease progression that is characteristic of most lentiviral infections (Cheevers and McGuire, 1985).

The clinical course of EIAV infection is divided into three distinct stages: acute, chronic and inapparent. The symptoms associated with acute disease usually occur within one to four weeks after infection and are of short duration. Symptoms of acute EIA include fever, depression, rapid weight loss, anemia, thrombocytopenia, and high levels of viremia (Oaks et al., 1998; Russell et al., 1999). Some infections progress to chronic EIA, in which infected animals develop recurrent cycles of fever, associated with high viral load and clinical signs similar to the acute phase (McGuire et al., 1990; Sellon, 1993). Recurrences appear during an interval of 6 to 8 months and are interspersed with normal clinical periods (weeks or months).

Approximately 8 to 12 months post-infection, more than 90% of infected horses progress to a life-long inapparent carrier stage characterized by very low viral loads and lack of clinical signs (Li et al., 2003; Sellon et al., 1994). The inapparent carrier stage seems to be associated with the establishment of strict immunological control over virus

replication. Inapparent carriers are a constant source of transmission to uninfected horses (Hammond et al., 2000; Issel et al., 1982).

In addition to encoding the *gag*, *pol* and *env* genes common to all retroviruses, EIAV encodes a dUTPase in the *pol* gene that is required for productive viral replication in non-dividing cells such as macrophages (Lichtenstein et al., 1995; Threadgill et al., 1993). EIAV also encodes four regulatory/accessory proteins: Tat, Rev, Ttm and S2. The S2 gene, located in the *pol*-*env* intergenic region encodes a 65 amino acid 7 kDa protein, which is synthesized in the late phase of the viral life cycle (Carroll and Derse, 1993; Schiltz et al., 1992). S2 is mainly localized in the cytoplasm and may interact with the EIAV Gag precursor in cell culture (Yoon et al., 2000). The S2 open reading frame is highly conserved, being found in all published EIAV sequences, indicating that it carries out a vital function *in vivo* (Leroux et al., 2004; Li et al., 2000). *In vitro*, S2 is not required for viral replication in cultured equine monocyte derived macrophages (eMDM), the natural target for EIAV replication (Li et al., 1998). However, the biological importance of S2 in viral pathogenesis has been demonstrated by experimental infection in Shetland ponies (Fagerness et al., 2006; Li et al., 2000). Ponies infected with a virus derived from the highly virulent molecular clone, $EIAV_{17,}$ experience severe febrile episodes accompanied by a significant decrease in platelet count and an increase in viral load, similar to those seen in natural infection. In contrast, ponies infected with a highly virulent molecular clone lacking a functional S2 protein ($EIAV_{17\Delta S2}$) display a decrease in viral replication and fail to develop any clinical signs of disease (Fagerness et al., 2006). Despite its essential role, the mechanisms by which

S2 influences EIAV pathogenesis are not understood. Since S2 does not display significant sequence homology with any other retroviral or cellular proteins, it has been difficult to predict its mode of action.

Macrophages are considered the predominant cell type for EIAV infection. It has been shown that blood monocytes are permissive for EIAV, but differentiation of monocytes into macrophages is a prerequisite step for EIAV replication (Maury, 1994; Schiltz et al., 1992; Sellon et al., 1996). In addition to the role as reservoirs, infected monocytes may serve as vehicles capable of disseminating the virus to macrophage-rich organs such as the spleen, liver and kidney, which are the primary sites associated with high levels of EIAV replication in persistently infected horses (Oaks et al., 1998). Cells of the monocyte/macrophage lineage play an important role in the immune response against pathogens; these cells produce soluble factors such as cytokines and chemokines, which can orchestrate the immune response to infection.

During EIAV infection, serum levels of tumor necrosis factor alpha (TNF-α), transforming growth factor beta (TGF-β) and interferon alpha (IFN-α) which can act as negative regulators of platelet production are increased before the clinical onset of thrombocytopenia (Tornquist et al., 1997). In addition, eMDMs infected with $EIAV_{17}$ displayed significantly increased expression of interleukin-1 (IL-1) α, IL-1 β, IL-6, IL-10 and TNF-α early during infection (0.5-1 h post-infection) suggesting a role of these pro-inflammatory cytokines during the initial response to EIAV infection (Lim et al., 2005). To examine the underlying immune mechanisms in the pathogenesis of EIAV and

the role, if any, of S2 in modulating this response, we studied the expression profiles of cytokines/chemokines over time in response to EIAV infection in eMDMs.

EIAV serves a valuable animal model not only as a macrophage-tropic lentivirus, but also as a model for host immune control of lentiviral infection. Although S2 is not the sole virulence determinant for EIAV, elucidating the specific role(s) of S2 in disease expression will advance our understanding of the patho-mechanism of lentiviral infection.

Materials and Methods

Monocyte-derived macrophage cell culture

Whole blood was collected from six adult EIA-negative healthy horses and centrifuged at 2100 rpm for 30 min to separate the buffy coat, which was then diluted 1:3 with Hank's balance salt solution (HBBS) containing 2 mM EDTA. Fifteen ml of endotoxin-free Histopaque-1077 (Sigma-Aldrich) was slowly layered underneath 20 ml of diluted buffy coat and centrifuged at 2100 rpm for 30 min at room temperature. Peripheral blood mononuclear cells (PBMCs) were harvested from the interface and washed by centrifugation at 1000 rpm for 10 min at 4 °C in cold entodoxin-free Alsever's solution (0.1M D-glucose, 0.027 M sodium citrate, 0.002 M citric acid, 0.07 M sodium chloride, pH 6.1) containing 1% penicillin-streptomycin, to remove platelets. Residual erythrocytes were lysed by incubation with 5 ml ACK lysis buffer (Invitrogen) for 3 min at 37 °C. After washing three times with 50 ml Alsever's solution, PBMCs were resuspended in RPMI 1640 medium supplemented with 10% heat-inactivated horse serum, penicillin (100 IU/ml), streptomycin (100μg/ml), and L-glutamine (2 mM). For

monocyte isolation by plastic adherence, 12 x 10^6 PBMC per well were seeded into 12-well plates (BD Falcon) and allowed to adhere overnight in a 37 °C humidified 5% CO2 incubator. Nonadherent cells were removed by gently washing the plates, twice, with prewarmed RPMI complete media and the remaining adherent monocyte-enriched cells were allowed to differentiate for a further 48 h before infection. All reagents were screened and found negative for endotoxin and mycoplasma contamination using the Limulus Amebocyte lysate kit (Associates of Cape Cod) and MycoFind Kit (Clongen laboratories) respectively.

Virus preparations

Virus stocks were generated as previously described (Lim et al., 2005). Briefly, D17 cells were transfected with 10 µg of the molecular clones $EIAV_{17}$ or $EIAV_{17\Delta S2}$ plasmids by using the calcium phosphate method and virus particles harvested 72 h post-transfection were used to infected eMDMs. Culture supernatants collected from 7 to 15 dpi, were removed from infected eMDMs and cleared of cell debris by low-spin centrifugation. Virus stocks were assayed for RT activity as a measure of virus replication. Virus stocks were purified and concentrated via ultrafiltration using a Vivaflow 200 tangential flow system with a 100 kDa MWCO filter (Sartorius). After ultrafiltration, maintenance of virus infectivity was confirmed by growth in eMDMs and RT activity. No detectable levels of endotoxin were present in the purified virus stocks. Viral infectious titers were determined by the Reed-Muench formula after infecting eMDMs with 10-fold serial dilutions of the virus in sextuplicates and maintaining the culture for two weeks.

Infection of eMDM

Three days post-plating, eMDM were mock infected (with cell culture media used to grow the cells), infected with $EAIV_{17}$ or $EIAV_{17\Delta S2}$ at a multiplicity of infection (MOI) of 3 to achieve a near synchronous infection. Supernatants and cell extracts were collected from day 1 to 4 post-infection. Virus replication was monitored for RT activity, cytopathic effect (CPE) and viral mRNA transcription in samples collected at various time points post-infection.

RNA isolation and cDNA synthesis

At each time point (1-4 dpi), cells were harvested in RLT buffer (QIAGEN) and cell pellets were stored at -80 °C until ready for RNA isolation. Total RNA was isolated using the RNeasy kit from Qiagen, including DNaseI digestion according to manufacturer's instructions. RNA was further assessed for quality and concentration using the Nano 6000 assay on the Agilent 2100 Bioanalyzer. cDNA was synthesized using the SuperScript Vilo cDNA Synthesis Kit (Invitrogen).

Real time PCR

TaqMan and SYBR Green based assays were used to analyze gene expression levels of 12 selected cytokine/chemokine target genes (Table 2.1). TaqMan real time PCR reactions were performed in a 10 μl total volume containing 0.5 μl of cDNA, 5 μl of EXPRESS qPCR SuperMix with premixed ROX (Invitrogen), 0.5μl of fluorescent primer/probe mix, and 4 μl of DEPC-treated water.

Table 2.1. Sequence of TaqMan primer/probe sets and SYBR Green primers*

Gene	Gene ID #	Primer/probe	Sequence 5'→3'	Product length (bp)
IL-1α	100064969	Forward	CAATATCTTGCGACTGCTGCATTAA	78
		Reverse	CTCTTCTGATGTATAAGCACCCATGT	
		Probe	FAM-ACGCAGTGAAATTT-NFQ	
IL-1β	100034237	Forward	TGTACCTGTCTTGTGGGATGAAAG	93
		Reverse	GCTTTTCCATTTTCCTCTTTGGGTAA	
		Probe	FAM-CCTACAGCTGGAGACAGT-NFQ	
IL-6	100034196	Forward	GAAAAAGACGGATGCTTCCAATCTG	74
		Reverse	TCCGAAAGACCAGTGGTGATTTT	
		Probe	FAM-CAGGTCTCCTGATTGAAC-NFQ	
IL-8	100037400	Forward	GCCACACTGCGAAAACTCA	95
		Reverse	GCACAATAATCTGCACCCACTTTG	
		Probe	FAM-ACGAGCTTTACAATGATTTC-NFQ	
TNF-α	100033834	Forward	TTCTCGAACCCCAAGTGACAAG	65
		Reverse	GCTGCCCCTCGGCTT	
		Probe	FAM-ATGTTGTAGCAAACCC-NFQ	
MCP-1	100034136	Forward	GCGGCCGCCTTCAG	66
		Reverse	GCAGCAGGTGACTGGAGAAT	
		Probe	FAM-CTCAGCCAGATGCAATTA-NFQ	
MCP-2	100033950	Forward	TCACCAGCAGCCAGTGTTC	67
		Reverse	GCACAGATCTCCTTGTCCACTTT	
		Probe	FAM-AAGCTGTGATCTTCAAGACC-NFQ	
MIP-1α	100057909	Forward	TCTGCAGCCAGGTCTTCTCT	61
		Reverse	GAGAAGCAGCAGGCAGTTG	
		Probe	FAM-TCGGCACCGAATGGTA-NFQ	
MIP-1β	100057859	Forward	GCTGGTGGCTGCCTTCTG	87
		Reverse	CGCAGGGTGTAAGAGAAGCA	
		Probe	FAM-CAGCACCAATGGGCTCA-NFQ	
IP-10	100050993	Forward	CAGAGTCCAAGACCGTCAAGAATTT	111
		Reverse	GCCATCCGTATCAGTAGTACCGTAATT	
		Probe	FAM-CAAAGGTCTAAAAGATCTCC-NFQ	
18S	AJ311673	Forward	AAACGGCTACCACATCCAA	54
		Reverse	TCGGGAGTGGGTAATTTGC	
		Probe	FAM-AAGGCAGCAGGCGC-NFQ	
IL-34*	100054703	Forward	TGCCCTTGCTGTAAACATAGC	100
		Reverse	CCACACACTGTGATGATGAGG	
IL-10*	100034187	Forward	GGCAGTGGAGCAGGTGAAGA	79
		Reverse	GATGTCAAACTCACTCATGGCTTT	
18S*	AJ311673	Forward	CACATCCAAGGAAGGCAGCA	66
		Reverse	TTTTCGTCACTACCTCCCCGG	
Beta-actin*	100033878	Forward	TCACGGAGCGTGGCTACAG	63
		Reverse	CCTTGATGTCACGCACGATTT	

SYBR Green real time PCR reactions contained 5 μl of SYBR GreenER™ qPCR with premixed ROX (Invitrogen), 200 nM of the primer mix, and DEPC-treated water. Amplification was carried out using the following parameters: 50 °C for 2 min, 95 °C for 10 min, followed by 40 cycles of 95 °C for 15 s and by 60 °C for 30 s. A dissociation stage was included for SYBR Green real time PCR to confirm the amplification of a single product. All RT reactions, including no-template controls, were run in triplicate on an ABI 7900HT real-time PCR system. Data were collected and analyzed with the SDS 2.3 software.

Data analysis and validation of chemokines TaqMan probes

The Pfaffl method (Pfaffl, 2001) was used to calculate relative fold changes in cytokine/chemokine gene expression between mock-infected and infected samples. Data were first normalized to the endogenous control 18S rRNA or beta-actin and the mock-infected samples from each time point were used as the calibrator control. TaqMan primer/probe sets for IL-1α, IL-1β, IL-6, IL-8, TNF-α and18S have been previously described and validated (Allen et al., 2007). TaqMan primer/probe sets for MCP-1, MCP-2, MIP-1α, MIP-1β, and IP-10, were obtained from Applied Biosystems. TaqMan probes and primers for SYBR Green real time PCR were designed to span at least one exon-exon junction to prevent amplification of genomic sequences. TaqMan probes were 5' labeled with 6-carboxyfluorescein (FAM) and 3' with a nonfluorescent quencher (NFQ). RT-PCR products were separated by 2% agarose gel electrophoresis to confirm product size and specificity of each primer/probe set. Fragments were also analyzed by sequence to validate the identity of the PCR products. PCR efficiency from each

primer/probe set was determined by performing a 6-log dilution range from 3 different cDNA samples. Each dilution was run in triplicate.

Viral RNA expression

SYBR Green real time PCR was used to detect viral transcripts with specific primers (forward 5'-CGGGACAGCAGAGGAGAACT-3' and reverse 5'-CAATCC CTAGAGACCTCAGGAAACAC-3') spanning the splice site used to generate the single spliced, tricistronic mRNA that encodes Tat, S2 and Env. In addition, specific primers bearing the S2 mutation (forward 5'-AACACAGGAGGACAGGAAGCA-3' and reverse 5'- TTACCCCTTTACCAAATACTCCCATA-3') were used to screen for contamination with wild-type sequences.

Statistical analysis

Fold changes for each cytokine/chemokine mRNA response were normalized by log-2 transformation prior to statistical analysis (data were not normally distributed). Transformed data were then analyzed using the Linear Mixed Model (LMM) (Repeated Measures - Type III sum of squares and diagonal repeated covariance) procedure for comparisons of changes in gene expression among treatments and across time. In this analysis, "horse" is considered the random factor and "day", "treatment" and "day x treatment" interactions considered as the fixed factors. The transformed fold changes corresponded to the response variable. This analysis allows for unsystematic variability of the data and provides greater power to detect effects. In this method, the covariance of errors is estimated and then used to constrain the error covariance matrix to derive the mean squares estimates of the effects. This method provides a way for modeling error

structures among the repeated dependent variables and avoids Type I errors, it is also used for unbalanced sets of data. In addition, independent t-tests were conducted on each separate date to compare mean values between $EAIV_{17}$ versus mock infected control, $EAIV_{17}$ versus $EIAV_{17\Delta S2}$ and $EIAV_{17\Delta S2}$ versus mock-infected control and to determine differences in gene expression that occurred across treatments on each day. The statistical package SPSS 15.0 (SPSS Inc. 2007) was used to perform these analyses. All data were expressed as mean value (log2) ± S.E.M. Results were considered significantly different when $p < 0.05$.

Results

Assay validation

PCR efficiency for each primer/probe set was determined from the slope of the standard curve generated from the serial dilutions of cDNA. A standard curve slope of -3.32 indicates a PCR reaction with 100% efficiency. Generally, efficiency between 90-110% is considered acceptable. For all the primer/probe sets, PCR efficiencies ranged between 93 and 105%. Moreover, the R^2 and standard deviation for each primer/probe set was >0.99 and ≤0.13 respectively, indicating overall assay precision (Table 2.2). To account for differences in PCR efficiencies, the Pfaffl method was used to determine the relative expression of the target genes (Pfaffl, 2001). A single band of expected size was obtained using each primer/probe set (Fig. 2.1). In addition sequence analysis confirmed the amplification of the target sequences (data not shown).

Table 2.2. Validation TaqMan primer/probe sets and SYBR Green primers*

Target Gene	PCR efficiency		
	Mean slope	%	R^2
MCP-1	-3.34±0.05	99	0.99
MCP-2	-3.34±0.11	99	1
MIP-1α	-3.31±0.03	100	1
MIP-1β	-3.19±0.13	105	1
IP-10	-3.27±0.06	102	0.99
IL-10*	-3.26±0.00	102	0.99
IL-34*	-3.48±0.07	93	0.99
18S*	-3.35±0.00	99	0.99
Beta-actin*	-3.28±0.03	101	0.99

Note: TaqMan primer/probe sets for IL-1α, IL-1β, IL-6, IL-8, TNF-α and18S have been previously described and validated (Allen et al., 2007).

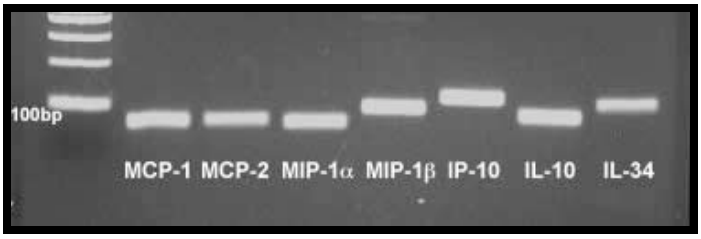

Figure 2.1. Validation real time PCR products. Products were analyzed by agarose gel electrophoresis to verify amplification of single products of the expected size. The 100 bp ladder is in lane 1.

Viral infectivity and mRNA expression

Viral infectivity of the purified stocks was verified by reverse transcriptase assay. Viral stocks remained infectious after purification and concentration and showed similar replication kinetics at an MOI of 3 (Fig. 2.2A). These data are in agreement with previously published reports that S2 is not required for efficient EIAV replication in cultured cells. During the course of EIAV infection in eMDMs, we also monitored the levels of viral transcription by real time PCR. As shown in Figure 2.2B, delta cycle

threshold (ΔCt) values were gradually decreased over time, indicating an increase in viral gene transcription. No differences in the levels of viral transcripts were observed between wild-type and S2-deleted viruses during the cytokine/chemokine time course experiment. Moreover, no evidence of contamination with wild-type sequences was observed during infection with the mutant virus (Fig. 2.3).

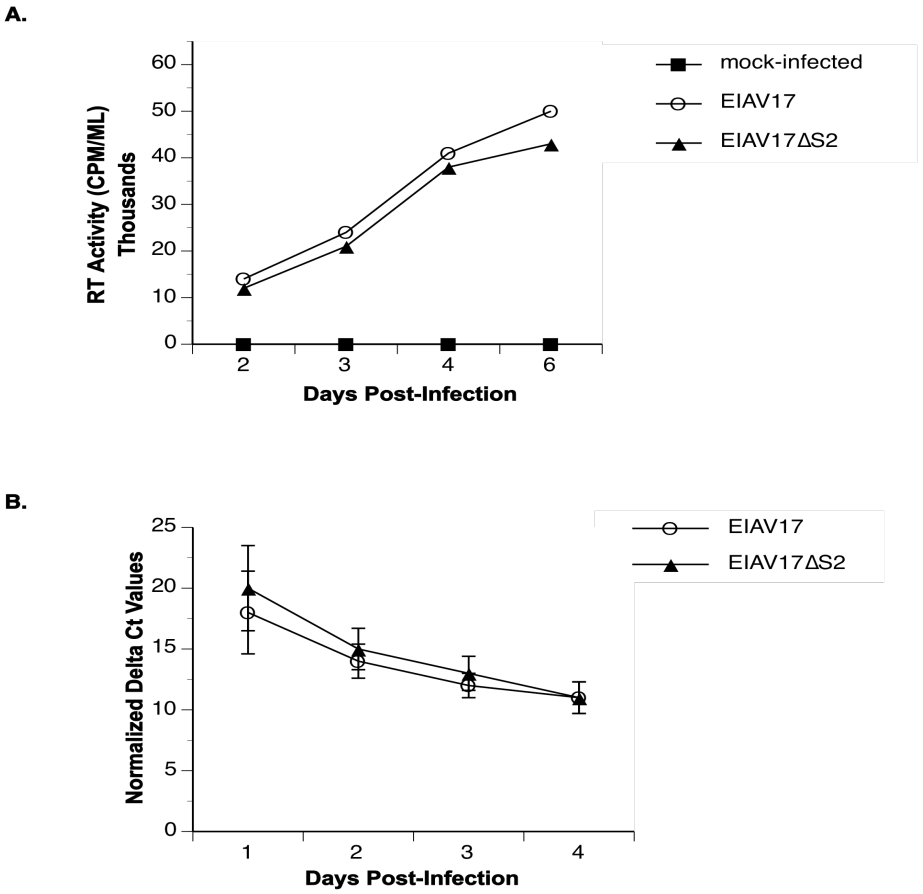

Figure 2.2. (A) Growth kinetics of viral stocks. eMDMs were infected at a multiplicity of infection (MOI) of 3 with $EIAV_{17}$ (○), $EIAV_{17\Delta S2}$ (▲), or mock-infected (■). Culture media were harvested at the indicated time points after infection and viral replication was monitored by measurement of reverse transcriptase (RT) activity. **(B)** Real time PCR detection of viral mRNA transcripts during the experiment depicted in Figure 2. Three sets of eMDM cells were infected with $EIAV_{17}$ (○) or $EIAV_{17\Delta S2}$ (▲) at an MOI of 3. RNA from infected cells were collected at the indicated time points then subjected to reverse transcription and amplified in the presence of EIAV specific primers. Viral mRNA was normalized against 18S mRNA levels. The error bars indicate the standard deviation from three horses (n =3). The data shown in Panels A and B are from separate experiments.

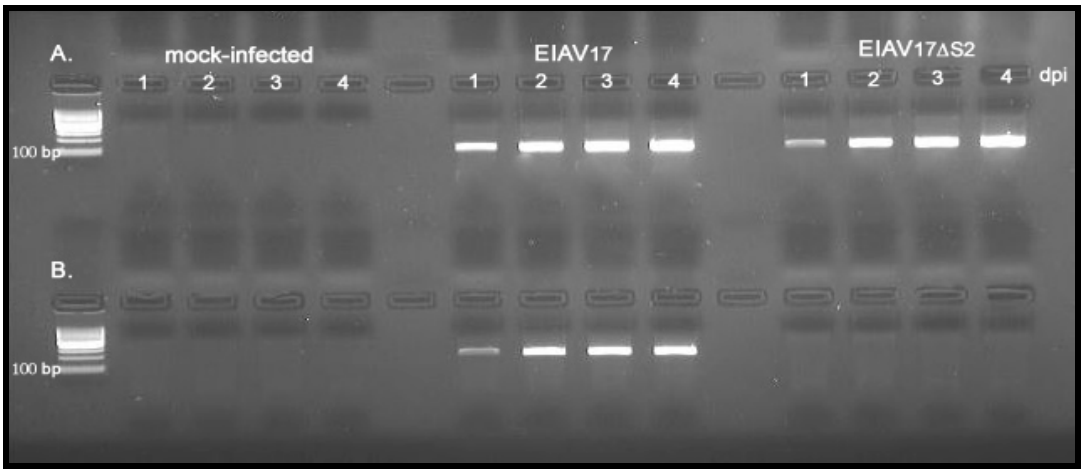

Figure 2.3. Detection of EIAV viral transcripts. (A) PCR with specific primers spanning the splice site used to generate the single spliced, tricistronic mRNA that encodes Tat, S2 and Env. **(B)** PCR with specific primers bearing the S2 mutation, used to screen for contamination of wild-type sequences. The 100 bp ladder is in lane 1. PCR was performed 1-4 days post-infection.

Cytokine/chemokine expression in EIAV infected eMDMs

To study the expression profiles of a set of equine cytokines and chemokines in response to EIAV infection and examine the role of S2 in regulating this response, we monitored the mRNA expression of 12 cytokines known to play a role in the immunopathogenesis of retroviral infections. As shown in Figure 2.4, there was a clear effect in the cytokine and chemokine mRNA levels in response to EIAV infection. Analysis of the expression data (Table 2.3) shows that following $EIAV_{17}$ infection, there was a statistically significant increase ($p < 0.05$) in the expression of IL-1β, IL-8, IL-34 and MCP-2 from days 1 to 4 post-infection compared with the mock-infected control. Levels of TNF-α, MCP-1, MIP-1β and IP-10 mRNA were significantly upregulated from day 2 to 4 days post-infection. IL-6 and MIP-1α were only induced significantly above the baseline levels at days 3 and 4 post-infection. Also, during the first 3 days

post-infection, the levels of IL-1α were significantly increased relative to the control. There was not a statistically significant difference in the expression of IL-10 at any of the time points examined, although there was a subtle decrease in expression compared with the control (Fig. 2.4).

Comparative analysis in the cytokine response between the wild-type virus and the S2-deleted virus showed that there is a pattern of enhancement in the cytokine/chemokine response in eMDMs infected with the wild-type virus (Fig. 2.4). There was a statistically significant difference in gene expression of IL-8 and MCP-2 from day 1 to 3 post-infection ($p < 0.05$) between the $EIAV_{17}$ and S2 mutant viruses. Moreover, levels of IL-1α and IL-1β mRNA were significantly increased in cells infected with $EIAV_{17}$ compared with S2-deleted virus at day 2, MIP-1β at day 3 and IP-10 at days 2 and 3 post infection (Table 2.3).

In the course of studying cytokine and chemokine profiles during EIAV infection, IL-34 was identified in an equine oligo microarray study to be upregulated upon EIAV infection (unpublished data). Therefore, we examined the gene expression profile of this newly discovered cytokine. When eMDMs were infected with the wild type virus, IL-34 was upregulated more than 2-fold during the course of the infection with significant differences in gene expression compared with mock-infected or $EIAV_{17\Delta S2}$ infected cells ($p < 0.01$) at all time points tested. Moreover, in contrast to other tested genes, IL-34 mRNA levels in cells infected with $EIAV_{17\Delta S2}$ were similar to those observed in mock-infected control at all time points.

Table 2.3. Comparison of cytokine/chemokine gene expression in $EIAV_{17}$ and $EIAV_{17\Delta S2}$ infected eMDM

Cytokine	$EIAV_{17b}$ vs $EIAV_{17b\Delta S2}$											
	1dpi			2dpi			3dpi			4dpi		
	$Mean_{17b}$	$Mean_{\Delta S2}$	*p* value	$Mean_{17b}$	$Mean_{\Delta S2}$	*p* value	$Mean_{17b}$	$Mean_{\Delta S2}$	*p* value	$Mean_{17b}$	$Mean_{\Delta S2}$	*p* value
IL-1alpha	**1.39**	0.63	0.101	**1.04a**	0.27b	0.024	**1.65**	0.93	0.203	1.52	0.92	0.442
IL-1beta	**2.17**	**1.56**	0.103	**2.31a**	**1.28b**	0.000	**1.83**	**0.93**	0.060	**1.79**	0.90	0.280
IL-6	0.15	-0.08	0.337	0.44	0.20	0.327	**0.93**	0.33	0.138	**1.58**	0.98	0.334
IL-8	**1.68a**	**1.00b**	0.011	**2.45a**	**1.36b**	0.000	**3.39a**	**2.05b**	0.018	**4.25**	**3.32**	0.278
IL-10	0.05	0.32	0.689	-0.22	0.05	0.675	-0.83	-0.32	0.331	-0.32	-0.53	0.630
IL-34	**0.91a**	0.22b	0.005	**1.30a**	0.23b	0.008	**1.20a**	-0.14b	0.000	**1.36a**	0.14b	0.006
TNF-alpha	0.22	-0.03	0.086	**0.56**	0.27	0.159	**0.70**	0.32	0.216	**1.13**	0.64	0.315
MCP-1	0.48	0.40	0.456	**0.87**	0.60	0.421	**0.95**	0.53	0.290	**0.88**	0.64	0.572
MCP-2	**1.65a**	**0.75b**	0.020	**2.66a**	**1.29b**	0.001	**3.03a**	**1.47b**	0.008	**3.65**	**2.31**	0.072
MIP-1alpha	-0.10	-0.20	0.642	0.26	0.12	0.619	**0.90**	0.32	0.099	**1.59**	0.98	0.157
MIP-1beta	0.14	-0.02	0.554	**0.70**	0.37	0.139	**2.06a**	**1.14b**	0.050	**3.50**	**2.61**	0.172
IP-10	0.47	0.47	0.995	**1.98a**	**0.87b**	0.003	**2.68a**	0.86b	0.016	**4.45**	2.58	0.258

Values represent the mean log2 fold change of infected relative to mock-infected control. Independent t-tests were conducted to compare mean values for $EIAV_{17}$ vs mock infected control ($Mean_{17}$ column), $EIAV_{17\Delta S2}$ vs mock infected control ($Mean_{17\Delta S2}$ column) and $EIAV_{17}$ vs $EIAV_{17\Delta S2}$. Bolded values indicate statistically significant ($p < 0.05$) changes in gene expression compared to the control (control values are constant and are not presented in the table; *p*-values for these comparisons are not presented in the table). Different letters indicate significant differences between $EIAV_{17}$ and $EIAV_{17\Delta S2}$. Results were considered significantly different when $p < 0.05$. *p*-values shown in the table describe the $EIAV_{17}$ vs $EIAV_{17\Delta S2}$ comparison.

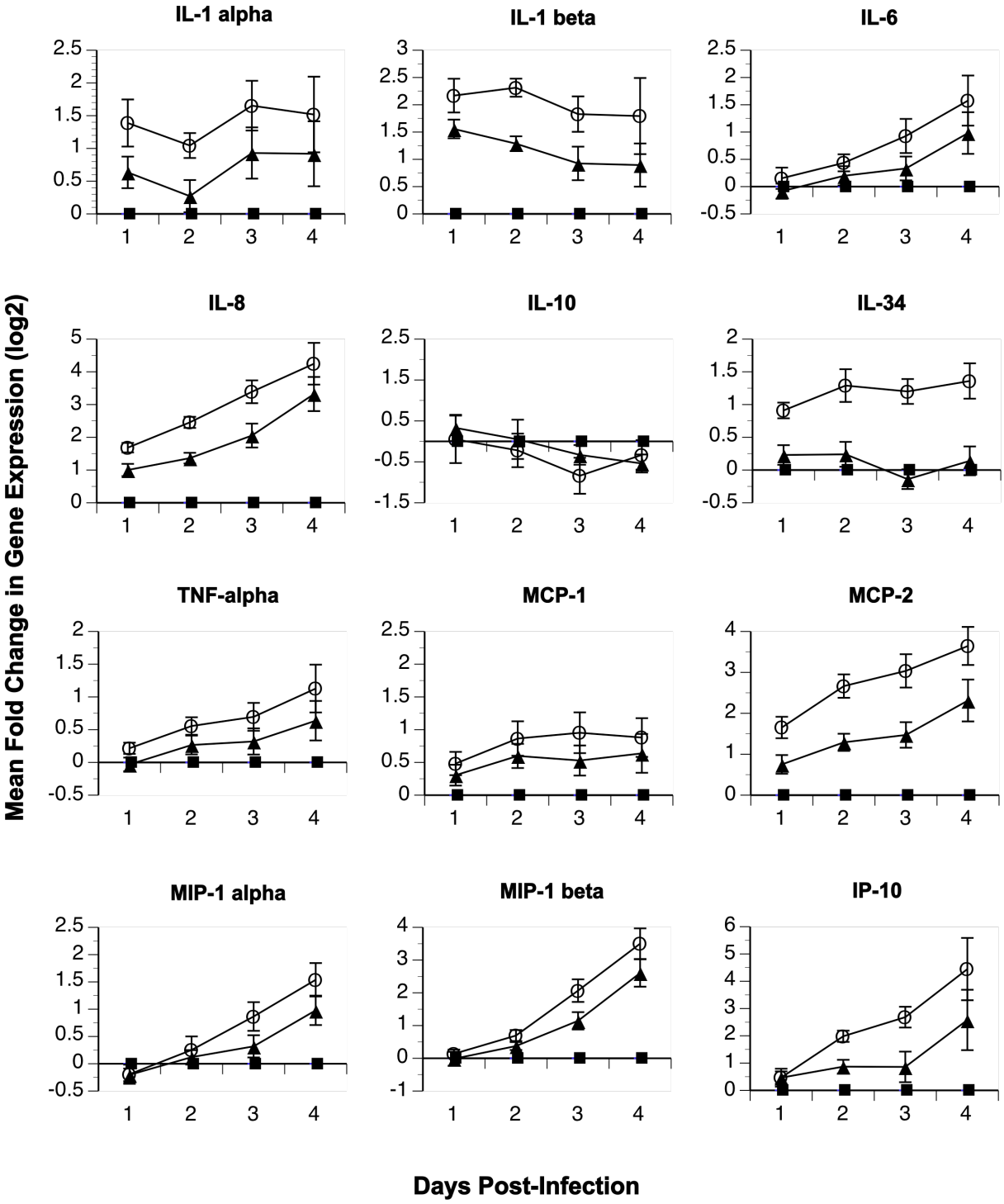

Figure 2.4. Time course of cytokine/chemokine mRNA expression in infected eMDM. $EIAV_{17}$ (○), $EIAV_{17\Delta S2}$ (▲), or mock-infected (■). Data was analyzed using the Pfaffl method (Pfaffl, M.W. 2001). All values were normalized to the endogenous control 18S or b-actin, and represent the log2 mean fold change in expression (relative to mock-infected control). Error bars represent ± SEM from six different horses (n =6).

Since out-bred horses were used in the study (n=6), there was considerable donor to donor variation in the cytokine response to EIAV infection. The greatest donor to donor variability in the response between $EIAV_{17}$ and $EIAV_{17\Delta S2}$ was observed at day 4 post-infection. Thus, although there was not an overall statistically significant difference in the induction of IL-8, MCP-2, MIP-1β and IP-10 between the two viruses at day 4 post-infection, there was a marked difference in the response among horses. For example, IP-10 gene expression varied from 1 to 18 fold in cells infected with $EIAV_{17}$ compared with $EIAV_{17\Delta S2}$ (data not shown).

Examining the kinetics of gene expression shows that IL-6, IL-8, TNF-α, MCP-2, MIP-1α, MIP-1β and IP-10 upregulation was minimal early during infection but gradually increased until the last time point examined. Levels of IL-1β were gradually decreased over time but significantly higher than the control at day 4 post-infection. IL-34 transcripts levels were significantly upregulated early in infection and remained steady during the course of infection. For IL-10 there was a subtle, although not statistically significant decrease in expression relative to the control. No significant changes in MCP-1 expression were detected over time (Fig. 2.4).

To clearly delineate the effect of S2 in cytokine dysregulation, we also analyzed the overall cytokine and chemokine response during EIAV infection. Similarly, the results showed that there is a significant effect of EIAV infection in the cytokine/chemokine response in eMDM (Fig. 2.5).

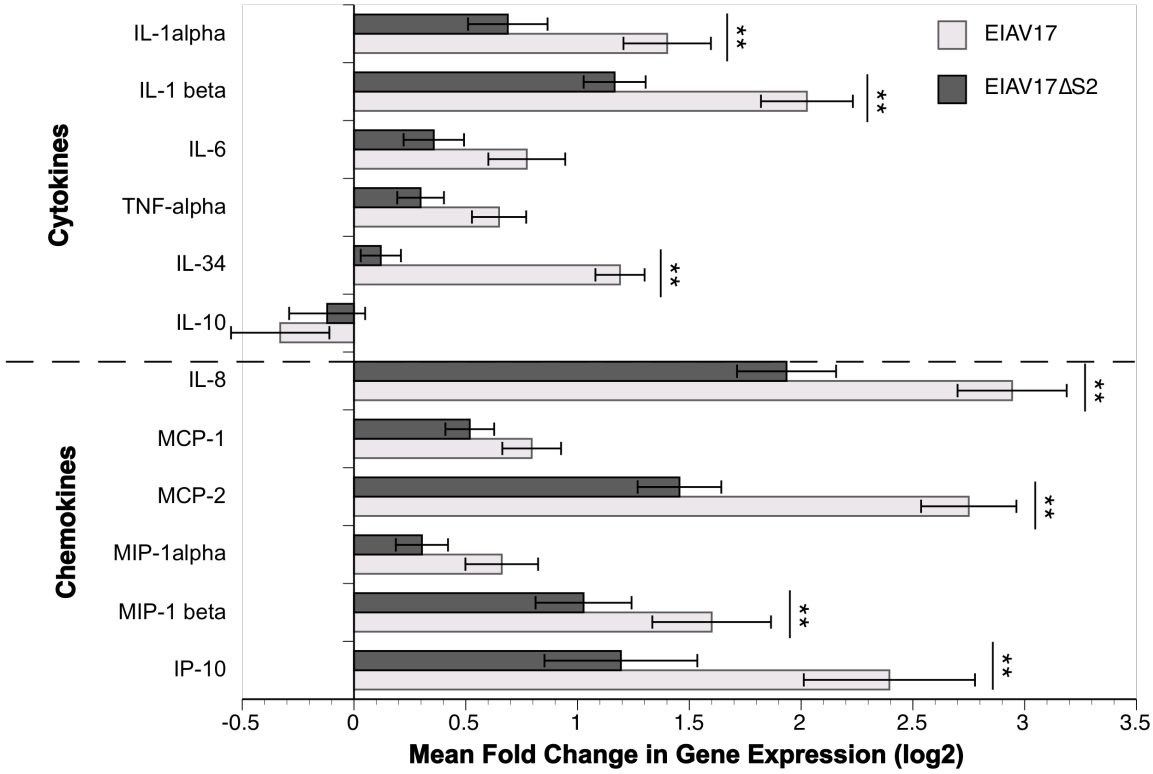

Figure 2.5. Overall cytokine and chemokine expression of eMDM infected with $EIAV_{17}$ (▒) or $EIAV_{17\Delta S2}$ (■). Bars represent the overall mean log2 fold change in expression relative to mock-infected control; mean was obtained by using means per date divided by the number of observed dates. Error bars represent ± SEM from six different horses (n =6). Linear mixed model (LMM) was used to determine whether or not significant differences occurred. **, indicates $p < 0.01$.

eMDM infection with $EIAV_{17}$ significantly upregulated the mRNA expression of IL-1α and β, IL-6, IL-8, IL-34, TNF-α, MIP-1β, MCP-1, MCP-2 and IP-10 ($p = 0.00$) and MIP-1α ($p = 0.02$) relative to the mock-infected cells. Moreover, the presence of S2 strongly enhanced mRNA expression of IL-1α, MIP-1β, IP-10 ($p = 0.01$), IL-1β, IL-8, IL-34 and MCP-2, ($p = 0.00$) compared with the $EIAV_{17\Delta S2}$ virus. However, the levels of IL-6, IL-10, TNF-α, MCP-1 and MIP-1α showed no statistically significant changes overall during infection ($p > 0.05$) compared with S2 deleted virus.

Discussion

A main feature of lentiviral infection is dysregulated expression of cytokines and chemokines. During the course of HIV, SIV, and FIV infections, cytokines are known to modulate viral replication, persistence and disease progression in the host (Dean and Pedersen, 1998; Kedzierska et al., 2003; Orandle et al., 2001). The modulation of the cytokine/chemokine response during the course of EIAV infection has not been as fully elucidated. It has been shown that early during infection (0.5-1 h post-infection) there is a pro- and anti-inflammatory response to EIAV infection *in vitro* (Lim et al., 2005), however the dynamics of cytokine response during the course of EIAV replication in horses is unknown. Changes in cytokine and chemokine levels during the course of EIAV infection could have a major impact on the immune system, influencing pathogenesis by enhancing or suppressing EIAV replication as well as favoring the formation of infected cell reservoirs. We undertook this study to further examine the effect of EIAV in modulating the cytokine and chemokine response in macrophages during the course of infection and to determine if the EIAV S2 protein has a role in modulating this response. Our results confirm that EIAV induces a strong pro-inflammatory response in eMDM and that S2 enhances this response. In light of the clearly demonstrated role of S2 in disease expression (Fagerness et al., 2006; Li et al., 2000) it is possible that a robust pro-inflammatory response is advantageous for the virus in the infected animal. In fact, pro-inflammatory cytokines/chemokines such as IL-1, IL-6, IL-8, TNF-α and IP-10, among others are known to stimulate HIV replication (Ott et al., 1998; (Lane et al., 2003).

In the current study we show significantly increased levels of TNF-α, IL-1α, IL-1β, IL-6, IL-8, IP-10, IL-34, MCP-1, MCP-2, MIP-1α and MIP-1β in EIAV-infected eMDM relative to uninfected controls. These results correspond to studies of EIAV infected foals where increased levels of TNF-α and IFN-α are found in association with high levels of viremia and are increased in the serum and bone marrow just before the onset of thrombocytopenia (Tornquist et al., 1997). IL-1 β and IL-8 are also associated with marked thrombocytopenia (Bozza et al., 2008); whether or not dysregulation of these cytokines contributes to the development of thrombocytopenia during EIAV infection needs to be determined.

IL-10 was the only anti-inflammatory cytokine monitored in the study. IL-10 strongly inhibits the production of a wide variety of inflammatory mediators in macrophages, T cells and B cells (de Waal Malefyt et al., 1991; Moore et al., 2001) and IL-10 decreases HIV replication in macrophages (Akridge et al., 1994). In our study IL-10 expression was not increased by EIAV infection; in fact there was a subtle decrease relative to the control. This result corroborates our findings that EIAV replication favors the induction of a pro-inflammatory response and that at least during the first days post-infection, this response is unlikely to have an antiviral effect.

EIAV infection also strongly stimulated gene expression levels of the chemokines IP-10, IL-8, MCP-1, MCP-2, MIP-1α and MIP-1β during the course of infection. The up-regulation of chemokine levels during EIAV infection could explain the accumulation of lymphocytes and macrophages in the spleen, lymph nodes, lungs and other tissues in EIAV infected horses (McGuire et al., 1990) and could play an

important role in disease progression. Increased IP-10 and IL-8 expression during HIV infection stimulates viral replication in macrophages and T cells (Lane et al., 2003; Lane et al., 2001). Moreover, dysregulation of theses chemokines have been implicated in the intensity and progression of HIV disease (Kinter et al., 1998; Reinhart, 2003; Schmidtmayerova et al., 1996).

Although MIP-1α and MIP-1β are closely related pro-inflammatory chemokines, they have distinctive biological properties. Both strongly induce chemotaxis of monocytes and macrophages and are potent pyrogens (Maurer and von Stebut, 2004; Menten et al., 2002; Minano et al., 1996). MIP-1α but not MIP-1β suppresses cell proliferation of granulocyte-macrophage (CFU-GM), erythroid (BFU-E) and multipotential (CFU-GEMM) progenitors from bone marrow cells *in vivo* and *in vitro* (Maze et al., 1992). Interestingly, MIP-1β acts specifically to block the inhibitory effect of MIP-1α, suggesting a synergy between these two chemokines to regulate proliferation of myeloid progenitor cells (Broxmeyer et al., 1993; Broxmeyer et al., 1991).

Analysis of the role of S2 in cytokine/chemokine expression indicates that S2 plays an overall enhancing role in the upregulation of proinflammatory cytokines and chemokines. S2 had a significant effect on expression of IL-1α, IL-1β, MIP-1β, IP-10, MCP-2, and IL-8. The difference in expression levels between S2-deleted and the parental virus was not significant for IL-6, TNF-α or MIP-1α, although cytokine expression was somewhat decreased for the S2-deleted virus. These results, together with *in vitro* studies of Lim et al. (2005) that describe a role for EIAV SU in the induction of proinflammatory cytokines in eMDM, and Payne et al. (Payne et al., 2004)

and Fagerness et al. (2006) that reveal roles of SU and S2 respectively in disease expression suggest a scenario whereby EIAV SU and S2 act in concert to produce a robust proinflammatory cytokine response that promotes vigorous virus replication, fever and thrombocytopenia.

IL-34 is a newly discovered cytokine without significant amino acid sequence homology to other cytokines or proteins. IL-34 is expressed in a wide variety of tissues including liver, kidney, thymus, brain and spleen. *In vitro*, IL-34 specifically binds to monocytes and stimulates their proliferation and/or survival. In addition, IL-34 promotes the differentiation of bone marrow cells into a macrophage progenitor known as colony-forming unit-macrophage (CFU-M), which in turn give rise to a homogenous population of macrophages (Lin et al., 2008). At the amino acid sequence level, equine IL-34 shares 85%, 75% and 71% pairwise sequence identity with bovine, human and mouse respectively.

Our results clearly showed that EIAV infection of eMDM increased the expression of IL-34. Since the S2-deleted virus failed to increase the mRNA levels above the baseline, this indicates a specific role for S2 in the upregulation of mRNA levels of this cytokine during infection. Interestingly, among all the cytokines and chemokines tested, IL-34 was the only cytokine to be solely affected by the presence of S2. These data underline the need for additional studies to determine the role, if any, of S2 in monocyte proliferation and survival through upregulation of IL-34 expression particularly as monocyte differentiation into macrophage is a prerequisite for a productive EIAV infection. Interestingly, IL-34 promotes the formation of

monocyte/macrophage lineage cells in the bone marrow, so it will be worth testing whether or not S2 has an essential role in regulating the proliferation of macrophage progenitors. A modulation of monocyte/macrophage lineage proliferation could in turn increase the pool of target cells available for infection having a profound effect in the pathogenesis of EIAV infection. In contrast with HIV, SIV and FIV infection where there is a suppression of bone marrow granulocyte/macrophage progenitor cells (Linenberger et al., 1991; Prost et al., 2008; Steinberg et al., 1991), EIAV is unique in that during the course of infection there is not an apparent inhibitory effect in the formation of granulocyte/macrophage progenitor cells (Swardson et al., 1992).

In summary, our study indicates that S2 is not solely responsible for the modulation of the cytokine responses during EIAV infection but supports the possibility of S2 as a contributing factor in cytokine dysregulation, exacerbating disease progression. Cytokine enhancement by S2 may promote a suitable cellular environment that is likely to promote viral replication and dissemination, having a major impact in viral pathogenesis and disease progression.

CHAPTER III

PROBING THE FUNCTION OF THE EIAV S2 PROTEIN USING AN EQUINE WHOLE GENOME OLIGONUCLEOTIDE ARRAY

Overview

EIAV is a macrophage-tropic lentivirus that causes persistent infection in horses. Studies have shown that the EIAV accessory protein S2 makes an important contribution to virulence, but the mechanism by which S2 modulates pathogenesis remains unclear. Ponies infected with the highly virulent molecular clone $EIAV_{17}$ experience severe febrile episodes accompanied by a significant decrease in platelet numbers and a high viral load, as seen in natural infections. In contrast, ponies infected with a deleted-S2 virus, $EIAV_{17\Delta S2}$, display reduced virus replication and fail to develop disease. In this study we used an equine whole genome oligonucleotide array to identify genes and predict cellular processes that are affected during infection of primary macrophages with virulent EIAV and to compare those with macrophages infected with an S2-deleted virus. Microarray data revealed 106 genes that were differentially expressed (compared with mock-infected) following infection with virulent EIAV. Comparison of virulent EIAV to the S2-deleted virus revealed 273 differentially expressed genes. Differentially expressed genes included those involved in immune response, transcription, translation, cell cycle and cell survival. Microarray results were validated for selected genes by quantitative real time PCR.

Introduction

EIAV is a lentivirus of the family *Retroviridae* that naturally infects horses and induces a disease characterized by three distinctive stages: acute, chronic and innaparent (Cheevers and McGuire, 1985). The acute stage occurs within a week to a month from the initial exposure, which is relatively fast compared with other lentiviral infections. Fever, thrombocytopenia and high levels of viremia are some of the characteristics symptoms of this stage (Payne, 2006). The chronic phase is associated with several recurrent episodes of the acute symptoms that can last 8-12 months post-infection, followed by an inapparent carrier stage (Craigo et al., 2006). One of the unique aspects of the pathogenesis of EIAV infection is that a high percentage of infected horses (90%) recover from the chronic infection to become asymptomatic carriers of the virus (Craigo et al., 2009).

The S2 gene, unique to EIAV, encodes a small 65 amino acid, 7 kDa protein that plays a critical role in disease expression in the infected horse. The S2 open reading frame (ORF) begins just downstream the second exon of tat and overlaps the 5' end of the *env* gene. S2 is synthesized at a late phase of the viral life cycle by a leaky ribosome scanning mechanism from either bicistronic or tricistronic mRNA encoding Tat, S2 and Env (Carroll and Derse, 1993; Schiltz et al., 1992). Examination of S2 viral sequences from natural or experimentally infected horses reveals a high level of conservation, indicating it plays an important role in the natural infection (Craigo et al., 2009; Leroux et al., 2004; Li et al., 2000). Moreover, amino acid sequence alignments of S2 reveal several conserved, well-characterized protein motifs: an N-terminal myristoylation

motif, the proline rich (PXXP) SH3 domain binding motif, the nucleoporin motif (GLFG) and the nuclear localization signal (RRKQETKK) motif (Leroux et al., 2004; Li et al., 2000).

The role of S2 during viral infection was first evaluated in several cultured equine cell systems infected with wild-type and S2-deleted molecular clones. It was found that S2 is not essential for viral replication in cultured cells, although its presence may slightly increase viral replication *in vitro* (Fagerness et al., 2006; Li et al., 1998). Later on, the pivotal role of S2 in EIAV infection came from studies using the Shetland pony model. In one study, ponies infected with a virus derived from $EIAV_{17}$, a highly virulent molecular clone, displayed the typical signs of equine infection anemia (EIA), including key features such as: febrile episodes, thrombocytopenia, and high levels of viremia. In contrast, ponies infected with an S2-deleted virus ($EIAV_{17\Delta S2}$) had a decreased viral load and failed to develop any clinical signs of the disease (Fagerness et al., 2006). These data indicate that S2 is an important determinant in EIAV pathogenesis *in vivo*.

The underlying mechanism(s) by which S2 enhances viral replication and influences disease expression, while unknown are under investigation. We recently reported that S2 enhances the expression of a variety of pro-inflammatory cytokine and chemokine genes suggesting a role for S2 in optimizing the host cell environment for viral replication and dissemination (Covaleda et al., 2009). In this study, to further elucidate the role of S2 in pathogenesis we employed an equine whole genome oligonucleotide array (Bright et al., 2009) to provide a global view in gene expression

patterns in macrophages infected with EIAV wild-type and S2-deleted mutant virus. This study is an important step toward identifying cellular processes affected during EIAV infection and also may give us clues as to the role of S2 in pathogenesis.

Materials and Methods

Culture of equine monocyte-derived macrophage cell culture (eMDM)

Whole blood was collected from six EIA-negative healthy adult horses and centrifuged at 2100 rpm for 30 min to separate the buffy coat, which was then diluted 1:3 with Hank's balance salt solution (HBBS) containing 2 mM EDTA. Fifteen ml of endotoxin-free Histopaque-1077 (Sigma-Aldrich) was slowly layered underneath 20 ml of diluted buffy coat and centrifuged at 2100 rpm for 30 min at room temperature. Peripheral blood mononuclear cells (PBMCs) were harvested from the interface and washed by centrifugation at 1000 rpm for 10 min at 4 °C in cold entodoxin-free Alsever's solution (0.1M D-glucose, 0.027 M sodium citrate, 0.002 M citric acid, 0.07 M sodium chloride, pH 6.1) containing 1% penicillin-streptomycin, to remove platelets. Residual erythrocytes were lysed by incubation with 5 ml ACK lysis buffer (Invitrogen) for 3 min at 37 °C. After washing three times with 50 ml Alsever's solution, PBMCs were resuspended in RPMI 1640 medium supplemented with 10% heat-inactivated horse serum, penicillin (100 IU/ml), streptomycin (100μg/ml), and L-glutamine (2 mM). For monocyte isolation by plastic adherence, 12 x 10^6 PBMC per well were seeded into 12-well plates (BD Falcon) and allowed to adhere overnight in a 37 °C humidified 5% CO2 incubator. Nonadherent cells were removed by gently washing the plates, twice, with prewarmed RPMI complete media and the remaining adherent monocyte-enriched cells

were allowed to differentiate for further 48 h before infection. All reagents were screened and found negative for endotoxin and mycoplasma contamination using the Limulus Amebocyte lysate kit (Associates of Cape Cod) and MycoFind Kit (Clongen laboratories) respectively.

Virus preparations

Virus stocks were generated as previously described (Lim et al., 2005). Briefly, D17 cells were transfected with 10 µg of the molecular clones $EIAV_{17}$ or $EIAV_{17\Delta S2}$ plasmids by using the calcium phosphate method and virus particles harvested 72 h post-transfection were used to infect eMDMs. Culture supernatants collected from 7 to 15 dpi, were removed from infected eMDMs and cleared of cell debris by low-spin centrifugation. Virus stocks were assayed for reverse transcriptase (RT) activity as a measure of virus replication. Virus stocks were purified and concentrated via ultrafiltration using a Vivaflow 200 tangential flow system with a 100 kDa MWCO filter (Sartorius). After ultrafiltration, maintenance of virus infectivity was confirmed by growth in eMDMs and RT activity. No detectable levels of endotoxin were present in the purified virus stocks. Viral infectivity titers were determined by the Reed-Muench formula after infecting eMDMs with 10-fold serial dilutions of the virus in sextuplicates and maintaining the culture for two weeks.

Infection of eMDM

Three days post-plating, eMDM were mock infected (with cell culture media used to grow the cells), infected with $EIAV_{17}$ or $EIAV_{17\Delta S2}$ at a multiplicity of infection (MOI) of 3 to achieve a near synchronous infection. Supernatants and cell extracts were

collected 72 h post-infection. Virus replication was monitored by measurement of RT activity, cytopathic effect (CPE) and viral mRNA transcription.

RNA isolation, amplification and labeling

At 72 h post-infection cells were harvested in RLT buffer (QIAGEN) and cell pellets were stored at -80 °C until ready for RNA isolation. Total RNA was isolated using the RNeasy kit from QIAGEN, including DNaseI digestion according to manufacturer's instructions. RNA was further assessed for quality and concentration using the Nano 6000 assay on the Agilent 2100 Bioanalyzer. Since microarray experiments require RNA in microgram quantities for hybridization, 500 ng of total RNA were used for one round of linear amplification using the senseAMP Plus kit (Genisphere). Amplified RNA (2 μg) was then used as a template to generate Cy3 or Cy5 tagged cDNA probes (Genisphere). Cy5 tagged cDNA probes were generated from wild-type and mutant samples and Cy3 tagged cDNA probes were generated from mock-infected control samples. The tagged cDNA probes were reversed in terms of dye labeling for samples obtained from the other three horses to offset potential dye bias. Shown in figure 3.1 is a flow diagram of the experimental design used.

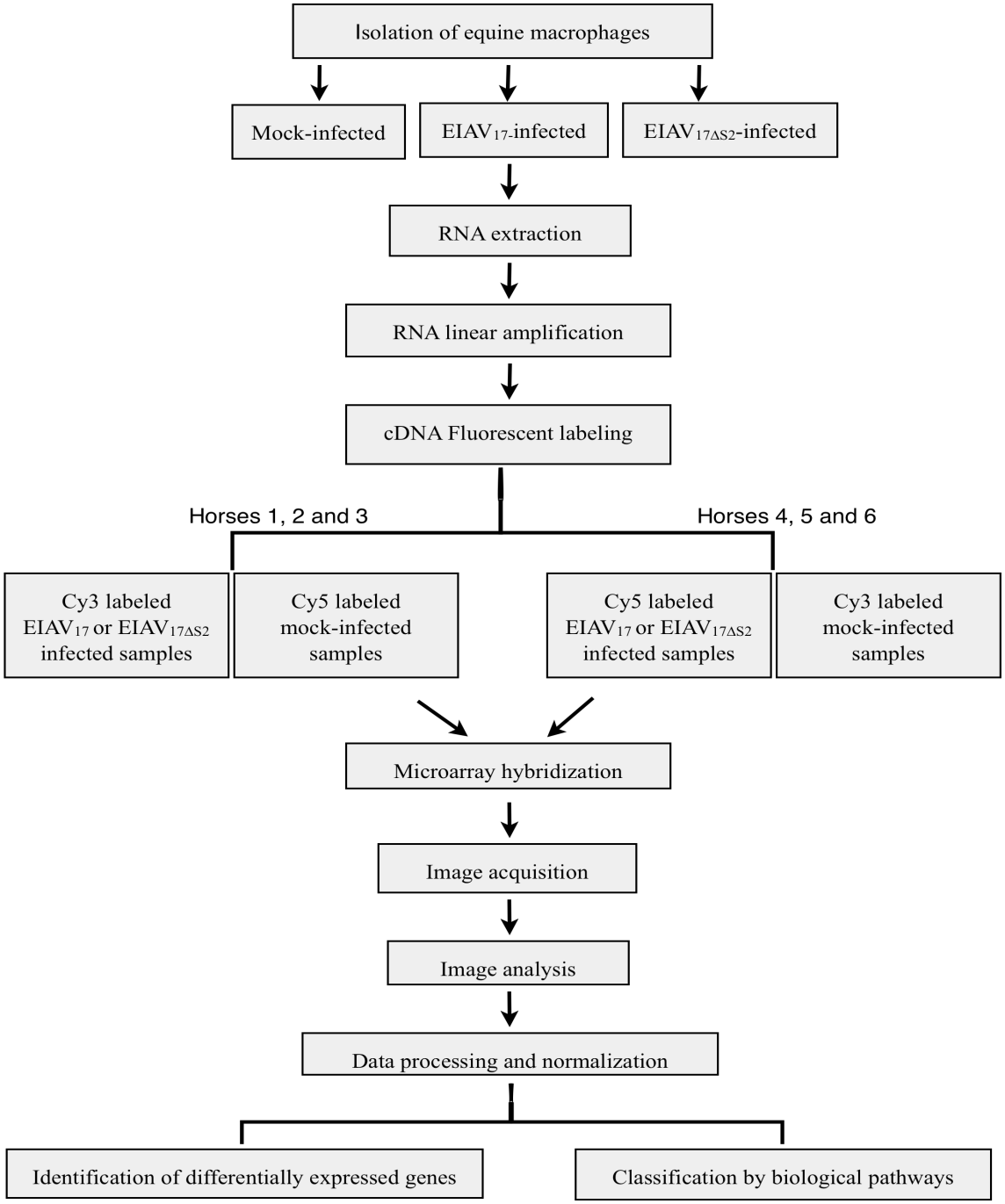

Figure 3.1. Flow diagram of the array experimental design.

Microarray hybridization and data collection

Prior to hybridization, printed oligo-microarray slides were: (**1)** rehydrated over a 50 °C water bath for 10 seconds (label-side down), (**2)** snap-dried at 65 °C in a heating block for 5 seconds (label-side up) and (**3)** allowed to cool for 1 minute. Steps 1-3 were repeated 3 times. The slides were then UV cross-linked at 750 mJoules. Twenty-eight μl of each Cy3 and Cy5 cDNA probe (mock-infected and wild-type or mock-infected and mutant) were combined with 290 μl 2X hybridization buffer plus 30 μl of TE, 2 μl LNA dT Blocker and 202 μl of nuclease-free water (Array 350 – Genisphere). The hybridization mixture was then incubated at 80 °C for 10 min, cooled to room temperature and then applied to the gasket slide in a microarray chamber (Agilent) with the rehydrated oligo-microarray slide laid on top (label-side down). The microarray-gasket slide sandwich was then incubated for 16 h at 55 °C in a hybridization rotation oven. Following hybridization, oligo-microarrays were washed for 15 min each in prewarmed 2X SSC plus 0.2% SDS solution (Ambion) at 42 °C, 2X SSC at room temperature and 0.2X SSC at room temperature. Finally, slides were spin-dried by centrifugation in 50 ml conical tubes. A second hybridization mixture contained 2.5 μl of Cy3 and Cy5 fluorescent 3DNA reagents, 25 μl of 2X hybridization buffer with SDS, 0.25 μl of anti-fade reagent and 20 μl of nuclease-free water. The hybridization mixture was then applied to the pre-hybridized microarray slide and covered with a glass cover slip. Slides were incubated in the dark at 55 °C for 4 h. Post-hybridization washes and spin-dry were repeated as before but in the dark. Oligo-microarrays were stored in the dark until scanned. Hybridized oligo-microarrays were scanned at 5 micron resolution

using a GenePix 4100A scanner and GENEPIX 6.0 analyzer software was used to process microarray images, locate spots and to obtain raw total spot intensities for both dyes in each spot (Axon Instruments / Molecular Devices).

Microarray analysis

Raw data from mean spot intensity and median background intensity was Lowess normalized to reduce the intra and inter-array variability that are commonly observed in microarray experiments (Park et al., 2003). In addition raw data was filtered to exclude spots with a signal to noise ratio ≤2 or a GenePix flag. A mixed model analysis was applied to the normalized log2 ratios to identify genes differentially expressed between the treatment groups. The mixed model included the effects of treatment, dye, slide and replicate in the analysis. List of genes were generated based on two criteria: a fold change ≥1.8 or ≤ -1.8 for genes upregulated or downregulated respectively and a *p*-value cutoff of ≤ 0.05. The statistical package SAS was used to perform these analyses.

Wild-type and delta-S2 infected samples (Cy5) were directly compared to the mock-infected control (Cy3). Differences in gene expression between wild-type and mutant were compared indirectly through those of the control samples.

Microarray validation

TaqMan and SYBR Green based assays were used to analyze and validate gene expression levels of selected genes (Table 3.1). TaqMan real time PCR reactions were performed in a 10 μl total volume containing 0.5 μl of cDNA, 5 μl of EXPRESS qPCR SuperMix with premixed ROX (Invitrogen), 0.5 μl of fluorescent primer/probe mix, and 4 μl of DEPC-treated water. SYBR Green real time PCR reactions contained 5 μl of

SYBR Greener qPCR with premixed ROX (Invitrogen), 200 nM of the primer mix, and DEPC-treated water. Amplification was carried out using the following parameters: 50 °C for 2 min, 95 °C for 10 min, followed by 40 cycles of 95 °C for 15 s and by 60 °C for 30 s. A dissociation stage was included for SYBR Green real time PCR to confirm the amplification of a single product. All RT reactions, including no-template controls, were run in triplicate on an ABI 7900HT real-time PCR system. Data were collected and analyzed with the SDS 2.3 software. The Pfaffl method (Pfaffl, 2001) was used to calculate relative fold changes in gene expression between mock-infected and infected samples. Data were first normalized to the endogenous control 18S rRNA or beta-actin and the mock-infected samples were used as calibrator. TaqMan primer/probe sets for IL-8 and 18S have been previously described and validated (Allen et al., 2007) and were obtained from Applied Biosystems. TaqMan probes and primers for SYBR Green real time PCR were designed to span at least one exon-exon junction to prevent amplification of genomic sequences. TaqMan probes were 5' labeled with 6-carboxyfluorescein (FAM) and 3' with a nonfluorescent quencher (NFQ). RT-PCR products were separated by 2% agarose gel electrophoresis to confirm product size and specificity of each primer/probe set. Fragments were also analyzed by sequencing to validate the identity of the PCR products. PCR efficiency from each primer/probe set was determined by performing a 6-log dilution range from 3 different cDNA samples. Each dilution was run in triplicate.

Table 3.1. Sequence of primer and probes used in real time quantitative PCR

Gene	Gene ID #	Primer/probe	Sequence 5'→3'	Product length (bp)
IL-8 *	100037400	Forward	GCCACACTGCGAAAACTCA	95
		Reverse	GCACAATAATCTGCACCCACTTTG	
		Probe	FAM-ACGAGCTTTACAATGATTTC-NFQ	
MCP-2 *	100033950	Forward	TCACCAGCAGCCAGTGTTC	67
		Reverse	GCACAGATCTCCTTGTCCACTTT	
		Probe	FAM-AAGCTGTGATCTTCAAGACC-NFQ	
18S*	AJ311673	Forward	AAACGGCTACCACATCCAA	54
		Reverse	TCGGGAGTGGGTAATTTGC	
		Probe	FAM-AAGGCAGCAGGCGC-NFQ	
IL-34	100054703	Forward	TGCCCTTGCTGTAAACATAGC	100
		Reverse	CCACACACTGTGATGATGAGG	
RANTES	100033925	Forward	AGTCGTCTTTGTCACCCGAAAG	62
		Reverse	GCACCCATTTCTTCTCTGCATT	
ISG15	100066364	Forward	TGCAGGCCGACCAGTTCT	94
		Reverse	ACTGTGCACCCGGCTGTAA	
MMP-9	100056599	Forward	GCGCTCATGTACCCCATGTA	90
		Reverse	GCGAGGACCATAGAGATACTGGAT	
CD63	100051450	Forward	CAAGGGCTGTGTGGAGAAGATT	100
		Reverse	AATTCCCAGGACCTCCACAAA	
DNM3	100060156	Forward	TGAAAGTGCGAGATGTGGAAAA	90
		Reverse	AGTCTTTGTAAACATTCCTTTGTTCAGT	
HMG-1	100050136	Forward	GCGGACAAGGCCCGTTAT	90
		Reverse	AGGTGCATTGGGATCCTTGA	
CHMP1B	100071734	Forward	TGAAGCTGGCCTTGATCTCA	64
		Reverse	ACTTGTGCCAACAGAACCTGTCT	
Beta-actin	100033878	Forward	TCACGGAGCGTGGCTACAG	63
		Reverse	CCTTGATGTCACGCACGATTT	

*TaqMan primer/probes sets

Fold changes for each target gene were log-2 transformed prior to statistical analysis and statistically significant difference was determined using Student's *t* test. All data were expressed as mean value (log2) ± S.E.M. Results were considered significantly different when $p < 0.05$.

Results

EIAV replication and transcription in eMDM cultures

To obtain a global view of gene expression patterns induced by EIAV infection and the contribution of S2, this study was performed with the highly virulent molecular clone $EIAV_{17}$ and its S2-deleted counterpart ($EIAV_{17\Delta S2}$). Gene expression profiles from infected samples were analyzed relative to the mock-infected control, to accurately evaluate the changes in cellular gene expression.

Cultured equine macrophages were infected at an MOI of 3 to achieve a near synchronous infection and ensure that each cell was infected. This allowed us to clearly analyze the cellular response that occurs upon EIAV infection and minimize bystander cell responses. To evaluate viral infectivity of the purified stocks, supernatants from infected cells and the mock-infected control were collected at different time points and assayed for RT activity as a measure of viral replication. As shown in Fig. 3.2A, the viral stocks showed similar replication kinetics. Moreover, we also monitored the levels of viral transcription by real time PCR with EIAV primers spanning the splice site used to generate the single spliced, tricistronic mRNA that encodes Tat, S2 and Env. As shown in Fig. 3.2B, no significant differences in the levels of the specific viral transcript were observed between wild-type and S2-deleted virus. In this experiment, a decrease in delta cycle threshold (ΔCt) values indicates an increase in viral gene transcription.

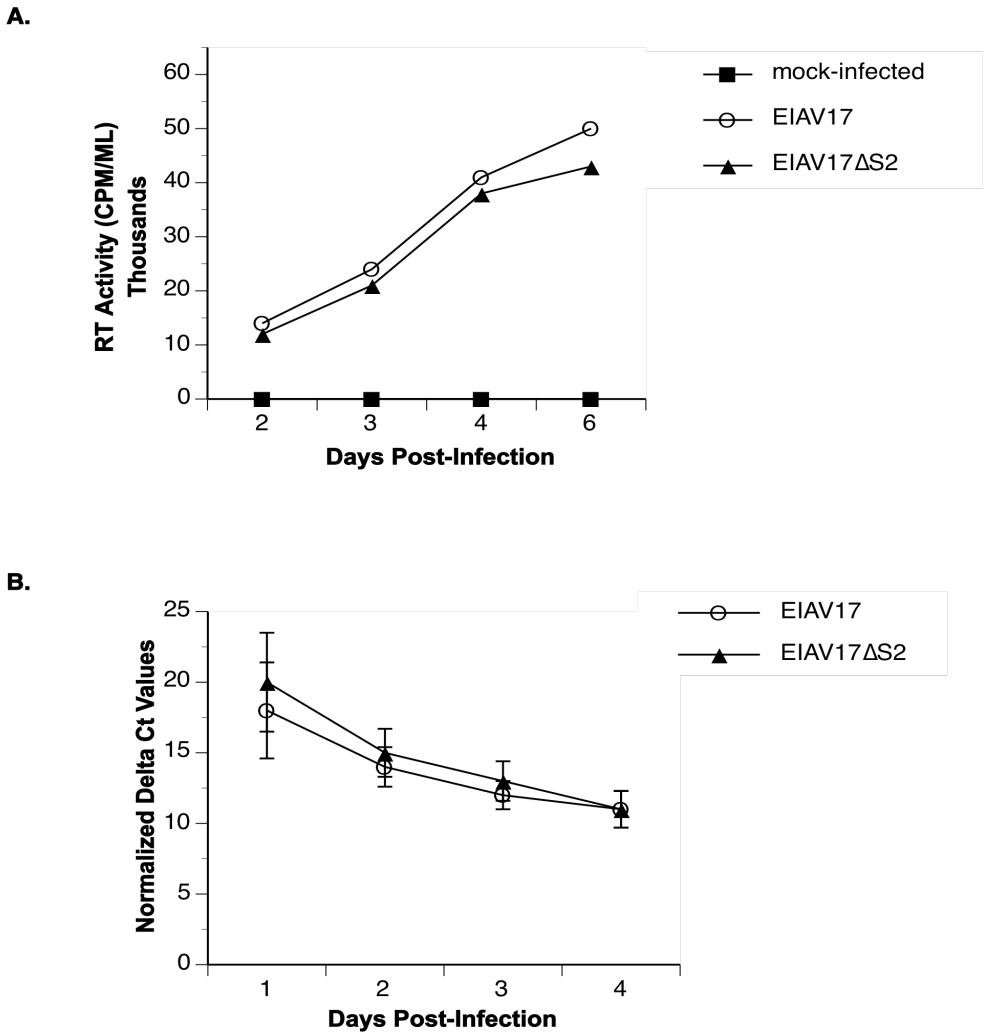

Figure 3.2. Viral infectivity and mRNA expression. (A) Growth kinetics of viral stocks. **(B)** Real time PCR detection of viral mRNA transcripts. The error bars indicate the standard deviation from three horses (n=3). The data shown in Panels A and B are from separate experiments.

Gene expression profiles in eMDMs after infection with $EIAV_{17}$ and $EIAV_{17\Delta S2}$

In a previous study from our lab (Covaleda et al., 2009), we showed that the majority of changes in cytokine and chemokine expression in macrophages infected with EIAV occurred three days post-infection. For that reason, as a first step to delineate changes in cellular gene expression induced by EIAV we chose to initially carry out this study with samples collected at 72 h post-infection.

Since the amount of total RNA obtained in our experiment was too low to perform array analysis, RNA samples were subjected to one round of linear amplification (Genisphere). Cy3 and Cy5 dye-labeled cDNA probes (mock-infected and infected samples, respectively) were hybridized to equine oligonucleotide arrays and ratios of signal intensities were calculated at each spot. Samples obtained from three out of the six horses used in the study were labeled reversed in terms of dye labeling to offset potential dye bias due to sequence-specific dye incorporation. The equine whole genome oligonucleotide array kindly provided by Dr Bhanu Chowdhary (Texas A&M University) has 21,351 probes representing a genomic coverage of approximately 97.5% (Bright et al., 2009). After array normalization, data from 78% of the array spots were further used for mixed model analysis to identify genes differentially expressed between the treatment groups.

To determine gene expression profiles and establish gene expression differences between treatments, differentially expressed genes were selected based on two criteria, a significance level of $p<0.05$ and a fold change greater than 1.8 up or down regulated.

On the basis of the mixed model analysis, approximately 109 genes were differentially expressed upon EIAV infection with the highly virulent virus ($EIAV_{17}$), 290 genes were differentially expressed between $EIAV_{17}$ and the S2-deleted virus ($EIAV_{17\Delta S2}$) and 30 genes were differentially regulated by the S2-deleted virus relative to the mock infected control ($p<0.05$). Of these significantly regulated genes, a high percentage had not been annotated yet. Thirty-five of these unannotated genes are from the analysis of $EIAV_{17}$ versus mock-infected control, 89 from the $EIAV_{17}$ versus $EIAV_{17\Delta S2}$ and 6 from the $EIAV_{17\Delta S2}$ versus mock-infected control.

Differentially expressed genes with increased or decreased expression were classified by the Swiss-Prot keyword "biological process". Partial lists of the top differentially expressed genes are shown in Tables 3.2 to 3.5. Genes up-regulated during EIAV infection include genes that we previously have reported as induced in EIAV infected macrophages, such as interleukin-8 (IL-8), monocyte chemotactic protein-2 (MCP-2) and interleukin-1 alpha (IL-1α), providing support of the validity of the array results. Overall, more genes involved in immune response, transcription regulation, mRNA splicing, cell cycle, cell survival and the ubiquitin pathway were stimulated (Table 3.2). Whereas a lower percentage of genes involved in transcription, immune response, cell cycle and cell survival were down-regulated (Table 3.3). Strikingly, genes involved in translation were only down-regulated upon EIAV infection; these included several ribosomal proteins (RPL17, RPL27A, RPL34, RPL31, RPS25, S6, 16S) and eukaryotic translation initiation factor 3 (EIF3F).

Table 3.2. Selected up-regulated genes in EIAV wild-type infected macrophages classified by Swiss-Prot keyword

Gene ID	Gene name	Fold change
Immune response		
LOC100037400	Interleukin-8 (IL-8)	2.2
LOC100033927	Monocyte chemoattractant protein-2 (MCP-2)	4.8
LOC100033925	RANTES	2.0
LOC100064969	Interleukin-1 alpha (IL-1a)	1.8
LOC100053534	Immunoglobulin-like transcript 8 (ILT8)	1.9
LOC100070878	Interferon, gamma-inducible protein 30 (IP-30)	2.0
Transcription regulation and mRNA splicing		
LOC100051665	RuvB-like 2 (RUVBL2)	2.6
LOC100068414	Cysteine-serine-rich nuclear protein-1 (CSRNP-1)	2.1
LOC100146801	Jun B proto-oncogene (Jun-b)	2.0
LOC100056571	CREB regulated transcription coactivator 2 (CRTC2)	1.9
LOC100034223	Superoxide dismutase-2 (SOD2)	2.1
LOC100058690	RNA binding motif protein 4 (RBM4)	3.2
Cell cycle and proliferation		
LOC100055960	G1 to S phase transition-1 (GSPT-1)	2.3
LOC100072415	Serpin peptidase inhibitor, clade F (SERPINF1)	2.1
LOC100054703	Interleukin-34 (IL-34)	1.9
LOC100061408	Dedicator of cytokinesis-3 (DOCK3)	1.9
LOC100053929	Interferon stimulated exonuclease gene-20 (ISG20)	1.9
LOC100034223	Superoxide dismutase-2 (SOD2)	1.1
LOC100064022	Cyclin-dependent kinase inhibitor 1A, p21 (CDKN1A)	1.8
Ubl conjugation pathway and antiviral defense		
LOC100065188	Ring finger protein 182 (RNF182)	2.6
LOC100052084	Murine double minute 2 oncogene (MDM2)	2.5
LOC100066364	Interferon stimulated gene 15 (ISG15) - ubiquitin-like modifier	2.3
LOC100071433	Ubiquitin specific peptidase 47 (USP47)	2.0
LOC100068894	Baculoviral IAP repeat-containing 3 (BIRC3)	1.9
AY509556	2'-5'-oligoadenylate synthetase 2 (OAS2)	1.9
LOC100053929	Interferon stimulated exonuclease gene-20 (ISG20)	1.9
LOC100052688	Fem-1 homolog b, transcript variant 2 (FEM1B)	1.9
Cell death and survival		
LOC100061755	BCL2-antagonist/killer 1 (BAK1)	2.0
LOC100068894	Baculoviral IAP repeat-containing 3 (BIRC3)	1.9
LOC100034223	Superoxide dismutase-2 (SOD2)	2.1
LOC100068414	Cysteine-serine-rich nuclear protein-1 (CSRNP-1)	2.1
Signal transduction		
LOC100051866	Growth factor receptor-bound protein 2 (GRB2)	2.0
LOC100067361	Signal-regulatory protein beta 1 (SIRPB1)	2.0
Others		
LOC100072671	Vacuolar protein sorting 26 homolog A (VPS26A)	2.6
LOC100052051	Barrier to autointegration factor 1 (BANF1)	2.1
LOC100051102	RNA binding motif protein 42 (RBM42)	1.9
LOC100066372	Zinc finger protein 385B (ZNF385B)	1.8

Table 3.3. Selected down-regulated genes in EIAV wild-type infected macrophages classified by Swiss-Prot keyword

Gene ID	Gene name	Fold change
Immune response		
LOC100057478	Thrombospondin 1 (TSP1)	-4.3
LOC100065481	Apolipoprotein E (APOE)	-2.8
LOC100056599	Matrix metallopeptidase 9 (MMP9)	-2.3
Transcription regulation and mRNA splicing		
LOC100050136	High-mobility group box 1	-4.0
LOC100051444	TGFB-induced factor homeobox 1 (TGIF1)	-2.6
LOC100066520	Polymerase (RNA) I polypeptide E (POLR1E)	-2.5
LOC100066265	DEK oncogene	-2.0
LOC100052973	Forkhead box N3 (FOXN3)	-1.8
Cell death and survival		
LOC100060183	p21 protein-activated kinase 2 (PAK2)	-7.0
LOC100057478	Thrombospondin 1 (TSP1)	-4.3
LOC100050136	High-mobility group box 1 (HMGB1)	-4.0
LOC100072241	Annexin A5 (ANXA5)	-3.2
LOC100053396	Glutathione peroxidase 1 (GPX1)	-2.5
LOC100053958	Cytochrome c (CYCS)	-2.0
LOC100063318	Protein kinase C (PRKCA)	-1.9
Cell cycle		
LOC100071734	Chromatin modifying protein 1B (CHMP1B)	-1.9
LOC100052973	Forkhead box N3 (FOXN3)	-1.8
Translation		
LOC100056788	Ribosomal protein L34 (RPL34)	-2.5
LOC100071004	Ribosomal protein L27a (RPL27A)	-2.3
CD466522	Ribosomal 16S RNA gene	-2.3
LOC100052368	Ribosomal protein S6	-2.1
LOC100053716	Ribosomal protein L17 (RPL17)	-2.1
LOC100059235	Ribosomal protein L31 (RPL31)	-2.0
LOC100063216	Ribosomal protein S25 (RPS25)	-2.0
LOC100070877	Eukaryotic translation initiation factor 3, F (EIF3F)	-1.9
Others		
LOC100050663	Lymphocyte cytosolic protein 1 (LCP1)	-2.1
LOC100050835	Cystatin B (CSTB)	-2.1
LOC100051450	CD63 antigen (CD63)	-1.8

Even though we amplified the RNA to obtain enough material to perform the microarray experiment, it was not sufficient to carry out a direct experimental design method where we could compare, in the same array slide, the $EIAV_{17}$ versus $EIAV_{17\Delta S2}$ treatments. Instead, we used an alternative approach using indirect comparisons to evaluate differences in gene expression profiles between macrophages infected with the wild-type and S2-deleted viruses (Speed and Yang, 2002).

Similar to the results obtained with the $EIAV_{17}$ versus mock-infected cells, genes up-regulated in macrophages infected with $EIAV_{17}$ compared with the S2-deleted virus are involved in the immune response, transcription, cell death, cell cycle and antiviral defense. The majority of the differentially expressed genes are different from those genes found to be increased in the $EIAV_{17}$ versus mock-infected analysis (Table 3.4).

Genes that were decreased in cells infected with $EIAV_{17}$ when compared with the mutant virus were found to encode proteins involved in the immune response, translation, cell death and transcription (Table 3.5). Some of the common genes down-regulated are matrix metallopeptidase 9 (MMP9), cystatin B (CSTB), forkhead box N3 (FOXN3), high-mobility group box 1 (HMGB1) and ribosomal proteins, RLP27A, RPL31 and RPL36A.

Table 3.4. Selected up-regulated genes in EIAV wild-type versus EIAV S2- deleted infected macrophages classified by Swiss-Prot keyword

Gene ID	Gene name	Fold change
Immune response		
LOC100064969	Interleukin-1 alpha (IL-1a)	2.0
DN507662	Human microRNA host gene 2- MIRHG2 (BIC)	2.0
LOC100053534	Immunoglobulin-like transcript 8 (ILT8)	2.3
LOC100066223	Signal transducing adaptor family member 1 (STAP1)	2.3
Transcription regulation and mRNA splicing		
LOC100061235	Zinc finger protein 568 (ZNF568)	2.5
LOC100055527	GA binding protein transcription factor (GABPB2)	2.3
LOC100058395	Zinc finger protein 207 (ZNF207)	2.0
LOC100063879	Nuclear receptor subfamily 2 (NR2E3)	2.0
LOC100071307	Ring finger protein 141 (RFN141)	1.8
LOC100066388	cAMP responsive element binding protein 1 (CREB1)	1.8
LOC100050857	Retinoblastoma binding protein 8 (RBBP8)	1.8
LOC100068168	Smu-1 suppressor of mec-8 (SMU1)	2.0
Cell cycle		
LOC100060949	Arginine vasopressin-induced 1 (AVPI1)	2.1
LOC100057138	DEAD/H box polypeptide (DDX11)	2.0
LOC100050857	Retinoblastoma binding protein 8 (RBBP8)	1.8
LOC100056044	Protein tyrosine phosphatase type IVA (PTP4A2)	1.8
LOC100060513	Cell cycle associated protein 1 (CAPRIN1)	2.0
Cell death		
LOC100051773	Programmed cell death 2 (PDCD2)	1.9
Ubl conjugation pathway and antiviral defense		
LOC100061587	Zyg-11 homolog B (ZYG11B)	2.1
LOC100060728	F-box protein 38 (FBXO38)	1.9
LOC100066866	Ubiquitin-conjugating enzyme E2L 6 (UBE2L6)	1.8
LOC100062815	ATP-binding cassette, sub-family E (ABCE1)	2.0
Translation		
LOC100064307	Eukaryotic translation initiation factor 3, K (EIF3K)	2.0
LOC100055350	Eukaryotic translation initiation factor 3, G (EIF3G)	2.3
Others		
LOC100065130	Protein tyrosine phosphatase, liprin alpha 4 (PPFIA4)	8.6
LOC100065531	Nucleotide binding protein 2 (NUBP2)	3.0
LOC100065366	RAB6B, member RAS oncogene (RAB6B)	2.5
LOC100062835	Integrin, beta-like 1 (ITGBL1)	2.3
LOC100054426	Cadherin 18, type 2 (CDH18)	2.1
LOC100060652	Scavenger receptor class A (SCARA3)	2.1
LOC100071763	Rho GTPase activating protein 11A	2.0

Table 3.5. Selected down-regulated genes in EIAV wild-type versus EIAV S2- deleted infected macrophages classified by Swiss-Prot keyword

Gene ID	Gene name	Fold change
Immune response		
LOC100055841	Phospholipase A2, group VII (PLA2G7)	-2.1
LOC100062762	Cholinergic receptor, nicotinic beta 2 (CHRNB2)	-2.3
LOC100056599	Matrix metallopeptidase 9 (MMP9)	-2.5
LOC100033933	Heat shock protein 90kDa beta (GRP94)	-3.2
LOC100066928	Interleukin 4 induced 1 (IL4I1)	-1.9
Transcription regulation and mRNA splicing		
LOC100051444	TGFB-induced factor homeobox 1 (TGIF1)	-2.0
LOC100050136	High-mobility group box 1 (HMGB1)	-1.8
LOC100050121	Small nuclear ribonucleoprotein D3 (SNRPD3)	-1.8
Translation		
Human ID 6189	Ribosomal protein S3A (RPS3A)	-2.6
LOC100071004	Ribosomal protein L27A (RPL27A)	-2.3
LOC100052368	Ribosomal protein S6 (RPS6)	-2.0
LOC100060331	Ribosomal protein L36A (RPL36A)	-2.0
LOC100059235	Ribosomal protein L31 (RPL31)	-1.9
Cell death and survival		
LOC100050835	Glutathione peroxidase 1 (GPX1)	-2.5
LOC100055170	BCL2/adenovirus E1B interacting protein like (BNIPL)	-1.9
Human ID 9423	Netrin 1 (NTN1)	-2.1
Cell cycle		
LOC100052973	Forkhead box N3 (FOXN3)	-1.8
Others		
LOC100060156	Dynamin 3 (DNM3)	-3.2
LOC100050835	Cystatin B (CSTB)	-2.5
LOC100070766	Protein kinase inhibitor gamma (PKIG)	-2.1
Human ID 5569	Protein kinase inhibitor alpha (PKIA)	-1.8
LOC100052644	Ribosomal protein S27	-2.0
LOC100071944	Ubiquitin protein ligase E3 component n-recognin 4 (UBR4)	-1.8

Validation of microarray data

We selected a number of genes for validation by quantitative real time PCR. PCR efficiency for each primer/probe set was determined (Table 3.6). To account for differences in PCR efficiencies, the Pfaffl method was used to determine the relative expression of the target genes (Pfaffl, 2001).

Table 3.6. Validation of TaqMan primer/probe sets and SYBR Green primers

Target Gene	PCR efficiency		
	Mean slope	%	R^2
MCP-2*	-3.34	99	1
IL-8	-3.29	101	0.98
IL-34	-3.48	93	0.99
RANTES	-3.29	101	0.98
ISG15	-3.15	107	0.99
MMP-9	-3.21	104	0.99
CD63	-3.20	105	1
DNM3	-3.29	101	0.98
HMG-1	-3.22	104	0.98
CHMP1B	-3.29	101	1
18S	-3.57	90	0.99
Beta-actin	-3.28	101	0.99

* TaqMan primer/probe

Although fold changes were similar or slightly greater than what was measured by microarray, the direction of gene expression pattern (up or down-regulation) was similar (Fig. 3.3).

Expression of genes encoding proteins involved in the pro-inflammatory response, IL-8, MCP-2 and RANTES were validated by RT-PCR (Fig. 3.3). For IL-8 and MCP-2 there was a statistically significant difference between macrophages infected with $EIAV_{17}$ versus the mock-infected control and also between macrophages infected with the S2-deleted virus. In contrast, expression of RANTES was significantly higher in the $EIAV_{17}$ infected cells compared to the mock-infected control but not when compared to the mutant virus. Interferon-stimulated gene 15 (ISG15) that is involved in antiviral defense and immune response among other functions (Dao and Zhang, 2005), was significantly up-regulated in $EIAV_{17}$ infected macrophages compared with the mock-infected control and S2-deleted virus infected macrophages. There was a significant

difference in gene expression with IL-34, a novel cytokine, in cells infected with the wild-type virus compared with the control or with $EIAV_{17\Delta S2}$ infected eMDMs.

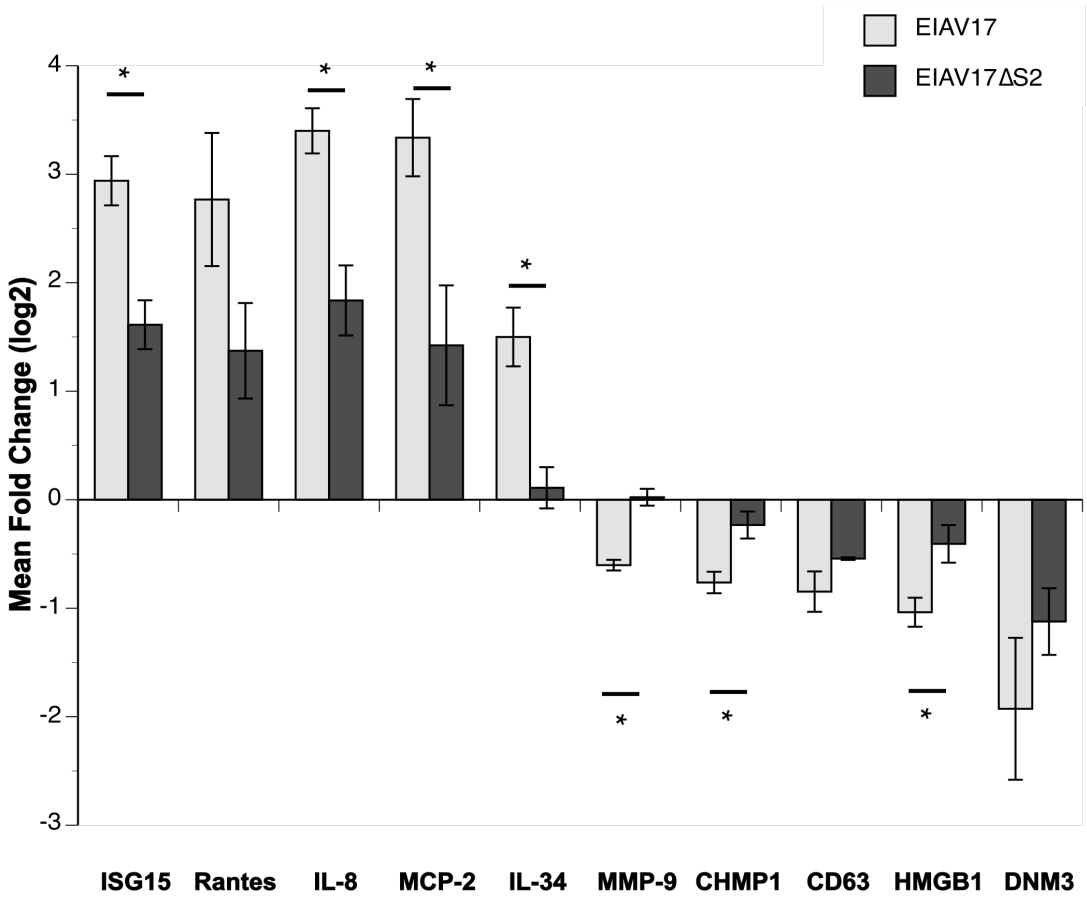

Figure 3.3. Validation of microarray results. Showing mRNA expression of selected genes in EMDM infected with $EIAV_{17b}$ (■) or $EIAV_{17b\Delta S2}$ (■). Data was analyzed using the Pfaffl method. All values were normalized to the endogenous control 18S or b-actin, and represent the log2 mean fold change in expression (relative to mock-infected control). Error bars represent ± SEM between three different horses (n =3). Student's *t*-test was used to determine whether or not significant differences occurred. *, indicates $p< 0.05$.

Interestingly, the EIAV S2-deleted virus did not appear to significantly increase IL-34 mRNA expression above the control (Fig. 3.3).

Among the down-regulated genes, the array results of all except one, dynamin 3 (DNM3) were validated by real time PCR (Fig. 3.3). Array data indicated a significant down-regulation (3.2 fold) of DNM3 in cells infected with $EIAV_{17}$ compared with cells infected with $EIAV_{17\Delta S2}$. However, by quantitative PCR there was not a significant difference in the expression levels between $EIAV_{17}$ and $EIAV_{17\Delta S2}$. MMP9, important for the migration of immune cells (Jintang et al., 2009), charged multivesicular body protein /chromatin modifying protein 1 (CHMP1), involved in modification of chromatin structure and endosomal vesicle sorting (Howard et al., 2001) and HMGB1, a chromatin associated nuclear factor (Girard, 2007), were found to be significantly down-regulated after EIAV infection and significant differences were detected between wild-type virus and S2-deleted virus (Fig. 3.3). CD63, a lysosome protein involved in HIV replication in macrophages (Chen et al., 2008) is down-regulated upon EIAV infection and similar to the array data, no differences were found between $EIAV_{17}$ and $EIAV_{17\Delta S2}$ infected cells.

Discussion

Analyses of gene expression profiles are central to the understanding of the mechanisms of viral pathogenesis. Until now, there have been no studies addressing the global transcription patterns that occur during EIAV infection. In the present study we used microarray analysis to examine the response of macrophages upon EIAV infection and compared those with macrophages infected with an S2-deleted virus.

EIAV infection induced the expression of genes involved in a variety of biological processes such as the immune response, transcription, cell cycle, cell survival and antiviral defense. Some of the immune response genes found to be differentially expressed during EIAV infection were IL-8 and MCP-2. In agreement with our previous study, IL-8 and MCP-2 expression were highly up-regulated in eMDM cells following EIAV infection and the response was significantly higher with the wild-type virus compared with the S2-deleted virus. IL-8 and MCP-2 are major chemoattractants for monocytes and macrophages (Lane et al., 2003(Loetscher et al., 1994). Moreover, gene expression of RANTES, also a potent chemotactic protein for monocytes and macrophages, was highly increased upon EIAV infection (Kuna et al., 1992). These data indicate enhancement of the chemokine response is mediated by S2 or by S2 interaction with other immune modulators that lead to a more robust wave of monocytes and macrophages recruitment to the site of infection, likely contributing to viral dissemination and disease progression.

Genes involved in cell cycle and proliferation were up-regulated upon EIAV infection. One of the genes involved in cell proliferation, IL-34, is a novel cytokine that has been shown to stimulate monocyte proliferation and survival, and to promote the differentiation of human bone marrow cells into macrophage progenitor cells (Lin et al., 2008). In a recent report, IL-34 is shown to elicit macrophage proliferation from chicken bone marrow cells in culture (Garceau et al., 2010). Validation of the array data confirmed the up-regulation of IL-34 in macrophages infected with the highly virulent $EIAV_{17}$ virus relative to the mock-infected control. However, gene expression of IL-34

was not affected in macrophages infected with the S2-deleted virus, indicating S2 specifically plays a role in the induction of IL-34 during EIAV infection. This finding suggests that upon EIAV infection, S2 function is to stimulate the production of EIAV target cells. Another gene up-regulated during EIAV infection is the G1 to S phase transition protein 1 (GSPT-1) also known as eukaryotic release factor 3 (eRF3). eRF3 is part of the translation machinery involved in translation termination in eukaryotes (Kononenko et al., 2010). Studies have shown that eRF3 depletion induces cell cycle arrest at the G1 phase (Chauvin et al., 2007). Up-regulation of eRF3 upon EIAV infection may indicate that EIAV favors, at least at the time point studied, the progression from G1 to the S phase of the cell cycle.

It was also interesting to observe up-regulation of the cyclin-dependent kinase inhibitor 1A (CDKN1A), also known as p21, during EIAV infection in macrophages. p21, is a cell cycle regulator that mediates cell cycle arrest in response to a variety of stimuli such as DNA damage (Johnson and Walker, 1999). Studies have shown that inhibition of p21 leads to suppression of HIV replication in macrophages (Vazquez et al., 2005). Moreover, p21, is a target for the HIV Vpr accessory protein. One of the mechanisms of Vpr mediated cell cycle arrest in the G2/M phase is up-regulation of p21 expression (Chowdhury et al., 2003). Cell cycle arrest at G2 by Vpr is predicted to play an important role in HIV replication and pathogenesis (Yoshizuka et al., 2005). This suggests a pivotal role of p21 during the viral replication cycle in macrophages.

The murine double-minute protein 2 (MDM2) is an E3 ubiquitin ligase that inhibits the function of p53 tumor-suppressor protein (Dai et al., 2004). Overexpression

of MDM-2 inhibits p53-mediated apoptosis in response to DNA damage as well as p53-mediated G1 cell cycle arrest (Chen et al., 1996). Cell cycle arrest in the G1/S phase leads to the abrogation of a productive infection in macrophages (Schuitemaker et al., 1994). Moreover, studies have shown that the cell cycle status plays a key role in HIV replication (Groschel and Bushman, 2005; Katz et al., 2005). Cells arrested in G2 of the cell cycle support HIV replication more efficiently than cells arrested in the G1 phase (Goh et al., 1998). Taken together, these results suggest that EIAV modulates expression of genes involved in cell cycle progression and inhibition of apoptosis to provide a more favorable environment for viral replication.

Several genes involved in the ubiquitin degradation pathway such as f-box protein 38 (FBXO38), baculoviral IAP repeat-containing protein 3 (also known as cIAP2), fem-1 homolog b (FEM1B) and ubiquitin-conjugating enzyme E2L6 (UBE2L6) were differentially expressed upon EIAV infection. Many viruses are known to utilize the ubiquitin-degradation pathway to their advantage, not only by altering the cell cycle but also to modulate viral replication and the immune response (Isaacson and Ploegh, 2009). An interesting example is seen with the HIV Vpu accessory protein. Vpu targets CD4 (cell surface glycoprotein present on the surface of T helper lymphocytes) for proteasomal degradation through binding to βTrCP, a component of the E3 ubiquitin ligase complex. Binding of Vpu to βTrCP leads to CD4 ubiquitination and subsequent degradation (Nomaguchi et al., 2008). CD4 down-regulation is required for efficient virus replication and infectivity (Hanna et al., 2006). In addition, MDM2, up-regulated during EIAV infection, has also been involved in mediating HIV Tat ubiquitination both

in vivo and *in vitro*. Interestingly, MDM2 mediated ubiquitination of Tat, does not target Tat for degradation by the proteosome. Instead, ubiquitination positively modules Tat transactivation, which is required for efficient replication of HIV (Bres et al., 2003).

A major group of down-regulated genes during EIAV infection were those encoding ribosomal proteins. This observation differs from data previously reported during HIV infection. Gene expression analysis of HIV Tat and Vpr expressing cells revealed a marked induction of ribosomal genes, suggesting a mechanism by which HIV may stimulate viral protein production (de la Fuente et al., 2002; Janket et al., 2004). Further studies need to be conducted to determine if a down-regulation of ribosomal genes during EIAV infection, specifically at the time point analyzed, correlates with a decrease in viral protein synthesis. If a correlation is detected could this be a mechanism by which EIAV controls cellular and/or viral protein production to prevent ER overload and premature cell death?. In addition to the established roles in protein synthesis, several ribosomal proteins have been implicated in extra-ribosomal functions (Warner and McIntosh, 2009). For example, the ribosomal protein S3a (RPS3a), a component of the small ribosomal 40S subunit, is involved in cell transformation and apoptosis (Naora et al., 1998). Moreover, ribosomal protein L34 (RPL34), a component of the 60S ribosomal subunit, that is down-regulated upon EIAV infection, is an efficient inhibitor of the cyclin D-Cdk4 activity, an important cellular complex for cell progression of the G1 phase (Moorthamer and Chaudhuri, 1999).

Another gene down-regulated during EIAV infection, the high mobility group B1 protein (HMGB1), is involved in repressing HIV-1 gene expression by causing

repression of the LTR-mediated transcription (Naghavi et al., 2003) and acts as a DNA-binding cytokine, promoting the expression of multiple pro-inflammatory cytokines (Andersson et al., 2002).

Overall these data show that EIAV induces expression of transcription, cell cycle, ubiquitin and immune related genes that likely play a role in viral transcription, replication and pathogenesis. A down-modulation of translation related genes could be a mechanism by which EIAV controls cellular and/or viral protein production to prevent ER overload and premature cell death. The role of S2 in macrophage gene dysregulation during EIAV infection is not clear. However, the results presented herein identified key target genes to continue our studies into the role of S2 in viral replication and disease expression *in vivo* and may aid other investigators in their studies of EIAV pathogenesis.

Lastly, evaluation of additional time points post EIAV infection will give a more complete picture of the global changes in host gene expression that occur during an EIAV infection and thereby contribute to our understanding of lentiviral pathogenesis.

CHAPTER IV

IDENTIFICATION OF CELLULAR PROTEINS INTERACTING WITH EQUINE INFECTIOUS ANEMIA VIRUS S2 PROTEIN

Overview

The EIAV S2 gene encodes a 65 amino acid accessory protein of ~7 kDa. Although S2 is dispensable for EIAV replication *in vitro*, it is essential for the maintenance of high levels of viral replication and pathogenesis *in vivo*. Despite its essential role in disease expression, the mechanism(s) of S2 action *in vivo* remain elusive. By analogy with other retroviral accessory proteins S2 is likely to exert its function by interacting with cellular factor(s). To gain insight into the role of S2 during pathogenesis, we sought cellular factors that interact with S2 in a yeast two-hybrid screen. In this screen, we identified osteosarcoma amplified 9 (OS-9) and proteasome 26S ATPase subunit 3 (PSMC3) proteins as interacting partners of S2. These interactions were confirmed by co-immunoprecipitation experiments. To our knowledge this is the first report regarding S2 interactions with equine cellular proteins, an important step to gain understanding of protein-protein interactions that are involved in EIAV replication and disease development. Additional evidence is needed to demonstrate the physiological relevance of these interactions *in vivo*.

Introduction

Equine infectious anemia virus (EIAV) is a macrophage-tropic retrovirus (genus Lentivirus) of equids. Natural transmission occurs mechanically when biting flies move between infected and naïve animals during feeding (Kemen et al., 1978). Upon infection, acute disease may develop within days to weeks and is characterized by a high titer viremia accompanied by fever and pronounced thrombocytopenia. Clinical outcomes depend on the infecting virus strain, as well as host factors; horses frequently survive the acute disease episode to become life-long carriers. However some infected animals will develop a chronic form of the disease, manifested by recurring febrile episodes with clinical symptoms that include lethargy, edema, anemia, weight loss and diarrhea in addition to fever and thrombocytopenia (Clements and Payne, 1994; Montelaro et al., 1993; Payne et al., 2006).

EIAV genome organization is relatively simple when compared to primate lentivirus genomes (Payne et al., 2006). EIAV encodes gag, pol, env, tat and rev genes, but few additional auxiliary genes. In fact, EIAV appears to encode only two additional proteins, S2 and Ttm, neither of whose functions have been well characterized (Fagerness et al., 2006). The approximately 7 kDa (65-68 amino acid) S2 polypeptide is encoded by a short open reading frame (ORF) that overlaps env. S2 translation presumably occurs by leaky scanning of a tricistronic mRNA encoding Tat, S2 and Env or from a bicitronic mRNA encoding S2 and Env (Li et al., 1998; Schiltz et al., 1992).

The S2 ORF is present in all EIAV strains characterized to date suggesting functional significance (Fagerness et al., 2006; Li et al., 2000). Overall the S2 protein

has no obvious sequence homology to other viral or host cell proteins (Fagerness et al., 2006). S2 function has been probed by generating S2 mutant proviruses and assessing viral replication in permissive cell lines or in primary monocyte-derived-macrophages (Fagerness et al., 2006; Li et al., 2000; Li et al., 1998). Cell culture-based assays suggest that S2 does not play a major role in virion production or particle morphology, nor does it appear to be packaged into virions, although its presence may subtly enhance viral replication (Fagerness et al., 2006; Li et al., 2000; Li et al., 1998; Yoon et al., 2000). In contrast to effects observed in cultured cells, S2-deletion has profound effects on replication and virulence when assayed in horses or Shetland ponies where S2 is required for high titer virus replication and the development of acute disease (Fagerness et al., 2006). To gain insight into possible activities of the EIAV S2 protein, we performed a yeast 2-hybrid screen to identify host cell proteins that interact with S2. In the current report we describe the interaction of EIAV S2 with the cellular proteins amplified in osteosarcoma (OS-9) and proteasome 26S ATPase subunit 3 (PSMC3), a protein component of the 19S regulatory cap of the 26S proteasome (Hoyle et al., 1997; Tanahashi et al., 1998).

Materials and Methods

Yeast strain and media

The yeast strain used in the two-hybrid study, MaV203, was grown in YPD medium (1% yeast extract, 2% peptone, 2% dextrose). Yeast transformants harboring both prey and bait plasmids were maintained on synthetic complete (SC) medium lacking leucine and tryptophan. Yeast cells were grown at 30 °C.

Yeast two-hybrid screen

The ProQuest™ Two-Hybrid System with Gateway® Technology (Invitrogen) was used to identify potential EIAV S2-interacting proteins. The S2 open reading frame was amplified by PCR and was moved into pDEST™ 32 bait plasmid using recombination mediated cloning (Gateway® BP Clonase™) according to the manufacturer's instructions. The sequences of the primers used for amplification were S2 attB1 forward 5'-GGGG*ACAAGTTTGTACAAAAAAGCAGCCTTG*ATGGGAGTATT TGGT-3' and S2 attB2 reverse 5'-GGGG*ACCACTTTGTACAAGAAAGCTGGGT*TTTC TTGGTCTCTTGC-3'. The *att*B recombination sites are italicized and S2 specific sequences are indicated (underlined). Recombinants were isolated and subjected to DNA sequence analysis to confirm recovery of the desired constructs. The selected pDEST32-S2 bait construct was tested for self-activation (in the presence of pEXP-AD502) as recommended by the manufacturer. pDEST32-S2 was co-transformed into the yeast reporter strain MaV203 (Invitrogen) with a commercially available human spleen cDNA library (pPC86 vector, Invitrogen). Transformants were plated onto SC-Leu-Trp (to determine the total number of transformants) and the selective media SC-Leu-Trp-His +3AT. Patching and replica plating were performed exactly as described by the manufacturer to identify transformants that activate the three reporter genes His3, Ura3 and LacZ. After identification of the possible S2-interactors, both bait and prey plasmids were isolated from the yeast and transformed into *E. coli* followed by selection on LB agar with gentamicin and ampicillin respectively. Plasmid minipreps were performed followed by DNA sequence analysis. The proteins encoded by the cDNAs were

identified by performing BLAST searches.

ß-gal assay

The yeast ß-galactosidase assay kit (Pierce) was used to detect ß -galactosidase activity in transformed yeast cells. Briefly, single colonies of yeast transformants were diluted in 100 µl of the Y-PER reagent, gently mixing to create a homogenous solution. An equal volume of assay buffer was added and the reactions were incubated at 37 °C until a color change was observed. Reactions were stopped by adding 100 µl of the 2X ß -galactosidase stop solution.

Generation and expression of tagged fusion proteins

The EIAV S2 coding sequence was amplified by PCR with primers containing restriction sites for BamHI and HindIII. The resulting PCR product was digested with BamHI and HindIII and ligated into the similarly digested pET32 vector (Novagen). The S2 protein was expressed as a carboxyl-terminal histidine-tag fusion protein in *E coli* BL21 (DE3) cells. To purify S2, the S2-his tagged protein in *E coli* lysates were added to a Ni-agarose affinity column following the manufacturer's specifications (Invitrogen).

For expression in mammalian cells, the S2 coding sequence was PCR amplified using the forward primer 5'-GAGCTCAAGCTTCGAATTCATGGGATT ATTTG-3' and the reverse primer 5'-ACTGCAGAATTCTCATTTCTTGGTCTCTTG-3'. HindIII and EcoRI sites are underlined. The amplified fragments were double-digested with HindIII and EcoRI and then cloned into the pEGFP-C2 vector (BD Biosciences). The resultant amino-terminal GFP-tagged construct, GFP-S2, was used for transient

transfection in Chinese hamster ovary (CHO-K1) cells and expression was confirmed by western blot.

The hOS9, eOS9 and ePSMC3 cDNAs were amplified by PCR and cloned into the mammalian expression vector pcDNA^{TM}3.2/V5-DEST (Invitrogen) using recombination mediated cloning (Gateway® BP Clonase™) according to the manufacturer's instructions. Primer sequences used to generate the mammalian expression constructs are as follow: hOS9 attB1 inner forward 5'-*AAAAAGCAGGCT*TCACCATGGGTGCTGCACCGCAGGCCAT-3' and hOS9 attB2 inner reverse 5'-*AGAAAGCTGGGT*CAAATTCGTCCAGGTCCCCTGT-3', eOS9 attB1 inner forward 5'-*AAAAAGCAGGCT*TCACCATGGGGTGGACGTATGAATTCTG-3' and eOS9 attB2 reverse 5'-*AGAAAGCTGGGT*AGAAGTCAAATTCATCCA-3', ePSMC3 attB1 inner forward 5'-*AAAAAGCAGGCT*TCATGGCGGAGGAGATCATCC-3' and ePSMC3 attB2 inner reverse 5'-*AGAAAGCTGGGT*TGTAGTATTGTAGGTTG-3'. The *att*B recombination sites are italicized and gene specific sequences are underlined. The adaptor primer sequences, attB1: 5'-GGGGACAAGTTTGTACAAAA AAGCAGGCT-3' and attB2 5'-GGGGACCACTTTGTACAAGAAAGCTGGGT-3' were subsequently used to add the complete recombination site sequences. Constructs were expressed as carboxyl-terminal V5-tagged fusion proteins in CHO-K1 cells. Expression of GFP-S2, hOS9-V5, eOS9-V5 and ePSMC3-V5 were confirmed by western blot.

Western blot analysis and antibodies

To perform Western blot analysis, SDS-PAGE separated proteins were electro-transferred onto nitrocellulose membranes. Primary antibodies used in these studies were: mouse anti-his monoclonal antibody and mouse anti-V5 monoclonal antibody at a 1:5000 dilution (Invitrogen). Mouse anti-GFP monoclonal antibody was used at a 1:1000 dilution (Santa Cruz Biotechnology), mouse anti-human OS-9 (Center for Biomedical Invention, University of Texas Southwestern Medical School, Dallas TX) and goat anti-EIAV S2-his were used at a 1:500 dilution (generated at Bethel Laboratories, Inc). Secondary antibodies were horseradish peroxidase conjugates were used at a 1:3000 dilution (Pierce) and were detected using the ECL Western blotting detection system (Amersham). Chemiluminescence was detected by exposure to X-Omat AR film (Kodak).

Far Western blot

Purified S2-his and bovine serum albumin (~1 μg) were electrophoresed on 12% SDS-PAGE and then transferred onto a nitrocellulose membrane. After the membranes were blocked in Tris-buffered saline tween-20 (TBST) containing 5% skim milk for 1 h at room temperature, the bound membranes were incubated overnight at 4 ºC with a lysate containing the hOS9-V5 protein diluted in TBST. After washing with TBST to remove unbound proteins the membrane was incubated with antibodies against the V5 tag followed by incubation with HRP-conjugated antibody.

Cloning equine OS-9 and equine PSMC3

Total RNA was prepared from equine monocyte-derived macrophages and cDNA

was prepared using SuperScript® II Reverse Transcriptase (Invitrogen) and reverse PCR primers. Initial PCR products were recovered by TOPO TA (Invitrogen). As the equine genome sequence was unavailable at the time these studies were initiated, available sequences from other species were compared and used to design degenerate primers for amplification of equine OS-9 and equine PSMC3 by RT-PCR. The initial primer set used to amplify equine OS-9 was forward primer 5'-ATGGCGGCGGARDCGCTG CTGT-3' and reverse primer 5'-GGGTCAGAAGTCAAAYTCRTCCAGGTCCCCTGT -3'). The primer set used to amplify equine PSMC3 was forward primer 5'-TCCACGGAGGAGATCATC-3' and reverse primer 5'-CTAGGCGTAGTATTGTAG-3'. All PCR reactions were performed using Platinum® *Taq* DNA Polymerase High Fidelity (Invitrogen). The final concentrations of each reagent were 0.2 μM forward and reverse primers, 0.2 mM dNTPs, 2 mM $MgSO_4$, 1X High Fidelity PCR buffer, and 1 unit Platinum® *Taq* DNA Polymerase High Fidelity. All plasmids were purified using QIAprep spin columns (Qiagen). DNA sequencing reactions were performed using the ABI BigDye® Terminator Cycle Sequencing Kit; sequences were generated with an ABI PRISM® 3100 Genetic Analyzer.

Co-immunoprecipitation assays

Co-immunoprecipitation (Co-IP) analyses were used to confirm the interaction between S2 and the interacting proteins identified by the yeast-two hybrid assay. CHO-K1 cells were transiently cotransfected with GFP-S2 and either hOS9-V5, eOS9-V5 or ePSMC3 for 24 h. Cells were washed with PBS and harvested in RIPA buffer containing a protease inhibitor cocktail (Pierce). The crude cell lysate was then incubated with the

appropriate antibody (anti-V5 or anti-GFP) overnight at 4 ºC on a rotation wheel. Fifty µl of agarose G beads (Invitrogen) was used to collect the immunocomplex by gently incubation for 2 h at room temperature. The immunocomplex was then washed five times with IP wash buffer (Modified Dulbecco's PBS) and eluted in 100 µl of elution buffer (Pierce). Samples were subjected to SDS-PAGE electrophoresis and transferred onto nitrocellulose membranes. Western blots were performed using anti-V5 and anti-GFP antibodies.

Results

Identification of cellular proteins interacting with EIAV S2 using the yeast two hybrid system

One of the most commonly used approaches to aid in the understanding of viral protein function is the elucidation of interactions between the viral protein and the host cell. Analysis of viral-protein interactions is an important step to understand viral pathogenesis. Therefore, in an attempt to identify the host cellular proteins involved in S2 function, we employed the yeast two-hybrid system to search for S2 binding partners. Due to a lack of a validated equine cDNA library for yeast two-hybrid screening, a well-characterized human spleen cDNA library (Invitrogen) was used in this initial screen. Fig. 4.1 shows a schematic representation of the yeast two-hybrid system and the expected phenotypes of a positive interaction.

Briefly, S2 was fused to the Gal4-DNA binding domain "bait" plasmid and assayed for interaction with a Gal4 activation domain cDNA library used as the "prey". Both bait plasmid and prey library were cotransformed into the yeast reporter strain

MaV203, which contains the HIS3, URA3 and lacZ genes under the control of a GAL4 promoter.

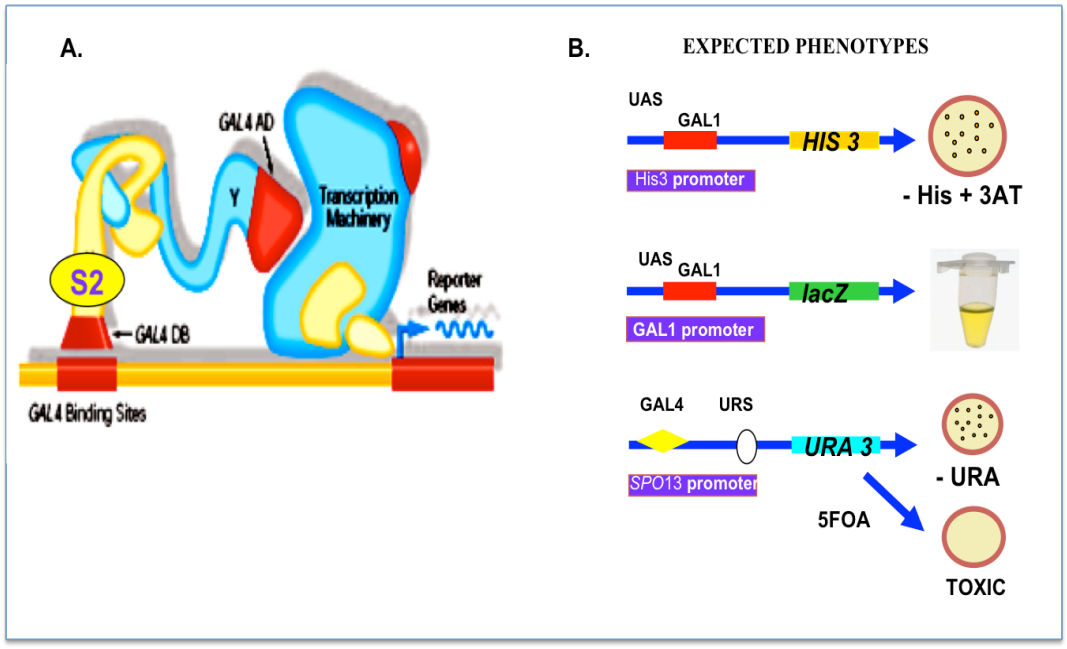

Figure 4.1. The principle of the yeast-two hybrid system. (A) Schematic representation of Gal4-DNA binding domain fusion with S2 and the Gal4 activation domain present in the cDNA clones of the human spleen cDNA library. **(B)** Expected phenotypes of a positive interaction.

If bait and prey physically interact with each other, they activate the transcription of the three reporter genes. Yeast clones containing interacting proteins grow in histidine and uracil deficient medium and activate ß-galactosidase expression. Moreover, an additional phenotype can be assayed by the inhibition of growth in media containing 5FOA (5-fluoroorotic acid) (ProQuest Two Hybrid Sytem, Invitrogen). The strength of the interaction can be measure by the activation of two (weak) to four (strong) of the reporter genes.

The screen resulted in recovery of three cDNAs, encoding two different cellular proteins. Fig. 4.2 demonstrates the pattern of reporter gene activation observed for each clone and a positive and negative control. Two cDNAs encoding human OS-9 (hOS-9) were recovered; both displayed strong interaction phenotypes, activating the three reporter genes in the system. One clone (designated LC14.1.1) encodes 430 amino acids of hOS-9; the second cDNA (LC10.1) encodes 419 amino acids. These partial cDNAs are probably derived from the alternatively spliced isoforms 1 and 2 of hOS-9 shown schematically in Fig. 4.3. A cDNA encoding 425 amino acids of the human PSMC3 (hPSMC3) also was recovered. Co-expression of PSMC3 with EIAV S2 reproducibly activated two of three reporter genes in a pattern indicating a weak interaction (Fig. 4.2).

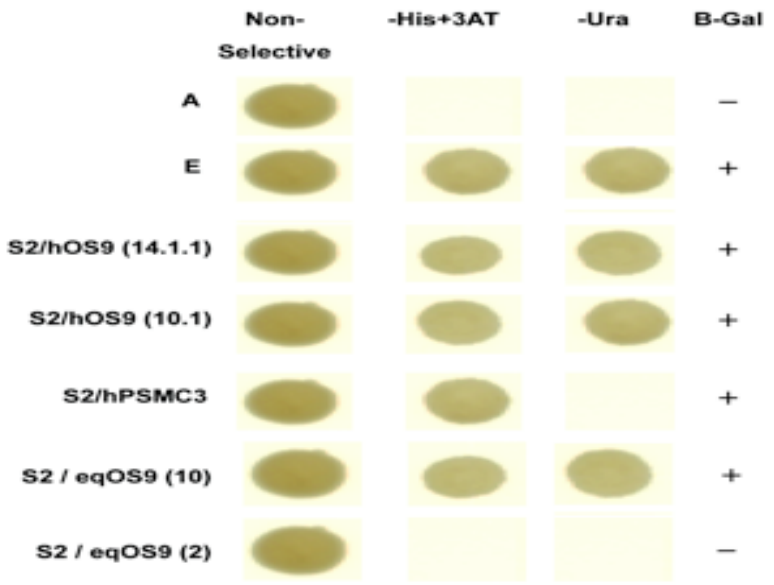

Figure 4.2. Summary of yeast two hybrid screen results. Figure shows a strong interaction phenotype for two human OS9 cDNAs and the weak interaction of phenotype of human PMCS3 with EIAVS2 in the yeast two-hybrid screen. Also shown are the interaction phenotypes of two equine OS9 clones. **A**, is the non-interaction control, and E is the strong interaction control.

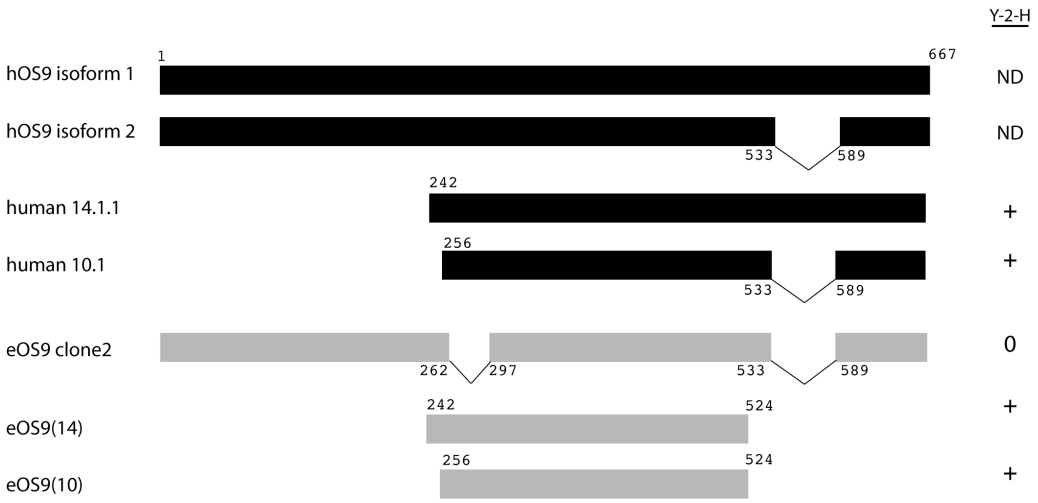

Figure 4.3. Schematic representation of known OS9 isoforms. Comparison of OS9 isoform 1 and 2 with cDNAs recovered from the yeast-two hybrid screen. Fragments of equine OS9 tested in the yeast-two hybrid assay are also shown schematically.

Validation of the yeast-two hybrid screen

To confirm the results from the yeast-two hybrid screen, we chose to validate the strong interaction between hOS-9 and EIAV S2 by performing far-western blot assays, using his-tagged EIAV S2 and V5-tagged hOS-9. As shown in Fig. 4.4, interactions between hOS-9 and S2 were observed between membrane-bound S2 and soluble hOS-9 (Fig. 4.4, panel A) and between soluble S2 and membrane-bound OS9 (Fig. 4.4, panel B). We also assayed equine macrophage for OS-9 expression and detected an abundantly expressed protein of the appropriate molecular weight by western blot using antisera to human OS-9 (Fig. 4.4, panel C).

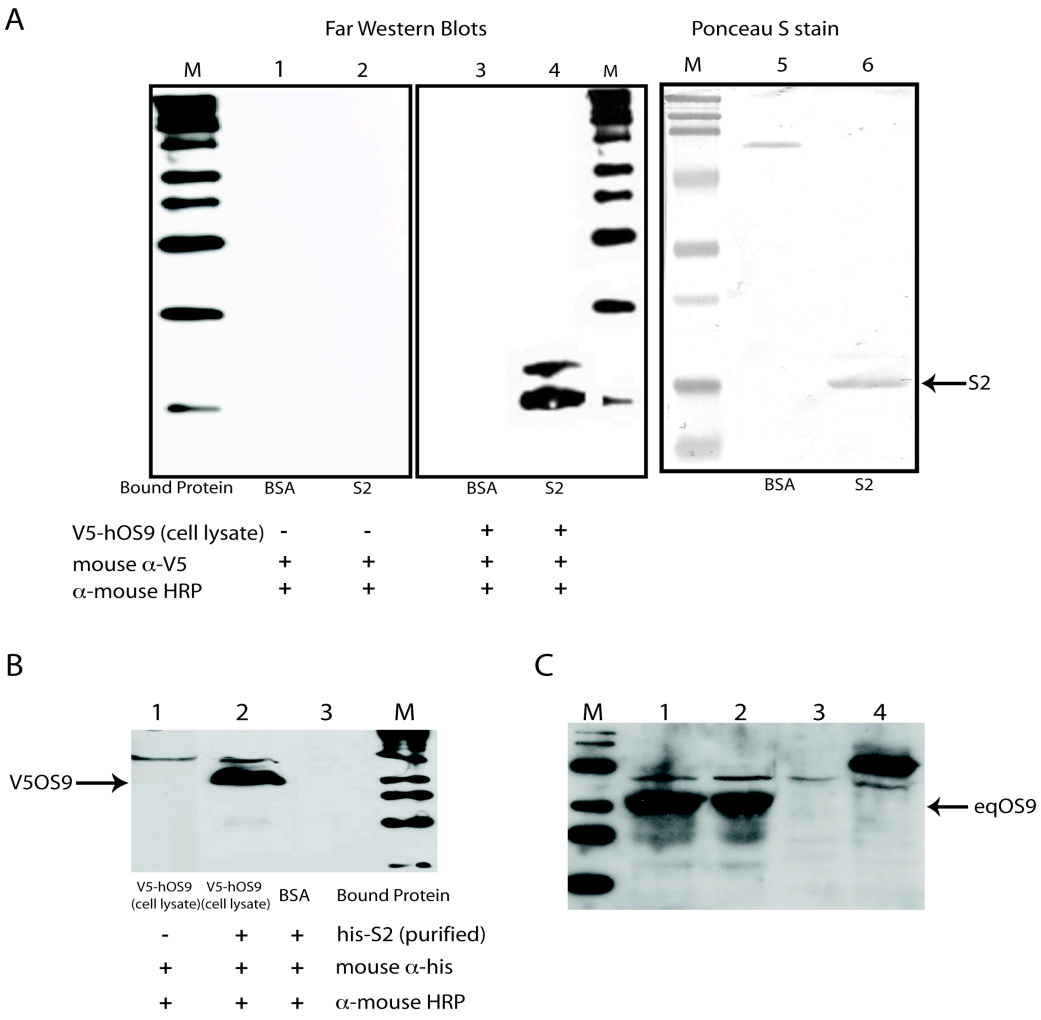

Figure 4.4. Far western blot assay results. Panel (A) Far western blots showing the interaction of immobilized recombinant S2 with recombinant V5-tagged hOS9 in CHO cell lysates. Lanes 1-3 are reagent controls. Lane 4 shows the binding of V5-OS9 to the membrane at the position of EIAV S2. OS9 is detected using mouse anti-V5. Lanes 5 and 6 show the positions of S2 and the control protein, bovine serum albumin. Panel (B) Far western blot showing the interaction of immobilized V5-OS9 with histidine tagged S2 (bacterially expressed). Panel (C) Western blot using anti human OS9. Lanes 1 and 2 contain lysates from equine monocyte-derived macrophages. Lane 3, CHO-K1 cell lysate. Lane 4, V5-tagged human OS9.

Cloning and amino acid sequence comparison of the equine OS9 and PSMC3

As the complete equine genome sequence was not publicly available at the time these studies, initial cDNA clones were obtained using degenerate primers. Partial cDNAs of equine OS-9 (eqOS-9) similar to hOS-9 isoforms 1 and 2 were recovered; a cDNA indicating a novel splice variant-labeled eOS9 clone_2 was also recovered (Fig. 4.5).

```
hOS9_isoform_2          MAAETLLSSLLGLLLLGLLLPASLTGGVGSLNLEELSEMRYGIEILPLPVMGGQSQSSDV
hOS9_clone_10.1         MAAETLLSSLLGLLLLGLLLPASLTGGVGSLNLEELSEMRYGIEILPLPVMGGQSQSSDV
hOS9_clone_14.1.1       MAAETLLSSLLGLLLLGLLLPASLTGGVGSLNLEELSEMRYGIEILPLPVMGGQSQSSDV
hOS9_isoform_1          MAAETLLSSLLGLLLLGLLLPASLTGGVGSLNLEELSEMRYGIEILPLPVMGGQSQSSDV
eOS9_clone_2            MAAEALLSSVLGLLLLGLLLPASLTGGVGSLNLEELSEMRYGIEILPLPVMGGQSQASDV
eOS9_isoform_1          MAAEALLSSVLGLLLLGLLLPASLTGGVGSLNLEELSEMRYGIEILPLPVMGGQSQASDV
                        ****:****:*********************************************:***

hOS9_isoform_2          VIVSSKYKQRYECRLPAGAIHFQREREEETPAYQGPGIPELLSPMRDAPCLLKTKDWWTY
hOS9_clone_10.1         VIVSSKYKQRYECRLPAGAIHFQREREEETPAYQGPGIPELLSPMRDAPCLLKTKDWWTY
hOS9_clone_14.1.1       VIVSSKYKQRYECRLPAGAIHFQREREEETPAYQGPGIPELLSPMRDAPCLLKTKDWWTY
hOS9_isoform_1          VIVSSKYKQRYECRLPAGAIHFQREREEETPAYQGPGIPELLSPMRDAPCLLKTKDWWTY
eOS9_clone_2            VIVSSKYKQRYECRLPAGAIHFQREREEETPAYQGPGIPELLSPMKDAPCLLKTKDWWTY
eOS9_isoform_1          VIVSSKYKQRYECRLPAGAIHFQREREEETPAYQGPGIPELLSPMKDAPCLLKTKDWWTY
                        ********************************************:**************

hOS9_isoform_2          EFCYGRHIQQYHMEDSEIKGEVLYLGYYQSAFDWDDETAKASKQHRLKRYHSQTYGNGSK
hOS9_clone_10.1         EFCYGRHIQQYHMEDSEIKGEVLYLGYYQSAFDWDDETAKASKQHRLKRYHSQTYGNGSK
hOS9_clone_14.1.1       EFCYGRHIQQYHMEDSEIKGEVLYLGYYQSAFDWDDETAKASKQHRLKRYHSQTYGNGSK
hOS9_isoform_1          EFCYGRHIQQYHMEDSEIKGEVLYLGYYQSAFDWDDETAKASKQHRLKRYHSQTYGNGSK
eOS9_clone_2            EFCYGRHIQQYHMEDSEIKGEVLYLGYYHSAFDWDDETAKASKQHRLKRYHSQTYGNGSK
eOS9_isoform_1          EFCYGRHIQQYHMEDSEIKGEVLYLGYYHSAFDWDDETAKASKQHRLKRYHSQTYGNGSK
                        ****************************:*******************************

hOS9_isoform_2          CDLNGRPREAEVRFLCDEGAGISGDYIDRVDEPLSCSYVLTIRTPRLCPHPLLRPPPSAA
hOS9_clone_10.1         CDLNGRPREAEVRFLCDEGAGISGDYIDRVDEPLSCSYVLTIRTPRLCPHPLLRPPPSAA
hOS9_clone_14.1.1       CDLNGRPREAEVRFLCDEGAGISGDYIDRVDEPLSCSYVLTIRTPRLCPHPLLRPPPSAA
hOS9_isoform_1          CDLNGRPREAEVRFLCDEGAGISGDYIDRVDEPLSCSYVLTIRTPRLCPHPLLRPPPSAA
eOS9_clone_2            CDLNGRPREAEVRFLCDEGAGISGDYIDRVDEPLSCSYVLTIRTSRLCPHPLLRPPPSAA
eOS9_isoform_1          CDLNGRPREAEVRFLCDEGAGISGDYIDRVDEPLSCSYVLTIRTSRLCPHPLLRPPPSAA
                        *******************************************.**************

hOS9_isoform_2          PQAILCHPSLQPEEYMAYVQRQADSKQYGDKIIEELQDLGPQVWSETKSGVAPQKMAGAS
hOS9_clone_10.1         PQAILCHPSLQPEEYMAYVQRQADSKQYGDKIIEELQDLGPQVWSETKSGVAPQKMAGAS
hOS9_clone_14.1.1       PQAILCHPSLQPEEYMAYVQRQADSKQYGDKIIEELQDLGPQVWSETKSGVAPQKMAGAS
hOS9_isoform_1          PQAILCHPSLQPEEYMAYVQRQADSKQYGDKIIEELQDLGPQVWSETKSGVAPQKMAGAS
eOS9_clone_2            PQAILCHPALQPEEYMAYIQRQA--------------------------------GAG
eOS9_isoform_1          PQAILCHPALQPEEYMAYIQRQADSKQYGEKIMEELPDPDPQMWRETKPGMVPPKRAGAG
                        ********:*********:****                                **.
```

Figure 4.5. Amino acid sequence comparison of human and equine OS9. * indicates single, fully conserved residues (blue), : indicates conservation of strong groups (green) and – indicates no consensus sequence (black).

```
hOS9_isoform_2          PTKDDSKDSDFWKMLNEPEDQAPGGEEVPAEEQDPSPEAADSASGAPNDFQNNVQVKVIR
hOS9_clone_10.1         PTKDDSKDSDFWKMLNEPEDQAPGGEEVPAEEQDPSPEAADSASGAPNDFQNNVQVKVIR
hOS9_clone_14.1.1       PTKDDSKDSDFWKMLNEPEDQAPGGEEVPAEEQDPSPEAADSASGAPNDFQNNVQVKVIR
hOS9_isoform_1          PTKDDSKDSDFWKMLNEPEDQAPGGEEVPAEEQDPSPEAADSASGAPNDFQNNVQVKVIR
eOS9_clone_2            PTKDDSKESDFWKILHEPEDQAPGGEEAQVEEQEPSLEAAGPAPGSPDDFQNNVQVKVIR
eOS9_isoform_1          PTKDDSKESDFWKILHEPEDQAPGGEEAQAEEQEPSLEAADPAPGSPDDFQNNVQVKVIR
                        *******:*****:*:***********. .***:** ***..*.*:*:************

hOS9_isoform_2          SPADLIRFIEELKGGTKKGKPNIGQEQPVDDAAEVPQREPE-KERGDPERQREMEEEEDE
hOS9_clone_10.1         SPADLIRFIEELKGGTKKGKPNIGQEQPVDDAAEVPQREPE-KERGDPERQREMEEEEDE
hOS9_clone_14.1.1       SPADLIRFIEELKGGTKKGKPNIGQEQPVDDAAEVPQREPE-KERGDPERQREMEEEEDE
hOS9_isoform_1          SPADLIRFIEELKGGTKKGKPNIGQEQPVDDAAEVPQREPE-KERGDPERQREMEEEEDE
eOS9_clone_2            SPADLTRLIEELKGGTKKGKPNAGQEQPADDAAEVPQREPEVKEKGDREHQNEVEEEEED
eOS9_isoform_1          SPADLIRLIEELKGGTKKGKPNAGQEQPADDAAEVPQREPEVKEKGDREHQNEVEEEEED
                        ***** *:************** *****.************ **:** *:*.*:****::

hOS9_isoform_2          DEDEDEDEDERQLLGEFEKELEGILLPSDRDRLRSEVKAGMERELENIIQETEKELDPDG
hOS9_clone_10.1         DEDEDEDEDERQLLGEFEKELEGILLPSDRDRLRSEVKAGMERELENIIQETEKELDPDG
hOS9_clone_14.1.1       DEDEDEDEDERQLLGEFEKELEGILLPSDRDRLRSEVKAGMERELENIIQETEKELDPDG
hOS9_isoform_1          DEDEDEDEDERQLLGEFEKELEGILLPSDRDRLRSEVKAGMERELENIIQETEKELDPDG
eOS9_clone_2            DEDEDEDEDERQLLGEFEKELEGILLPSDRERLRSEVKAGMERELENIIQETEKELDPDG
eOS9_isoform_1          DEDEDEDEDERQLLGEFEKELEGILLPSDRERLRSEVKAGMERELENIIQETEKELDPDG
                        ********************************:****************************

hOS9_isoform_2          LKKESERDRAMLALTSTLNKLIKRLEEKQSPELVKKHKKKRVVPKKPPPSPQPT------
hOS9_clone_10.1         LKKESERDRAMLALTSTLNKLIKRLEEKQSPELVKKHKKKRVVPKKPPPSPQPT------
hOS9_clone_14.1.1       LKKESERDRAMLALTSTLNKLIKRLEEKQSPELVKKHKKKRVVPKKPPPSPQPTEEDPEH
hOS9_isoform_1          LKKESERDRAMLALTSTLNKLIKRLEEKQSPELVKKHKKKRVVPKKPPPSPQPTEEDPEH
eOS9_clone_2            LKKESERDRAMLALTSTLNKLIKRLEEKQSPELVKRHRKRRVVPKKPPPTPQPA------
eOS9_isoform_1          LKKESERDRAMLALTSTLNKLIKRLEEKQSPELVKRHRKRRVVPKKPPPTPQPAEEDPEH
                        ************************************:*:*:*********:***:

hOS9_isoform_2          --------------------------------------------------GKIEIKIVRPW
hOS9_clone_10.1         --------------------------------------------------GKIEIKIVRPW
hOS9_clone_14.1.1       RVRVRVTKLRLGGPNQDLTVLEMKRENPQLKQIEGLVKELLEREGLTAAGKIEIKIVRPW
hOS9_isoform_1          RVRVRVTKLRLGGPNQDLTVLEMKRENPQLKQIEGLVKELLEREGLTAAGKIEIKIVRPW
eOS9_clone_2            --------------------------------------------------GKIEIKIVRPG
eOS9_isoform_1          RVRVRVTKLRHGGPNQDLTVLEMKRENPQLKQIEGLVKELLEREGLTAEGKIEIKIVRPG
                                                                           **********

hOS9_isoform_2          AEGTEEGARWLTDEDTRNLKEIFFNILVPGAEEAQKERQRQKELESNYRRVWGSPGGEGT
hOS9_clone_10.1         AEGTEEGARWLTDEDTRNLKEIFFNILVPGAEEAQKERQRQKELESNYRRVWGSPGGEGT
hOS9_clone_14.1.1       AEGTEEGARWLTDEDTRNLKEIFFNILVPGAEEAQKERQRQKELESNYRRVWGSPGGEGT
hOS9_isoform_1          AEGTEEGARWLTDEDTRNLKEIFFNILVPGAEEAQKERQRQKELESNYRRVWGSPGGEGT
eOS9_clone_2            NEGSEDDARWLTDEDTKNLKEIFFNILVQGAEEAQKERQRQKELESNYRRVWGSPGGEGT
eOS9_isoform_1          NEGSEDDARWLTDEDTKNLKEIFFNILVQGAEEAQKERQRQKELESNYRRVWGSPGGEGT
                         **:*:.*********:*********** ********************************

hOS9_isoform_2          GDLDEFDF
hOS9_clone_10.1         GDLDEFDF
hOS9_clone_14.1.1       GDLDEFDF
hOS9_isoform_1          GDLDEFDF
eOS9_clone_2            GDLDEFDF
eOS9_isoform_1          GDLDEFDF
                        ********
```

Figure 4.5 continued

A full-length cDNA encoding the equine homologue of PSMC3 (eqPSMC3) was also recovered. The translation of this cDNA reveals strong amino acid sequence conservation between human and equine PSMC3 (Fig. 4.6). They differ by only two amino acids with conservation of strong groups.

```
ePSMC3          ------------------------------------MSTEEIIQRTRLLDSEIKIMRSEVL
hPSMC3          MNLLPNIESPVTRQEKMATVWDEAEQDGIGEEVLKMSTEEIIQRTRLLDSEIKIMKSEVL
                                                    ********************:****

ePSMC3          RVTHELQAMKDKIKENSEKIKVDKTLPYLVSNVIELLDVDPNDQEEDGANIDLDSQRKGK
hPSMC3          RVTHELQAMKDKIKENSEKIKVNKTLPYLVSNVIELLDVDPNDQEEDGANIDLDSQRKGK
                ***********************:************************************

ePSMC3          CAVIKTSTRQTYFLPVIGLVDAEKLKPGDLVGVNKDSYLILETLPTEYDSRVKAMEVDER
hPSMC3          CAVIKTSTRQTYFLPVIGLVDAEKLKPGDLVGVNKDSYLILETLPTEYDSRVKAMEVDER
                ************************************************************

ePSMC3          PTEQYSDIGGLDKQIQELVEAIVLPMNHKEKFENLGIQPPKGVLMYGPPGTGKTLLARAC
hPSMC3          PTEQYSDIGGLDKQIQELVEAIVLPMNHKEKFENLGIQPPKGVLMYGPPGTGKTLLARAC
                ************************************************************

ePSMC3          AAQTKATFLKLAGPQLVQMFIGDGAKLVRDAFALAKEKAPSIIFIDELDAIGTKRFDSEK
hPSMC3          AAQTKATFLKLAGPQLVQMFIGDGAKLVRDAFALAKEKAPSIIFIDELDAIGTKRFDSEK
                ************************************************************

ePSMC3          AGDREVQRTMLELLNQLDGFQPNTQVKVIAATNRVDILDPALLRSGRLDRKIEFPMPNEE
hPSMC3          AGDREVQRTMLELLNQLDGFQPNTQVKVIAATNRVDILDPALLRSGRLDRKIEFPMPNEE
                ************************************************************

ePSMC3          ARARIMQIHSRKMNVSPDVNYEELARCTDDFNGAQCKAVCVEAGMIALRRGATELTHEDY
hPSMC3          ARARIMQIHSRKMNVSPDVNYEELARCTDDFNGAQCKAVCVEAGMIALRRGATELTHEDY
                ************************************************************

ePSMC3          MEGILEVQAKKKANLQYYA
hPSMC3          MEGILEVQAKKKANLQYYA
                ******************
```

Figure 4.6. Amino acid sequence comparison of human and equine PSMC3. * indicates single, fully conserved residues (blue), : indicates conservation of strong groups (green) and – indicates no consensus sequence (black).

Detecting the interaction between S2 and eqOS9 using the yeast two-hybrid system

Three eqOS-9 fusions were tested in the yeast 2-hybrid assay. These included fragments starting at amino acids 242 and 256 and ending just upstream of the location of the alternatively spliced region of hOS-9 (Fig. 4.3). Both of these fragments showed strong interacting phenotypes when tested with S2 (Figs. 4.2 and 4.3). A full-length version of the novel eqOS-9 isoform was also tested, but this form failed to interact in the yeast 2-hybrid assay suggesting that a region of approximately 40 amino acids (262-297 of eqOS9) is necessary for the interaction of eOS9 and S2.

Validation of the interactions by co-immunoprecipitation asssay

Interaction between EIAV S2 and eqOS-9 was also probed using a co-immunoprecipitation assay. A full-length version of eqOS-9 clone 14 was fused to the V5 tag of pcDNA3.2V5 (Invitrogen). EIAV S2 was expressed as an N-terminal green fluorescent protein (GFP) fusion in the pEGFP-C2 vector (BD Biosciences). Plasmids expressing eqOS-9 or GFP-S2 were transfected individually into CHO-K1 cells and protein expression was verified by western blots using mouse anti-V5 or mouse anti-GFP antibodies. As shown in Fig. 4.7, panel A, when cell lysates were mixed, specific interactions between S2 and eqOS-9 were readily detected by co-immunoprecipitation.

As the hPSMC3 S2 interaction in the yeast-two hybrid assay was weak, ePSMC3 was not rescreened in that assay, but was instead tested for interaction with S2 using the co-immunoprecipitation assay. As shown in Fig. 4.7, panel B an interaction between S2 and eqPSMC3 was readily detected.

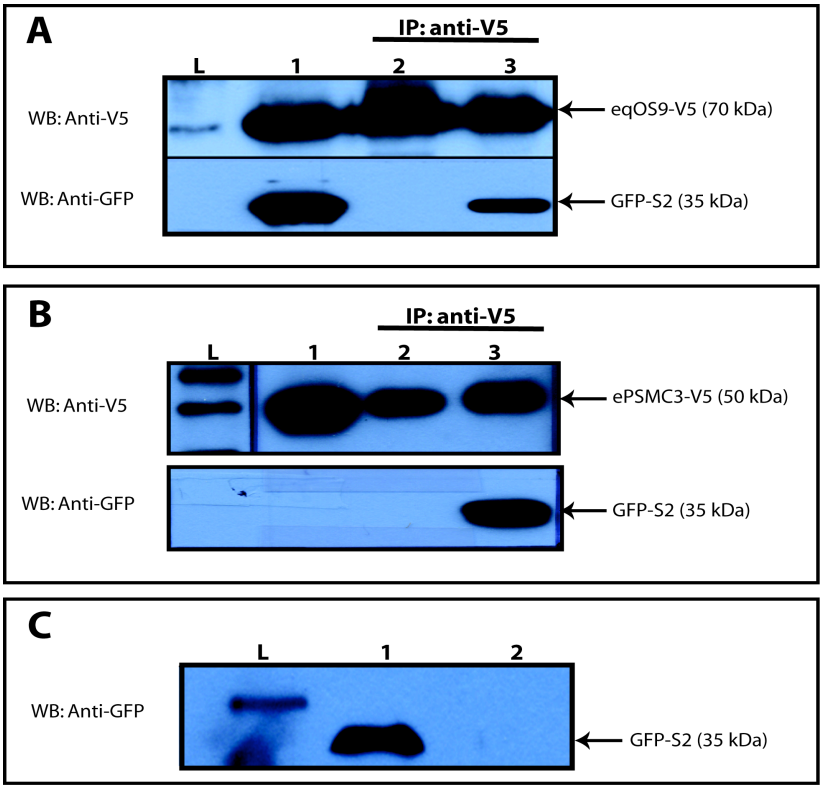

Figure 4.7. Co-immunoprecipitation of EIAV S2 with eqOS9 and eqPMSC3. Panel **(A)** Co-IP of eqOS9 and S2. Lane 1: Mixed lysates from eqOS9-V5 and GFP-S2 transfected cells. Lane 2: Mixed lysates, eqOS9 and GFP-control tranfected cells; immunoprecipitated with anti-V5. Lane 3: Mixed lysates, eqOS9 and GFP-S2 transfected cells; immunoprecipitated with anti-V5. Blots with anti-GFP or anti-V5 are as indicated. Panel **(B)** Co-IP of ePSMC3-V5 and GFP-S2. Lane 1: Lysate from ePSMC3-V5 transfected cells. Lane 2: ePSMC3-V5 transfected cell lysate mixed with GFP-control lysate; immunoprecipitated with anti-V5. Lane 3: ePSMC3-V5 transfected cell lysate mixed with GFP-S2 transfected cell lysate.; immunoprecipitated with anti-V5. Panel **(C)** GFP-S2 control. Lysate from GFP-S2 transfected cells was immunoprecipitated with anti-V5. Lane 1: Column flow-through. Lane 2. Column eluent. Protein markers (L)

Discussion

While largely dispensable for virus replication in cultured cells, EIAV S2 is required for efficient replication and disease expression in infected animals (Fagerness et al., 2006; Li et al., 2000). An S2-deleted virus, generated on the background of a highly virulent molecular clone, replicates at virus titers two to four logs lower than the parental virus in a Shetland pony model (Fagerness et al., 2006). No specific functions have yet been ascribed to the 66 amino acid S2 polypeptide and as it shares no overall amino acid sequence similarity with any other viral or cellular protein, hence sequence reveals little about possible function. To elucidate possible roles of S2 during infection, we sought for interacting proteins using a yeast two-hybrid screen against a human spleen cDNA library. OS9 and PSMC3 were identified as EIAV S2 interacting proteins.

OS-9 is encoded on human chromosome 12q 13-15, a region frequently amplified in human cancers (Su et al., 1996). OS-9 is ubiquitously expressed and four isoforms have been identified (Bernasconi et al., 2008; Kimura et al., 1998). Both cytoplasmic and ER localization of OS-9 have been reported and multiple protein activities have been proposed. An early report describes a role for OS-9 in the regulation of proteosome-mediated degradation of the transcription factor HIF1-α in an oxygen dependent manner (Baek et al., 2005). OS-9 has been reported to bind misfolded proteins in the ER lumen, directing them to the endoplasmic reticulum associated protein degradation pathway (Alcock and Swanton, 2009). Yet other studies suggest that OS9 plays a role in protein trafficking by serving as a multi-target adaptor of proteins moving from the ER to the Golgi (Jansen et al., 2009; Litovchick et al., 2002; Wang et al., 2007).

The various isoforms of OS-9 also may differ in their cellular location and/or function. Transport of meprin-β by OS-9 requires isoform 1 but is inhibited by isoform 2 (Litovchick et al., 2002). In contrast, transport of the dendritic cell-specific transmembrane protein (DC-STAMP) from the ER to the cis-golgi occurs in the presence of full-length OS9 isoforms 1 and 2, but is inhibited by a C-terminal OS-9 deletion (Jansen et al., 2009). In this study we report that EIAV S2 interacts with C-terminal deletions of both isoforms 1 and 2, but does not interact with a novel splice variant lacking amino acids 262 to 297. Thus the binding of S2 to OS9 may interrupt binding of some cellular OS9 partners, or may influence the trafficking or degradation of OS-9 containing complexes.

The interaction of EIAV S2 with PMSC3 is notable in that this cellular protein was first described as an HIV-1 Tat binding protein (thus its initial designation as Tat binding protein 1 or TBP1) (Nelbock et al., 1990). PMSC3/TBP1 is one of 6 ATPases found at the base of the 19S regulatory subunit of the proteasome (Tanahashi et al., 1998). In yeast these ATPases (rpt1-6) do not have redundant functions, as null mutants of any single rpt are lethal and cannot be rescued by overexpression of the others (Ferrell et al., 2000). PMSC3/TBP1 is a multifunctional protein involved in diverse cellular processes. For example, cellular levels of the tumor suppressor p14ARF are stabilized by PMSC3/TBP1 (Satoh et al., 2009). In contrast TBP-1/PMSC3 promotes degradation of hypoxia-inducible factor 1 (HIF-1) (Corn et al., 2003), a master regulator of oxygen homeostasis. PMSC3 also has been shown to have a crucial role in regulating the transcription of the class II transactivator (CIITA) (Truax et al.). CIITA, a positive

regulator of MHC class II genes is key in the regulation of the adaptive immune responses (Krawczyk et al., 2008). A number of other cellular proteins interact with PMSC3/TBP1 including tumor necrosis factor receptor associated factors (trafs) 4 and 6 (Rozan and El-Deiry, 2006).

It is difficult to predict any specific outcome of interaction between S2 and PMSC3/TBP1 as the proteasome itself is multifunctional and regulates many important cellular processes directly or indirectly through proteolysis of ubiquitinated and nonubiquitinated substrates (reviewed in (Bhaumik and Malik, 2008)). Recently the 19S regulatory subunits have been demonstrated to regulate cellular and viral promoters in both proteolytic and non-proteolytic modes (Bhaumik and Malik, 2008; Lassot et al., 2007). During HIV-1 infections, a 19S-like complex was determined to be required, in a nonproteolytic manner, for Tat-mediated transcription elongation from the HIV-1 promoter (Lassot et al., 2007).

There is certainly much precedent for roles of lentiviral accessory proteins in protein trafficking and degradation. HIV-1 Vpu, Vif and Vpr all induce the polyubiquitination and proteasomal degradation of their cellular targets (reviewed in (Malim and Emerman, 2008)). HIV-1 Vpu is an accessory protein similar to EIAV S2 with regard to its position in the lentiviral genome and its expression strategy. Both Vpu and S2 are encoded by open reading frames that overlap env and both are expressed via leaky ribosome scanning (Krummheuer et al., 2007; Schiltz et al., 1992; Schwartz et al., 1992). HIV-1 Vpu is an 81 aa protein whose activities include degradation of CD4 and interaction with proteasome members to inhibit IκB degradation (Malim and Emerman,

2008). Vpu is an integral membrane protein that contains a high proportion of charged residues in its cytoplasmic domain and has a pair of serine residues that are constitutively phosphorylated by casein kinase II (CKII) (Friborg et al., 1995). While S2 does not appear to have a transmembrane domain, it does have a myristoylation signal such that myristoylated S2 could direct the polypeptide to membranes. S2 also has a pair of conserved serine residues that could be substrates for CKII. We cannot rule out that the observed S2 interactions with OS9 and/or PSMC3 simply reflect the degradation of S2 itself, but given the important roles for other viral accessory proteins in influencing key host cell protein levels, this seems unlikely. The results presented herein indicate that one role of S2 could be that of altering host cell protein trafficking and/or degradation via OS9 and/or PSMC3/TBP1 interactions.

Although this is the first report to identify S2 host cellular binding partners, the identification of OS9 and PSMC3 as S2 interacting proteins does not provide a clear understanding of S2 function. Additional experiments will be needed to further elucidate the functional relevance of these interactions in vivo.

CHAPTER V

SUMMARY AND FUTURE DIRECTIONS

In the early 2000s the EIAV accessory protein S2 was found to be a critical factor in EIAV infection. S2 is not only necessary for maintaining high levels of viremia but also for disease development in the infected horse. A decade later, the mechanism(s) by which S2 induces disease remains a mystery. The studies presented in this dissertation provide an important starting point to elucidate the mode of action of EIAV S2.

The first study, EIAV S2 enhances pro-inflammatory cytokine and chemokine response in infected macrophages, published in Virology (Covaleda et al., 2010), addresses the role of S2 in cytokine/chemokine dysregulation. This is the first study to delineate the effect of S2 in cytokine and chemokine response during EIAV infection. Overall, we determined that S2 enhances the expression of IL-1α, IL-1β, IL-8, MCP-2, MIP-1β and IP-10, favoring a pro-inflammatory and chemotactic response. In support of this finding, the only anti-inflammatory cytokine evaluated in this study, IL-10, was not significantly affected during EIAV infection at the time points analyzed. Our results also indicated that S2 is not the sole determinant in cytokine induction, however suggested a role of S2 in optimizing a suitable environment for viral replication and dissemination by attracting target cells to the site of infection. These results, together with the *in vitro* studies by Lim et al. (2005) that describe a role for EIAV SU in the induction of

proinflammatory cytokines in eMDM, and Payne et al. (Payne et al., 2004) and Fagerness et al. (2006) that reveal roles of SU and S2 respectively in disease expression support the role of pro-inflammatory cytokines in virus replication and disease expression in the horse. These results suggest a scenario whereby EIAV SU and S2 act in concert to produce a robust pro-inflammatory cytokine response, which attracts target cells to the site of infection and promotes vigorous virus replication and disease expression.

Another finding was that S2 specifically up-regulates mRNA levels of IL-34, a novel cytokine specifically involved in monocyte proliferation and survival. This certainly is intriguing since monocytes/macrophages are the only target cells for EIAV infection, unlike HIV. Modulation of IL-34 expression by S2 could increase the pool of target cells available for infection greatly influencing disease expression.

An equine macrophage cell line was not available to use for this project. Thus, we used primary macrophage cell cultures to evaluate the cytokine/chemokine response upon EIAV infection. Three of the drawbacks with using primary cell lines are (i) limited amount of cells that can be obtained at one time from a single horse, (ii) activation of isolated cells, and (iii) the high degree of variability in the cytokine response among donors. Consequently, we screened for cell activation in each experiment to ensure that changes in the cytokine response were due to EIAV infection and not to activation of the cells due to manipulations during isolation. In addition, although not statistically significant, there were some marked differences in the expression of some cytokines and chemokines among donors. For example, IP-10 gene

expression at day 4 post-infection varied from 1 to 18 fold between $EIAV_{17}$ and $EIAV_{17\Delta S2}$ infected macrophages when examined from different horses. Although primary macrophages more closely reflect *in vivo* effects during EIAV infection, established cell lines can provide an unlimited supply of cells, easy standardization, reduced risk of cell activation and eliminate inter-donor variability. Recently, an equine macrophage cell line was characterized (Fidalgo-Carvalho et al., 2009); the use of this cell line will offer the advantage to continue studying several aspects of EIAV infection that have been hampered by the lack of a suitable equine macrophage-like cell line.

As for future studies, as equine immunological reagents become available it will be important to determine if the gene expression changes in cytokine and chemokines observed during EIAV infection correlate with changes at the protein level. This will give a more complete overview of the cytokine response upon EIAV infection.

To test the hypothesis that S2 enhances monocyte/macrophage chemotaxis through up-regulation of IL-8, MCP-2, MIP-1β and IP-10, the following experiments can be performed: (1) Measurement of chemokine protein levels in infected supernatants by ELISA and (2) Lymphocyte chemotaxis assays to evaluate whether supernatants from EIAV infected macrophages enhance lymphocyte chemotaxis compared with supernatants from S2-deleted virus.

In addition, it will be worth testing the extent in which S2 function is in regulating the proliferation of macrophage progenitors by increasing the levels of IL-34 in eMDMs.

In the second study, probing the function of the EIAV S2 protein using equine whole genome oligonucleotide array, the goals were to identify genes that are regulated post-infection and predict cellular processes that are affected during infection of primary macrophages with virulent EIAV and compared to those macrophages infected with the S2-deleted virus. Microarray analysis revealed a set of differentially expressed genes upon EIAV infection. Genes affected by EIAV were involved in the immune response, transcription, translation, cell cycle and cell survival.

Future studies should focus on obtaining a complete picture of gene expression profiles upon EIAV infection with additional time points post-infection and evaluating the contribution of the genes identified in this study in the pathogenesis of EIAV.

In the third study, we identified cellular proteins interacting with equine infectious anemia virus S2 protein (Accepted for publication April 2010, Virus Res). By analogy with other retroviral proteins, S2 is likely to accomplish an essential role in EIAV infection by interacting with host cellular factors. Therefore, our goal was to do a preliminary search for those factors by using a well-characterized human spleen cDNA library available for yeast two-hybrid studies. Here, we report the identification of osteosarcoma amplified 9 (OS-9) and proteasome 26S ATPase subunit 3 (PSMC3) proteins as interacting partners of S2. We cloned the equine homologs and confirmed the interactions by yeast two hybrid and co-immunoprecipitation assays. Both proteins are involved in protein trafficking and/or degradation, suggesting a role of S2 in this cellular pathway. Although this is the first report to identify S2 binding partners, the relevance of these interactions *in vivo* remains unclear. Additional experiments are needed to

demonstrate the physiological importance of these interactions *in vivo*. One approach is to silence OS-9 and/or TBP-1 expression in macrophages and determine the effect in viral replication, although since S2 is not required for viral replication *in vitro*, we may not necessarily see a direct effect. Another approach is to map the region where the interaction takes place, generate mutant viruses and test those mutants in the animal.

In this study, due to a lack of a validated equine cDNA library for yeast two-hybrid screening, we chose to do an initial search for S2 binding partners using a well characterized human cDNA library. However, we are aware that we could have missed important S2-interacting proteins due to an undeniable degree of genetic variation between humans and equids. Continuing studies to identify more cellular proteins that interact with S2 using a custom made equine cDNA library and/or pull-down assays combined with mass spectrometry would contribute to discerning the mechanism(s) of S2 mode of action.

Another line of S2 research that will help in the understanding of S2 function is the biochemical characterization of S2. As far as we know, no studies have been completed in the characterization of the putative motifs in S2. Alignments of available S2 proteins sequences indicate several putatively conserved, well-characterized protein motifs and therefore are presumed to play an important role in S2 function *in vivo*. These include an N-terminal myristoylation motif (GVTWSA), the nucleoporin motif (GLFG), the nuclear localization signal (RRKQETKK) motif, the proline rich (PxxP) SH3 binding motif, a casein kinase II (CKII) phosphorylation motif and at least two protein kinase phosphorylation sites (Leroux et al., 2004; Li et al., 2000). Similar to EIAV S2,

HIV Nef is dispensable for viral replication *in vitro* and is important for achieving high viral load and disease progression *in vivo* (Jamieson et al., 1994; Kestler et al., 1991). Studies have shown that the N-terminal myristoylation signal in Nef is essential for MHC class I and CD4 down-regulation, which enables HIV to escape from the host immune response (Peng and Robert-Guroff, 2001). Moreover, the PxxP motif present in Nef, is required for enhanced viral replication, MHC class I down-regulation and disease development (Brown et al., 2004; Chang et al., 2001; Khan et al., 1998). Similar to the role of the PxxP motif in Nef, it has been hypothesized that the PxxP motif in S2 plays also an important role in S2 function *in vivo*, due the high conservation of this motif in all but one of the known EIAV strains and isolates recovered from infected ponies during febrile episodes (Craigo et al., 2009; Li et al., 2000; Payne, 2006). Studies need to be conducted to determine the role of the different S2 motifs in viral replication and disease expression.

In summary, the results from this study contribute to our understanding of the role S2 in disease and allow the formulation of new hypotheses as to the potential mechanisms of action of S2 during EIAV infection.

REFERENCES

Akridge, R.E., Oyafuso, L.K., Reed, S.G., 1994. IL-10 is induced during HIV-1 infection and is capable of decreasing viral replication in human macrophages. J. Immunol. 153 (12), 5782-5789.

Alcock, F., Swanton, E., 2009. Mammalian OS-9 is upregulated in response to endoplasmic reticulum stress and facilitates ubiquitination of misfolded glycoproteins. J. Mol. Biol. 385 (4), 1032-1042.

Allen, C.A., Payne, S.L., Harville, M., Cohen, N., Russell, K.E., 2007. Validation of quantitative polymerase chain reaction assays for measuring cytokine expression in equine macrophages. J. Immunol. Methods. 328 (1-2), 59-69.

Anand, K., Schulte, A., Vogel-Bachmayr, K., Scheffzek, K., Geyer, M., 2008. Structural insights into the cyclin T1-Tat-TAR RNA transcription activation complex from EIAV. Nat. Struct. Mol. Biol. 15 (12), 1287-1292.

Andersson, U., Erlandsson-Harris, H., Yang, H., Tracey, K.J., 2002. HMGB1 as a DNA-binding cytokine. J. Leuk. Biol. 72 (6), 1084-1091.

Arts, E.J., Stetor, S.R., Li, X., Rausch, J.W., Howard, K.J., Ehresmann, B., North, T.W., Wohrl, B.M., Goody, R.S., Wainberg, M.A., Grice, S.F., 1996. Initiation of (-) strand DNA synthesis from tRNA(3Lys) on lentiviral RNAs: implications of specific HIV-1 RNA-tRNA(3Lys) interactions inhibiting primer utilization by retroviral reverse transcriptases. Proc. Natl. Acad. Sci. U.S.A. 93 (19), 10063-10068.

Askjaer, P., Jensen, T.H., Nilsson, J., Englmeier, L., Kjems, J., 1998. The specificity of the CRM1-Rev nuclear export signal interaction is mediated by RanGTP. J. Biol. Chem. 273 (50), 33414-33422.

Baek, J.H., Mahon, P.C., Oh, J., Kelly, B., Krishnamachary, B., Pearson, M., Chan, D.A., Giaccia, A.J., Semenza, G.L., 2005. OS-9 interacts with hypoxia-inducible factor 1alpha and prolyl hydroxylases to promote oxygen-dependent degradation of HIF-1alpha. Molecular Cell 17 (4), 503-512.

Ball, J.M., Swaggerty, C.L., Pei, X., Lim, W.S., Xu, X., Cox, V.C., Payne, S.L., 2005. SU proteins from virulent and avirulent EIAV demonstrate distinct biological properties. Virology 333 (1), 132-144.

Beisel, C.E., Edwards, J.F., Dunn, L.L., Rice, N.R., 1993. Analysis of multiple mRNAs from pathogenic equine infectious anemia virus (EIAV) in an acutely infected

horse reveals a novel protein, Ttm, derived from the carboxy terminus of the EIAV transmembrane protein. J. Virol. 67 (2), 832-842.

Belshan, M., Park, G.S., Bilodeau, P., Stoltzfus, C.M., Carpenter, S., 2000. Binding of equine infectious anemia virus rev to an exon splicing enhancer mediates alternative splicing and nuclear export of viral mRNAs. Mol. Cell. Biol. 20 (10), 3550-3557.

Bernasconi, R., Pertel, T., Luban, J., Molinari, M., 2008. A dual task for the Xbp1-responsive OS-9 variants in the mammalian endoplasmic reticulum: inhibiting secretion of misfolded protein conformers and enhancing their disposal. J. Biol. Chem. 283 (24), 16446-16454.

Bhaumik, S.R., Malik, S., 2008. Diverse regulatory mechanisms of eukaryotic transcriptional activation by the proteasome complex. Crit Rev Biochem Mol Biol. 43 (6), 419-433.

Bieniasz, P.D., Grdina, T.A., Bogerd, H.P., Cullen, B.R., 1999. Highly divergent lentiviral Tat proteins activate viral gene expression by a common mechanism. Mol. Cell. Biol. 19 (7), 4592-4599.

Bouillant, A.M., Nielsen, K., Ruckerbauer, G.M., Samagh, B.S., Hare, W.C., 1986. The persistent infection of a canine thymus cell line by equine infectious anaemia virus and preliminary data on the production of viral antigens. J. Virol. Methods. 13 (4), 309-321.

Bozza, F.A., Cruz, O.G., Zagne, S.M., Azeredo, E.L., Nogueira, R.M., Assis, E.F., Bozza, P.T., Kubelka, C.F., 2008. Multiplex cytokine profile from dengue patients: MIP-1beta and IFN-gamma as predictive factors for severity. BMC Infect Dis 8 (86), 1-11.

Bres, V., Kiernan, R.E., Linares, L.K., Chable-Bessia, C., Plechakova, O., Treand, C., Emiliani, S., Peloponese, J.M., Jeang, K.T., Coux, O., Scheffner, M., Benkirane, M., 2003. A non-proteolytic role for ubiquitin in Tat-mediated transactivation of the HIV-1 promoter. Nat. Cell. Biol. 5 (8), 754-761.

Bright, L.A., Burgess, S.C., Chowdhary, B., Swiderski, C.E., McCarthy, F.M., 2009. Structural and functional-annotation of an equine whole genome oligoarray. BMC Bioinformatics 10 (Suppl 11), 1-8.

Brown, A., Moghaddam, S., Kawano, T., Cheng-Mayer, C., 2004. Multiple human immunodeficiency virus type 1 Nef functions contribute to efficient replication in primary human macrophages. J. Gen. Virol. 85 (Pt. 6), 1463-1469.

Broxmeyer, H.E., Sherry, B., Cooper, S., Lu, L., Maze, R., Beckmann, M.P., Cerami, A., Ralph, P., 1993. Comparative analysis of the human macrophage inflammatory protein family of cytokines (chemokines) on proliferation of human myeloid progenitor cells. Interacting effects involving suppression, synergistic suppression, and blocking of suppression. J. Immunol. 150 (8), 3448-3458.

Broxmeyer, H.E., Sherry, B., Cooper, S., Ruscetti, F.W., Williams, D.E., Arosio, P., Kwon, B.S., Cerami, A., 1991. Macrophage inflammatory protein (MIP)-1 beta abrogates the capacity of MIP-1 alpha to suppress myeloid progenitor cell growth. J. Immunol. 147 (8), 2586-2594.

Carpenter, S., Chesebro, B., 1989. Change in host cell tropism associated with in vitro replication of equine infectious anemia virus. J. Virol. 63 (6), 2492-2496.

Carroll, R., Derse, D., 1993. Translation of equine infectious anemia virus bicistronic tat-rev mRNA requires leaky ribosome scanning of the tat CTG initiation codon. J. Virol. 67 (3), 1433-1440.

Carvalho, M., Kirkland, M., Derse, D., 1993. Protein interactions with DNA elements in variant equine infectious anemia virus enhancers and their impact on transcriptional activity. J. Virol. 67 (11), 6586-6595.

Chang, A.H., O'Shaughnessy, M.V., Jirik, F.R., 2001. Hck SH3 domain-dependent abrogation of Nef-induced class 1 MHC down-regulation. Eur. J. Immunol. 31 (8), 2382-2387.

Charman, H.P., Bladen, S., Gilden, R.V., Coggins, L., 1976. Equine infectious anemia virus: evidence favoring classification as a retravirus. J. Virol. 19 (3), 1073-1079.

Chauvin, C., Salhi, S., Jean-Jean, O., 2007. Human eukaryotic release factor 3a depletion causes cell cycle arrest at G1 phase through inhibition of the mTOR pathway. Mol. Cell. Biol. 27 (16), 5619-5629.

Cheevers, W.P., McGuire, T.C., 1985. Equine infectious anemia virus: immunopathogenesis and persistence. Rev Infect Dis. 7 (1), 83-88.

Chen, C., Montelaro, R.C., 2003. Characterization of RNA elements that regulate gag-pol ribosomal frameshifting in equine infectious anemia virus. J. Virol. 77 (19), 10280-10287.

Chen, H., Dziuba, N., Friedrich, B., von Lindern, J., Murray, J.L., Rojo, D.R., Hodge, T.W., O'Brien, W.A., Ferguson, M.R., 2008. A critical role for CD63 in HIV replication and infection of macrophages and cell lines. Virology 379 (2), 191-196.

Chen, J., Wu, X., Lin, J., Levine, A.J., 1996. mdm-2 inhibits the G1 arrest and apoptosis functions of the p53 tumor suppressor protein. Mol. Cell. Biol. 16 (5), 2445-2452.

Chowdhury, I.H., Wang, X.F., Landau, N.R., Robb, M.L., Polonis, V.R., Birx, D.L., Kim, J.H., 2003. HIV-1 Vpr activates cell cycle inhibitor p21/Waf1/Cip1: a potential mechanism of G2/M cell cycle arrest. Virology 305 (2), 371-377.

Clements, J.E., Payne, S.L., 1994. Molecular basis of the pathobiology of lentiviruses. Virus Res. 32 (2), 97-109.

Clements, J.E., Zink, M.C., 1996. Molecular biology and pathogenesis of animal lentivirus infections. Clin Microbiol Rev 9 (1), 100-117.

Coggins, L., Norcross, N.L., Nusbaum, S.R., 1972. Diagnosis of equine infectious anemia by immunodiffusion test. Am. J. Vet. Res. 33 (1), 11-18.

Cook, R.F., Cook, S.J., Bolin, P.S., Howe, L.J., Zhou, W., Montelaro, R.C., Issel, C.J., 2005. Genetic immunization with codon-optimized equine infectious anemia virus (EIAV) surface unit (SU) envelope protein gene sequences stimulates immune responses in ponies. Vet. Microbiol. 108 (1-2), 23-37.

Cook, R.F., Cook, S.J., Li, F.L., Montelaro, R.C., Issel, C.J., 2002. Development of a multiplex real-time reverse transcriptase-polymerase chain reaction for equine infectious anemia virus (EIAV). J. Virol. Methods. 105 (1), 171-179.

Corn, P.G., McDonald, E.R., 3rd, Herman, J.G., El-Deiry, W.S., 2003. Tat-binding protein-1, a component of the 26S proteasome, contributes to the E3 ubiquitin ligase function of the von Hippel-Lindau protein. Nat. Genet. 35 (3), 229-237.

Covaleda, L., Fuller, F.J., Payne, S.L., 2010. EIAV S2 enhances pro-inflammatory cytokine and chemokine response in infected macrophages. Virology 397 (1), 217-223.

Craigo, J.K., Barnes, S., Zhang, B., Cook, S.J., Howe, L., Issel, C.J., Montelaro, R.C., 2009. An EIAV field isolate reveals much higher levels of subtype variability than currently reported for the equine lentivirus family. Retrovirology 6 (95), 1-12.

Craigo, J.K., Sturgeon, T.J., Cook, S.J., Issel, C.J., Leroux, C., Montelaro, R.C., 2006. Apparent elimination of EIAV ancestral species in a long-term inapparent carrier. Virology 344 (2), 340-353.

Cullen, B.R., 2000. Nuclear RNA export pathways. Mol. Cell. Biol. 20 (12), 4181-4187.

Dai, M.S., Zeng, S.X., Jin, Y., Sun, X.X., David, L., Lu, H., 2004. Ribosomal protein L23 activates p53 by inhibiting MDM2 function in response to ribosomal perturbation but not to translation inhibition. Mol. Cell. Biol. 24 (17), 7654-7668.

Dao, C.T., Zhang, D.E., 2005. ISG15: a ubiquitin-like enigma. Front Biosci 10, 2701-2722.

de la Fuente, C., Santiago, F., Deng, L., Eadie, C., Zilberman, I., Kehn, K., Maddukuri, A., Baylor, S., Wu, K., Lee, C.G., Pumfery, A., Kashanchi, F., 2002. Gene expression profile of HIV-1 Tat expressing cells: a close interplay between proliferative and differentiation signals. BMC Biochem 3 (14), 1-22.

de Parseval, A., Elder, J.H., 1999. Demonstration that orf2 encodes the feline immunodeficiency virus transactivating (Tat) protein and characterization of a unique gene product with partial rev activity. J. Virol. 73 (1), 608-617.

de Waal Malefyt, R., Abrams, J., Bennett, B., Figdor, C.G., de Vries, J.E., 1991. Interleukin 10(IL-10) inhibits cytokine synthesis by human monocytes: an autoregulatory role of IL-10 produced by monocytes. J. Exp. Med. 174 (5), 1209-1220.

Dean, G.A., Pedersen, N.C., 1998. Cytokine response in multiple lymphoid tissues during the primary phase of feline immunodeficiency virus infection. J. Virol. 72 (12), 9436-9440.

Derse, D., Dorn, P.L., Levy, L., Stephens, R.M., Rice, N.R., Casey, J.W., 1987. Characterization of equine infectious anemia virus long terminal repeat. J. Virol. 61 (3), 743-747.

Derse, D., Newbold, S.H., 1993. Mutagenesis of EIAV TAT reveals structural features essential for transcriptional activation and TAR element recognition. Virology 194 (2), 530-536.

Fagerness, A.J., Flaherty, M.T., Perry, S.T., Jia, B., Payne, S.L., Fuller, F.J., 2006. The S2 accessory gene of equine infectious anemia virus is essential for expression of disease in ponies. Virology 349 (1), 22-30.

Ferrell, K., Wilkinson, C.R., Dubiel, W., Gordon, C., 2000. Regulatory subunit interactions of the 26S proteasome, a complex problem. Trends Biochem. Sci. 25 (2), 83-88.

Fidalgo-Carvalho, I., Craigo, J.K., Barnes, S., Costa-Ramos, C., Montelaro, R.C., 2009. Characterization of an equine macrophage cell line: Application to studies of EIAV infection. Vet. Microbiol. 136 (1-2), 8-19.

Foil, L.D., Issel, C.J., 1991. Transmission of retroviruses by arthropods. Annu Rev Entomol 36, 355-381.

Friborg, J., Ladha, A., Gottlinger, H., Haseltine, W.A., Cohen, E.A., 1995. Functional analysis of the phosphorylation sites on the human immunodeficiency virus type 1 Vpu protein. J Acquir Immune Defic Syndr Hum Retrovirol 8, 10-22.

Garber, M.E., Wei, P., KewalRamani, V.N., Mayall, T.P., Herrmann, C.H., Rice, A.P., Littman, D.R., Jones, K.A., 1998. The interaction between HIV-1 Tat and human cyclin T1 requires zinc and a critical cysteine residue that is not conserved in the murine CycT1 protein. Genes Dev 12 (22), 3512-3527.

Garceau, V., Smith, J., Paton, I.R., Davey, M., Fares, M.A., Sester, D.P., Burt, D.W., Hume, D.A., 2010. Pivotal advance: avian colony-stimulating factor 1 (CSF-1), interleukin-34 (IL-34), and CSF-1 receptor genes and gene products. J. Leukoc. Biol. 87, 1-12.

Girard, J.P., 2007. A direct inhibitor of HMGB1 cytokine. Chem Biol 14 (4), 345-347.

Goh, W.C., Rogel, M.E., Kinsey, C.M., Michael, S.F., Fultz, P.N., Nowak, M.A., Hahn, B.H., Emerman, M., 1998. HIV-1 Vpr increases viral expression by manipulation of the cell cycle: a mechanism for selection of Vpr in vivo. Nat. Med. 4 (1), 65-71.

Gonda, M.A., Charman, H.P., Walker, J.L., Coggins, L., 1978. Scanning and transmission electron microscopic study of equine infectious anemia virus. Am. J. Vet. Res. 39 (5), 731-740.

Groschel, B., Bushman, F., 2005. Cell cycle arrest in G2/M promotes early steps of infection by human immunodeficiency virus. J. Virol. 79 (9), 5695-5704.

Hammond, S.A., Li, F., McKeon, B.M., Sr., Cook, S.J., Issel, C.J., Montelaro, R.C., 2000. Immune responses and viral replication in long-term inapparent carrier ponies inoculated with equine infectious anemia virus. J. Virol. 74 (13), 5968-5981.

Hanna, Z., Priceputu, E., Hu, C., Vincent, P., Jolicoeur, P., 2006. HIV-1 Nef mutations abrogating downregulation of CD4 affect other Nef functions and show reduced pathogenicity in transgenic mice. Virology 346 (1), 40-52.

Harrold, S.M., Cook, S.J., Cook, R.F., Rushlow, K.E., Issel, C.J., Montelaro, R.C., 2000. Tissue sites of persistent infection and active replication of equine infectious anemia virus during acute disease and asymptomatic infection in experimentally infected equids. J. Virol. 74 (7), 3112-3121.

Hines, R., Maury, W., 2001. DH82 cells: a macrophage cell line for the replication and study of equine infectious anemia virus. J. Virol. Methods. 95 (1-2), 47-56.

Hines, R., Sorensen, B.R., Shea, M.A., Maury, W., 2004. PU.1 binding to ets motifs within the equine infectious anemia virus long terminal repeat (LTR) enhancer: regulation of LTR activity and virus replication in macrophages. J. Virol. 78 (7), 3407-3418.

Howard, T.L., Stauffer, D.R., Degnin, C.R., Hollenberg, S.M., 2001. CHMP1 functions as a member of a newly defined family of vesicle trafficking proteins. J. Cell. Sci. 114, 2395-2404.

Howe, L., Leroux, C., Issel, C.J., Montelaro, R.C., 2002. Equine infectious anemia virus envelope evolution in vivo during persistent infection progressively increases resistance to in vitro serum antibody neutralization as a dominant phenotype. J. Virol. 76 (21), 10588-10597.

Hoyle, J., Tan, K.H., Fisher, E.M., 1997. Localization of genes encoding two human one-domain members of the AAA family: PSMC5 (the thyroid hormone receptor-interacting protein, TRIP1) and PSMC3 (the Tat-binding protein, TBP1). Human Genetics 99 (2), 285-288.

Huffman, K.M., Arrigo, S.J., Schmidt, M.G., 1999. HIV-1 Rev promotes the nuclear export of unspliced and singly spliced RNAs in a mammalian cell-free export system. J. Biomed. Sci. 6 (3), 194-205.

Hussain, K.A., Issel, C.J., Rwambo, P.M., Arnizaut, A.B., Ball, J.M., Schnorr, K.L., Montelaro, R.C., 1988. Identification of gag precursor of equine infectious anaemia virus with monoclonal antibodies to the major viral core protein, p26. J. Gen. Virol. 69 (Pt. 7), 1719-1724.

Hussain, K.A., Issel, C.J., Schnorr, K.L., Rwambo, P.M., Montelaro, R.C., 1987. Antigenic analysis of equine infectious anemia virus (EIAV) variants by using monoclonal antibodies: epitopes of glycoprotein gp90 of EIAV stimulate neutralizing antibodies. J. Virol. 61 (10), 2956-2961.

Ihm, Y., Sparks, W.O., Lee, J.H., Cao, H., Carpenter, S., Wang, C.Z., Ho, K.M., Dobbs, D., 2009. Structural model of the Rev regulatory protein from equine infectious anemia virus. PLoS One 4 (1), e4178.

Isaacson, M.K., Ploegh, H.L., 2009. Ubiquitination, ubiquitin-like modifiers, and deubiquitination in viral infection. Cell. Host. Microbe. 5 (6), 559-570.

Issel, C.J., Adams, W.V., Jr., Meek, L., Ochoa, R., 1982. Transmission of equine infectious anemia virus from horses without clinical signs of disease. J Am Vet Med Assoc 180 (3), 272-275.

Issel, C.J., Cook, R.F., 1993. A review of techniques for the serologic diagnosis of equine infectious anemia. J Vet Diagn Invest 5 (1), 137-141.

Issel, C.J., Horohov, D.W., Lea, D.F., Adams, W.V., Jr., Hagius, S.D., McManus, J.M., Allison, A.C., Montelaro, R.C., 1992. Efficacy of inactivated whole-virus and subunit vaccines in preventing infection and disease caused by equine infectious anemia virus. J. Virol. 66 (6), 3398-3408.

Issel, C.J., McManus, J.M., Hagius, S.D., Foil, L.D., Adams, W.V., Jr., Montelaro, R.C., 1990. Equine infectious anemia: prospects for control. Developments in biological standardization 72, 49-57.

Jamieson, B.D., Aldrovandi, G.M., Planelles, V., Jowett, J.B., Gao, L., Bloch, L.M., Chen, I.S., Zack, J.A., 1994. Requirement of human immunodeficiency virus type 1 nef for in vivo replication and pathogenicity. J. Virol. 68 (6), 3478-3485.

Janket, M.L., Manickam, P., Majumder, B., Thotala, D., Wagner, M., Schafer, E.A., Collman, R.G., Srinivasan, A., Ayyavoo, V., 2004. Differential regulation of host cellular genes by HIV-1 viral protein R (Vpr): cDNA microarray analysis using isogenic virus. Biochem. Biophys. Res. Commun. 314 (4), 1126-1132.

Jansen, B.J., Eleveld-Trancikova, D., Sanecka, A., van Hout-Kuijer, M., Hendriks, I.A., Looman, M.G., Leusen, J.H., Adema, G.J., 2009. OS9 interacts with DC-STAMP and modulates its intracellular localization in response to TLR ligation. Mol. Immunol. 46 (4), 505-515.

Jing Zhang, N.T., Hwang, S., Garber, M.E., Huq, I., Jones, K.A., Rana, T.M., 2000. HIV-1 TAR RNA enhances the interaction between Tat and Cyclin T1. J. Biol. Chem. 275 (44), 34314–34319.

Jintang, S., Alei, F., Yun, Z., Shanzhen, S., Weixu, H., Meixiang, Y., Fengcai, W., Xun, Q., 2009. Fucoidan increases TNF-alpha-induced MMP-9 secretion in monocytic cell line U937. Inflamm Res. 59 (4), 271-276.

Johnson, D.G., Walker, C.L., 1999. Cyclins and cell cycle checkpoints. Annu Rev Pharmacol Toxicol 39, 295-312.

Karn, J., 1999. Tackling Tat. J. Mol. Biol. 293 (2), 235-254.

Katz, R.A., Greger, J.G., Skalka, A.M., 2005. Effects of cell cycle status on early events in retroviral replication. J. Cell. Biochem. 94 (5), 880-889.

Kedzierska, K., Crowe, S.M., Turville, S., Cunningham, A.L., 2003. The influence of cytokines, chemokines and their receptors on HIV-1 replication in monocytes and macrophages. Rev Med Virol 13 (1), 39-56.

Kemen MJ Jr, C.L., 1972. Equine infectious anemia: transmission from infected mares to foals. J Am Vet Med Assoc. 5 (161), 496-499.

Kemen, M.J., McClain, D.S., Matthysse, J.G., 1978. Role of horse flies in transmission of wquine infectious anemia from carrier ponies. J Am Vet Med Assoc 172 (3), 360-362.

Kestler, H.W., 3rd, Ringler, D.J., Mori, K., Panicali, D.L., Sehgal, P.K., Daniel, M.D., Desrosiers, R.C., 1991. Importance of the nef gene for maintenance of high virus loads and for development of AIDS. Cell 65 (4), 651-662.

Khan, I.H., Sawai, E.T., Antonio, E., Weber, C.J., Mandell, C.P., Montbriand, P., Luciw, P.A., 1998. Role of the SH3-ligand domain of simian immunodeficiency virus Nef in interaction with Nef-associated kinase and simian AIDS in rhesus macaques. J. Virol. 72 (7), 5820-5830.

Kimura, Y., Nakazawa, M., Yamada, M., 1998. Cloning and characterization of three isoforms of OS-9 cDNA and expression of the OS-9 gene in various human tumor cell lines. J. Biochem. 123 (5), 876-882.

Kinter, A., Catanzaro, A., Monaco, J., Ruiz, M., Justement, J., Moir, S., Arthos, J., Oliva, A., Ehler, L., Mizell, S., Jackson, R., Ostrowski, M., Hoxie, J., Offord, R., Fauci, A.S., 1998. CC-chemokines enhance the replication of T-tropic strains of HIV-1 in CD4(+) T cells: role of signal transduction. Proc. Natl. Acad. Sci. U.S.A. 95 (20), 11880-11885.

Klevjer-Anderson, P., Cheevers, W.P., Crawford, T.B., 1979. Characterization of the infection of equine fibroblasts by equine infectious anemia virus. Archives of Virology 60, 279-289.

Kono, Y., Kobayashi, K., Fukunaga, Y., 1973. Antigenic drift of equine infectious anemia virus in chronically infected horses. Arch Gesamte Virusforsch 41 (1), 1-10.

Kononenko, A.V., Mitkevich, V.A., Atkinson, G.C., Tenson, T., Dubovaya, V.I., Frolova, L.Y., Makarov, A.A., Hauryliuk, V., 2010. GTP-dependent structural rearrangement of the eRF1:eRF3 complex and eRF3 sequence motifs essential for PABP binding. Nucleic Acids Res 38 (2), 548-558.

Krawczyk, M., Seguin-Estevez, Q., Leimgruber, E., Sperisen, P., Schmid, C., Bucher, P., Reith, W., 2008. Identification of CIITA regulated genetic module dedicated for antigen presentation. PLoS Genet. 4 (4), e1000058.

Krummheuer, J., Johnson, A.T., Hauber, I., Kammler, S., Anderson, J.L., Hauber, J., Purcell, D.F., Schaal, H., 2007. A minimal uORF within the HIV-1 vpu leader allows efficient translation initiation at the downstream env AUG. Virology 363 (2), 261-271.

Kuna, P., Reddigari, S.R., Schall, T.J., Rucinski, D., Viksman, M.Y., Kaplan, A.P., 1992. RANTES, a monocyte and T lymphocyte chemotactic cytokine releases histamine from human basophils. J. Immunol. 149 (2), 636-642.

Lane, B.R., King, S.R., Bock, P.J., Strieter, R.M., Coffey, M.J., Markovitz, D.M., 2003. The C-X-C chemokine IP-10 stimulates HIV-1 replication. Virology 307 (1), 122-134.

Lane, B.R., Lore, K., Bock, P.J., Andersson, J., Coffey, M.J., Strieter, R.M., Markovitz, D.M., 2001. Interleukin-8 stimulates human immunodeficiency virus type 1 replication and is a potential new target for antiretroviral therapy. J. Virol. 75 (17), 8195-8202.

Lassot, I., Latreille, D., Rousset, E., Sourisseau, M., Linares, L.K., Chable-Bessia, C., Coux, O., Benkirane, M., Kiernan, R.E., 2007. The proteasome regulates HIV-1 transcription by both proteolytic and nonproteolytic mechanisms. Mol. Cell. 25 (3), 369-383.

Le Grice, S.F., Panin, M., Kalayjian, R.C., Richter, N.J., Keith, G., Darlix, J.L., Payne, S.L., 1991. Purification and characterization of recombinant equine infectious anemia virus reverse transcriptase. J. Virol. 65 (12), 7004-7007.

Lee, J.H., Murphy, S.C., Belshan, M., Sparks, W.O., Wannemuehler, Y., Liu, S., Hope, T.J., Dobbs, D., Carpenter, S., 2006. Characterization of functional domains of equine infectious anemia virus Rev suggests a bipartite RNA-binding domain. J. Virol. 80 (8), 3844-3852.

Leroux, C., Cadore, J.L., Montelaro, R.C., 2004. Equine Infectious Anemia Virus (EIAV): what has HIV's country cousin got to tell us? Vet. Res. 35 (4), 485-512.

Leroux, C., Issel, C.J., Montelaro, R.C., 1997. Novel and dynamic evolution of equine infectious anemia virus genomic quasispecies associated with sequential disease cycles in an experimentally infected pony. J. Virol. 71 (12), 9627-9639.

Li, F., Craigo, J.K., Howe, L., Steckbeck, J.D., Cook, S., Issel, C., Montelaro, R.C., 2003. A live attenuated equine infectious anemia virus proviral vaccine with a

modified S2 gene provides protection from detectable infection by intravenous virulent virus challenge of experimentally inoculated horses. J. Virol. 77 (13), 7244-7253.

Li, F., Leroux, C., Craigo, J.K., Cook, S.J., Issel, C.J., Montelaro, R.C., 2000. The S2 gene of equine infectious anemia virus is a highly conserved determinant of viral replication and virulence properties in experimentally infected ponies. J. Virol. 74 (1), 573-579.

Li, F., Puffer, B.A., Montelaro, R.C., 1998. The S2 gene of equine infectious anemia virus is dispensable for viral replication in vitro. J. Virol. 72 (10), 8344-8348.

Lichtenstein, D.L., Craigo, J.K., Leroux, C., Rushlow, K.E., Cook, R.F., Cook, S.J., Issel, C.J., Montelaro, R.C., 1999. Effects of long terminal repeat sequence variation on equine infectious anemia virus replication in vitro and in vivo. Virology 263 (2), 408-417.

Lichtenstein, D.L., Issel, C.J., Montelaro, R.C., 1996. Genomic quasispecies associated with the initiation of infection and disease in ponies experimentally infected with equine infectious anemia virus. J. Virol. 70 (6), 3346-3354.

Lichtenstein, D.L., Rushlow, K.E., Cook, R.F., Raabe, M.L., Swardson, C.J., Kociba, G.J., Issel, C.J., Montelaro, R.C., 1995, Replication in vitro and in vivo of an equine infectious anemia virus mutant deficient in dUTPase activity. J. Virol. 69 (5), 2881-2888.

Lim, W.S., Payne, S.L., Edwards, J.F., Kim, I., Ball, J.M., 2005. Differential effects of virulent and avirulent equine infectious anemia virus on macrophage cytokine expression. Virology 332 (1), 295-306.

Lin, H., Lee, E., Hestir, K., Leo, C., Huang, M., Bosch, E., Halenbeck, R., Wu, G., Zhou, A., Behrens, D., Hollenbaugh, D., Linnemann, T., Qin, M., Wong, J., Chu, K., Doberstein, S.K., Williams, L.T., 2008. Discovery of a cytokine and its receptor by functional screening of the extracellular proteome. Science 320 (5877), 807-811.

Linenberger, M.L., Shelton, G.H., Persik, M.T., Abkowitz, J.L., 1991. Hematopoiesis in asymptomatic cats infected with feline immunodeficiency virus. Blood 78 (8), 1963-1968.

Litovchick, L., Friedmann, E., Shaltiel, S., 2002. A selective interaction between OS-9 and the carboxyl-terminal tail of meprin beta. J. Biol. Chem. 277 (37), 34413-34423.

Loetscher, P., Seitz, M., Clark-Lewis, I., Baggiolini, M., Moser, B., 1994. Monocyte chemotactic proteins MCP-1, MCP-2, and MCP-3 are major attractants for human CD4+ and CD8+ T lymphocytes. FASEB J 8 (13), 1055-1060.

Malim, M.H., Emerman, M., 2008. HIV-1 accessory proteins-ensuring viral survival in a hostile environment. Cell Host & Microbe 3 (6), 388-398.

Martarano, L., Stephens, R., Rice, N., Derse, D., 1994. Equine infectious anemia virus trans-regulatory protein Rev controls viral mRNA stability, accumulation, and alternative splicing. J. Virol. 68 (5), 3102-3111.

Maurer, M., von Stebut, E., 2004. Macrophage inflammatory protein-1. Int J Biochem Cell Biol 36 (10), 1882-1886.

Maury, W., 1994. Monocyte maturation controls expression of equine infectious anemia virus. J. Virol. 68 (10), 6270-6279.

Maury, W., 1998. Regulation of equine infectious anemia virus expression. Journal of Biomedical Science 5 (1), 11-23.

Maury, W., Bradley, S., Wright, B., Hines, R., 2000. Cell specificity of the transcription-factor repertoire used by a lentivirus: motifs important for expression of equine infectious anemia virus in nonmonocytic cells. Virology 267 (2), 267-278.

Maury, W., Thompson, R.J., Jones, Q., Bradley, S., Denke, T., Baccam, P., Smazik, M., Oaks, J.L., 2005. Evolution of the equine infectious anemia virus long terminal repeat during the alteration of cell tropism. J. Virol. 79 (9), 5653-5664.

Maury, W.J., Carpenter, S., Graves, K., Chesebro, B., 1994. Cellular and viral specificity of equine infectious anemia virus Tat transactivation. Virology 200 (2), 632-642.

Maze, R., Sherry, B., Kwon, B.S., Cerami, A., Broxmeyer, H.E., 1992. Myelosuppressive effects in vivo of purified recombinant murine macrophage inflammatory protein-1 alpha. J Immunol 149 (3), 1004-1009.

McGuire, T.C., Crawford, T.B., Henson, J.B., 1971. Immunofluorescent localization of equine infectious anemia virus in tissue. Am J Pathol. 62 (2), 283-294.

McGuire, T.C., Fraser, D.G., Mealey, R.H., 2002. Cytotoxic T lymphocytes and neutralizing antibody in the control of equine infectious anemia virus. Viral Immunol 15 (4), 521-531.

McGuire, T.C., Fraser, D.G., Mealey, R.H., 2004. Cytotoxic T lymphocytes in protection against equine infectious anemia virus. Anim Health Res Rev 5 (2), 271-276.

McGuire, T.C., O'Rourke, K.I., Perryman, L.E., 1990. Immunopathogenesis of equine infectious anemia lentivirus disease. Dev. Biol Stand. 72, 31-37.

Menten, P., Wuyts, A., Van Damme, J., 2002. Macrophage inflammatory protein-1. Cytokine Growth Factor Rev 13 (6), 455-481.

Metcalf, E.S., 2001. The role of international transport of equine semen on disease transmission. Anim Reprod Sci 68 (3-4), 229-237.

Miller, R.J., Cairns, J.S., Bridges, S., Sarver, N., 2000. Human immunodeficiency virus and AIDS: insights from animal lentiviruses. J. Virol. 74 (16), 7187-7195.

Minano, F.J., Fernandez-Alonso, A., Myers, R.D., Sancibrian, M., 1996. Hypothalamic interaction between macrophage inflammatory protein-1 alpha (MIP-1 alpha) and MIP-1 beta in rats: a new level for fever control? J Physiol. 491 (Pt. 1), 209-217.

Montelaro, R.C., Chen, C., 2003. Characterization of RNA elements that regulate Gag-Pol ribosomal frameshifting in equine infectious anemia virus. J. Virol. 77 (19), 10280–10287.

Montelaro, R.C., Ball, J.M., Rushlow, K.E., 1993. Equine retroviruses, In The Retroviridae (L. J. A., Ed). Vol. 2, pp. 257-360. Plenum Press, New York.

Montelaro, R.C., Parekh, B., Orrego, A., Issel, C.J., 1984. Antigenic variation during persistent infection by equine infectious anemia virus, a retrovirus. J. Biol. Chem. 259 (16), 10539-10544.

Moore, K.W., de Waal Malefyt, R., Coffman, R.L., O'Garra, A., 2001. Interleukin-10 and the interleukin-10 receptor. Annu. Rev. Immunol. 19, 683-765.

Moorthamer, M., Chaudhuri, B., 1999. Identification of ribosomal protein L34 as a novel Cdk5 inhibitor. Biochem Biophys Res Commun. 255 (3), 631-638.

Nagarajan, M.M., Simard, C., 2001. Detection of horses infected naturally with equine infectious anemia virus by nested polymerase chain reaction. J. Virol. Method. 94 (1-2), 97-109.

Naghavi, M.H., Nowak, P., Andersson, J., Sonnerborg, A., Yang, H., Tracey, K.J., Vahlne, A., 2003. Intracellular high mobility group B1 protein (HMGB1) represses HIV-1 LTR-directed transcription in a promoter- and cell-specific manner. Virology 314 (1), 179-189.

Nakajima, H., Yoshino, T., Ushimi, C., 1974. Equine infectious anemia virus from infected horse serum. Infect Immun. 10 (3), 667-668.

Naora, H., Takai, I., Adachi, M., 1998. Altered cellular responses by varying expression of a ribosomal protein gene: sequential coordination of enhancement and suppression of ribosomal protein S3a gene expression induces apoptosis. J. Cell Biol. 141 (3), 741-753.

Nelbock, P., Dillon, P.J., Perkins, A., Rosen, C.A., 1990. A cDNA for a protein that interacts with the human immunodeficiency virus Tat transactivator. Science 248 (4963), 1650-1653.

Noiman, S., Yaniv, A., Sherman, L., Tronick, S.R., Gazit, A., 1990. Pattern of transcription of the genome of equine infectious anemia virus. J. Virol. 64 (4), 1839-1843.

Noiman, S., Yaniv, A., Tsach, T., Miki, T., Tronick, S.R., Gazit, A., 1991. The Tat protein of equine infectious anemia virus is encoded by at least three types of transcripts. Virology 184 (2), 521-530.

Nomaguchi, M., Fujita, M., Adachi, A., 2008. Role of HIV-1 Vpu protein for virus spread and pathogenesis. Microbes Infect 10 (9), 960-967.

Oaks, J.L., McGuire, T.C., Ulibarri, C., Crawford, T.B., 1998. Equine infectious anemia virus is found in tissue macrophages during subclinical infection. J. Virol. 72 (9), 7263-7269.

Oaks, J.L., Ulibarri, C., Crawford, T.B., 1999. Endothelial cell infection in vivo by equine infectious anaemia virus. J. Gen. Virol. 80 (Pt. 9), 2393-2397.

Orandle, M.S., Williams, K.C., MacLean, A.G., Westmoreland, S.V., Lackner, A.A., 2001. Macaques with rapid disease progression and simian immunodeficiency virus encephalitis have a unique cytokine profile in peripheral lymphoid tissues. J. Virol. 75 (9), 4448-4452.

Orrego, A., Issel, C.J., Montelaro, R.C., Adams, W.V., Jr., 1982. Virulence and in vitro growth of a cell-adapted strain of equine infectious anemia virus after serial passage in ponies. Am J Vet Res. 43 (9), 1556-1560.

Otero, G.C., Harris, M.E., Donello, J.E., Hope, T.J., 1998. Leptomycin B inhibits equine infectious anemia virus Rev and feline immunodeficiency virus rev function but not the function of the hepatitis B virus posttranscriptional regulatory element. J. Virol. 72 (9), 7593-7597.

Park, T., Yi, S.G., Kang, S.H., Lee, S., Lee, Y.S., Simon, R., 2003. Evaluation of normalization methods for microarray data. BMC Bioinformatics 4 (33).

Payne, S., Lim, W.S., Fuller, F.J., Ball, J.M., 2006. Equine infectious anemia virus as a model for lentiviral pathogenesis, In: Friedman, H., Specter, S., Bendinelli, M. (Eds.) In Vivo Models of HIV Disease and Control / edited by Herman Friedman, Steven Specter, Mauro Bendinelli. Springer, New York, pp. 365-390.

Payne, S.L., Fang, F.D., Liu, C.P., Dhruva, B.R., Rwambo, P., Issel, C.J., Montelaro, R.C., 1987. Antigenic variation and lentivirus persistence: variations in envelope gene sequences during EIAV infection resemble changes reported for sequential isolates of HIV. Virology 161 (2), 321-331.

Payne, S.L., La Celle, K., Pei, X.F., Qi, X.M., Shao, H., Steagall, W.K., Perry, S., Fuller, F., 1999. Long terminal repeat sequences of equine infectious anaemia virus are a major determinant of cell tropism. J. Gen. Virol. 80 (Pt. 3), 755-759.

Payne, S.L., Pei, X.F., Jia, B., Fagerness, A., Fuller, F.J., 2004. Influence of long terminal repeat and env on the virulence phenotype of equine infectious anemia virus. J. Virol. 78 (5), 2478-2485.

Peng, B., Robert-Guroff, M., 2001. Deletion of N-terminal myristoylation site of HIV Nef abrogates both MHC-1 and CD4 down-regulation. Immunol Lett 78 (3), 195-200.

Pfaffl, M.W., 2001. A new mathematical model for relative quantification in real-time RT-PCR. Nucleic Acids Res. 29 (9), e45.

Prost, S., Le Dantec, M., Auge, S., Le Grand, R., Derdouch, S., Auregan, G., Deglon, N., Relouzat, F., Aubertin, A.M., Maillere, B., Dusanter-Fourt, I., Kirszenbaum, M., 2008. Human and simian immunodeficiency viruses deregulate early hematopoiesis through a Nef/PPARgamma/STAT5 signaling pathway in macaques. J. Clin. Invest. 118 (5), 1765-1775.

Raabe, M.L., Issel, C.J., Cook, S.J., Cook, R.F., Woodson, B., Montelaro, R.C., 1998a. Immunization with a recombinant envelope protein (rgp90) of EIAV produces a spectrum of vaccine efficacy ranging from lack of clinical disease to severe enhancement. Virology 245 (1), 151-162.

Raabe, M.R., Issel, C.J., Montelaro, R.C., 1998b. Equine monocyte-derived macrophage cultures and their applications for infectivity and neutralization studies of equine infectious anemia virus. J. Virol. Method. 71 (1), 87-104.

Reinhart, T.A., 2003. Chemokine induction by HIV-1: recruitment to the cause. Trends Immunol. 24 (7), 351-353.

Rice, N.R., Henderson, L.E., Sowder, R.C., Copeland, T.D., Oroszlan, S., Edwards, J.F., 1990. Synthesis and processing of the transmembrane envelope protein of equine infectious anemia virus. J. Virol. 64 (8), 3770-3778.

Rozan, L.M., El-Deiry, W.S., 2006. Identification and characterization of proteins interacting with Traf4, an enigmatic p53 target. Cancer Biol Ther. 5 (9), 1228-1235.

Russell, K.E., Perkins, P.C., Hoffman, M.R., Miller, R.T., Walker, K.M., Fuller, F.J., Sellon, D.C., 1999. Platelets from thrombocytopenic ponies acutely infected with equine infectious anemia virus are activated in vivo and hypofunctional. Virology 259 (1), 7-19.

Sandri-Goldin, R.M., 2004. Viral regulation of mRNA export. J. Virol. 78 (9), 4389-4396.

Satoh, T., Ishizuka, T., Tomaru, T., Yoshino, S., Nakajima, Y., Hashimoto, K., Shibusawa, N., Monden, T., Yamada, M., Mori, M., 2009. Tat-binding protein-1 (TBP-1), an ATPase of 19S regulatory particles of the 26S proteasome, enhances androgen receptor function in cooperation with TBP-1-interacting protein/Hop2. Endocrinology 150 (7), 3283-3290.

Schiltz, R.L., Shih, D.S., Rasty, S., Montelaro, R.C., Rushlow, K.E., 1992, Equine infectious anemia virus gene expression: characterization of the RNA splicing pattern and the protein products encoded by open reading frames S1 and S2. J. Virol. 66 (6), 3455-3465.

Schmidtmayerova, H., Nottet, H.S., Nuovo, G., Raabe, T., Flanagan, C.R., Dubrovsky, L., Gendelman, H.E., Cerami, A., Bukrinsky, M., Sherry, B., 1996. Human immunodeficiency virus type 1 infection alters chemokine beta peptide expression in human monocytes: implications for recruitment of leukocytes into brain and lymph nodes. Proc. Natl. Acad. Sci. U.S.A. 93 (2), 700-704.

Schuitemaker, H., Kootstra, N.A., Fouchier, R.A., Hooibrink, B., Miedema, F., 1994. Productive HIV-1 infection of macrophages restricted to the cell fraction with proliferative capacity. EMBO J. 13 (24), 5929-5936.

Schwartz, S., Felber, B.K., Pavlakis, G.N., 1992. Mechanism of translation of monocistronic and multicistronic human immunodeficiency virus type 1 mRNAs. Mol. Cell. Biol. 12 (1), 207-219.

Selby, M.J., Bain, E.S., Luciw, P.A., Peterlin, B.M., 1989. Structure, sequence, and position of the stem-loop in tar determine transcriptional elongation by tat through the HIV-1 long terminal repeat. Genes Dev. 3 (4), 547-558.

Sellon, D.C., 1993. Equine infectious anemia. Vet Clin North Am Equine Pract. 9 (2), 321-336.

Sellon, D.C., Fuller, F.J., McGuire, T.C., 1994. The immunopathogenesis of equine infectious anemia virus. Virus Res. 32 (2), 111-138.

Sellon, D.C., Perry, S.T., Coggins, L., Fuller, F.J., 1992. Wild-type equine infectious anemia virus replicates in vivo predominantly in tissue macrophages, not in peripheral blood monocytes. J. Virol. 66 (10), 5906-5913.

Sellon, D.C., Walker, K.M., Russell, K.E., Perry, S.T., Covington, P., Fuller, F.J., 1996. Equine infectious anemia virus replication is upregulated during differentiation of blood monocytes from acutely infected horses. J. Virol. 70 (1), 590-594.

Shen, R.X., Wang, Z., 1985. Development and use of an equine infectious anemia donkey leucocyte attenuated vaccine. In: Proceedings of the International Symposium on Immunity to Equine Infection Anemia, Chinese Academy of Agricultural Sciences Harbin Veterinary Research Institute, Harbin. p. 34-35.

Shen, T., Liang, H., Tong, X., Fan, X., He, X., Ma, Y., Xiang, W., Shen, R., Zhang, X., Shao, Y., 2006. Amino acid mutations of the infectious clone from Chinese EIAV attenuated vaccine resulted in reversion of virulence. Vaccine 24 (6), 738-749.

Speed, T., Yang, Y.H., 2002. Direct versus indirect designs for cDNA microarray experiments. Indian J. Stat. 64, 707-721.

Stauber, R.H., Afonina, E., Gulnik, S., Erickson, J., Pavlakis, G.N., 1998. Analysis of intracellular trafficking and interactions of cytoplasmic HIV-1 Rev mutants in living cells. Virology 251 (1), 38-48.

Stein, C.D., J. C. Lotze, and L. O. Mott., 1942. Transmission of equine infectious anemia by the stablefly, Stomoxys calcitrans, the horsefly, Tabanus sulcifrons (Macquart), and by injection of minute amounts of virus. Am. J. Vet. Res. 3, 183–193.

Steinberg, H.N., Crumpacker, C.S., Chatis, P.A., 1991. In vitro suppression of normal human bone marrow progenitor cells by human immunodeficiency virus. J. Virol. 65 (4), 1765-1769.

Su, Y.A., Hutter, C.M., Trent, J.M., Meltzer, P.S., 1996. Complete sequence analysis of a gene (OS-9) ubiquitously expressed in human tissues and amplified in sarcomas. Molecular Carcinogenesis 15 (4), 270-275.

Sun, C., Zhang, B., Jin, J., Montelaro, R.C., 2008. Binding of equine infectious anemia virus to the equine lentivirus receptor-1 is mediated by complex discontinuous sequences in the viral envelope gp90 protein. J. Gen. Virol. 89 (Pt. 8), 2011-2019.

Sune, C., Goldstrohm, A.C., Peng, J., Price, D.H., Garcia-Blanco, M.A., 2000. An in vitro transcription system that recapitulates equine infectious anemia virus tat-mediated inhibition of human immunodeficiency virus type 1 Tat activity demonstrates a role for positive transcription elongation factor b and associated proteins in the mechanism of Tat activation. Virology 274 (2), 356-366.

Swardson, C.J., Kociba, G.J., Perryman, L.E., 1992. Effects of equine infectious anemia virus on hematopoietic progenitors in vitro. Am. J. Vet. Res. 53 (7), 1176-1179.

Tanahashi, N., Suzuki, M., Fujiwara, T., Takahashi, E., Shimbara, N., Chung, C.H., Tanaka, K., 1998. Chromosomal localization and immunological analysis of a family of human 26S proteasomal ATPases. Biochem. Biophys. Res. Comm. 243 (1), 229-232.

Taube, R., Fujinaga, K., Irwin, D., Wimmer, J., Geyer, M., Peterlin, B.M., 2000. Interactions between equine cyclin T1, Tat, and TAR are disrupted by a leucine-to-valine substitution found in human cyclin T1. J. Virol. 74 (2), 892-898.

Threadgill, D.S., Steagall, W.K., Flaherty, M.T., Fuller, F.J., Perry, S.T., Rushlow, K.E., Le Grice, S.F., Payne, S.L., 1993. Characterization of equine infectious anemia virus dUTPase: growth properties of a dUTPase-deficient mutant. J. Virol. 67 (5), 2592-2600.

Tornquist, S.J., Oaks, J.L., Crawford, T.B., 1997. Elevation of cytokines associated with the thrombocytopenia of equine infectious anaemia. J. Gen. Virol. 78 (Pt.10), 2541-2548.

Truax, A.D., Koues, O.I., Mentel, M.K., Greer, S.F., 2010. The 19S ATPase S6a (S6'/TBP1) regulates the transcription initiation of class II transactivator. J. Mol. Biol. 395 (2), 254-269.

Vallée H., C.H., 1904. Sur la nature infectieuse de l'anémie du cheval. C.R. Hebd. Seances Acad. Sci. Ser. D Sci. Nat. 139, 331–333.

Vazquez, N., Greenwell-Wild, T., Marinos, N.J., Swaim, W.D., Nares, S., Ott, D.E., Schubert, U., Henklein, P., Orenstein, J.M., Sporn, M.B., Wahl, S.M., 2005. Human immunodeficiency virus type 1-induced macrophage gene expression includes the p21 gene, a target for viral regulation. J. Virol. 79 (7), 4479-4491.

Wang, S.Z., Rushlow, K.E., Issel, C.J., Cook, R.F., Cook, S.J., Raabe, M.L., Chong, Y.H., Costa, L., Montelaro, R.C., 1994. Enhancement of EIAV replication and disease by immunization with a baculovirus-expressed recombinant envelope surface glycoprotein. Virology 199 (1), 247-251.

Wang, Y., Fu, X., Gaiser, S., Kèottgen, M., Kramer-Zucker, A., Walz, G., Wegierski, T., 2007. OS-9 regulates the transit and polyubiquitination of TRPV4 in the endoplasmic reticulum. J. Biol. Chem. 282 (50), 36561-36570.

Warner, J.R., McIntosh, K.B., 2009. How common are extraribosomal functions of ribosomal proteins? Mol Cell. 34 (1), 3-11.

Wei, L., Fan, X., Lu, X., Zhao, L., Xiang, W., Zhang, X., Xue, F., Shao, Y., Shen, R., Wang, X., 2009. Genetic variation in the long terminal repeat associated with the transition of Chinese equine infectious anemia virus from virulence to avirulence. Virus Genes. 38 (2), 285-288.

Wohrl, B.M., Howard, K.J., Jacques, P.S., Le Grice, S.F., 1994. Alternative modes of polymerization distinguish the subunits of equine infectious anemia virus reverse transcriptase. J. Biol. Chem. 269 (11), 8541-8548.

Yoon, S., Kingsman, S.M., Kingsman, A.J., Wilson, S.A., Mitrophanous, K.A., 2000. Characterization of the equine infectious anaemia virus S2 protein. J. Gen. Virol. 81 (Pt. 9), 2189-2194.

Yoshizuka, N., Yoshizuka-Chadani, Y., Krishnan, V., Zeichner, S.L., 2005. Human immunodeficiency virus type 1 Vpr-dependent cell cycle arrest through a mitogen-activated protein kinase signal transduction pathway. J. Virol. 79 (17), 11366-11381.

Zhang, X., Wang, Y., Liang, H., Wei, L., Xiang, W., Shen, R., Shao, Y., 2007. Correlation between the induction of Th1 cytokines by an attenuated equine infectious anemia virus vaccine and protection against disease progression. J. Gen. Virol. 88 (Pt. 3), 998-1004.

Zheng, Y.H., Sentsui, H., Kono, Y., Ikuta, K., 2000. Mutations occurring during serial passage of Japanese equine infectious anemia virus in primary horse macrophages. Virus Res. 68 (1), 93-98.

Zheng, Y.H., Sentsui, H., Nakaya, T., Kono, Y., Ikuta, K., 1997. In vivo dynamics of equine infectious anemia viruses emerging during febrile episodes: insertions/duplications at the principal neutralizing domain. J. Virol. 71 (7), 5031-5039.

VITA

Lina Maria Covaleda Salas

Texas A&M University
Department of Veterinary Pathobiology
College Station, TX, 77843-4458

Education

Ph.D. Veterinary Microbiology, Texas A&M University- May 2010

B.S. in Microbiology, Universidad de los Andes, Colombia- May 1999

Fellowships

Pre-doctoral Fellowship from the NIH Training Grant Faculty- 2006 and 2007

Publications

Covaleda, L., Gno, Bich-Ty., Fuller, F., and Payne S., 2010. Identification of cellular proteins interaction with Equine Infectious Anemia Virus S2 Protein. Virus Res. Accepted for publication April 2010.

Covaleda, L., Fuller, F., and Payne S., 2010. EIAV S2 enhances pro-inflammatory cytokine and chemokine response in infected macrophages. Virology 397 (1), 217-223.

Lungu, G., Covaleda, L., Mendes, O., Martini-Stoica, H., Stoica, G., 2008. FGF-1-induced matrix metalloproteinase-9 expression in breast cancer cells is mediated by increased activities of NF-kappaB and activating protein-1. Mol Carcinog. 47 (6), 424-435.

Xu Z, van den Berg MA, Scheuring C, Covaleda L, Lu H, Santos FA, Uhm T, Lee MK, Wu C, Liu S, Zhang HB., 2005. Genome physical mapping from large-insert clones by fingerprint analysis with capillary electrophoresis: a robust physical map of *Penicillium chrysogenum*. Nucleic Acids Res. 33 (5), 1-8.

He L, Du C, Covaleda L, Xu Z, Robinson AF, Yu JZ, Kohel RJ, Zhang HB., 2004. Cloning, characterization, and evolution of the NBS-LRR-encoding resistance gene analogue family in polyploid cotton (*Gossypium hirsutum L*). Mol. Plant. Microbe. Interact. 17 (11), 1234-1241.

Xu Z, Sun S, Covaleda L, Ding K, Zhang A, Wu C, Scheuring C, Zhang HB., 2004. Genome physical mapping with large-insert bacterial clones by fingerprint analysis: methodologies, source clone genome coverage, and contig map quality. Genomics 84 (6), 941-951.